

Genetic and Chemical Characterisation of the Cornexistin Pathway Provides Further Insight into Maleidride Biosynthesis

^aKatherine Williams,^a Agnieszka. J. Szwalbe,^b Claire Dickson,^b Tim R. Desson,^c Nicholas. P. Mulholland,^c Jason. L. Vincent,^c John. M. Clough,^c Andrew. M. Bailey,^d Craig. P. Butts,^b Christine. L. Willis,^b Thomas. J. Simpson^b and Russell. J. Cox^{a,b} ^aInstitute for Organic Chemistry, and BMWZ, Leibniz University of Hannover, Schneiderberg 1B, 30167, Germany

^bSchool of Chemistry, University of Bristol, Cantock's Close, Bristol, BS8 1TS, UK

^cSyngenta, Jealott's Hill, Bracknell, Berkshire, RG42 6EY, UK

^dSchool of Biological Sciences, Bristol Life Sciences Building, University of Bristol, 24 Tyndall Ave, Bristol BS8 1TH, UK

Electronic Supplementary Information

1	General Procedures	3
2	NMR Instruments	3
3	HRESIMS	3
4	Strains	3
5	Growth and Fermentation Conditions	3
6	Fungal Nucleic Acid Preparation	3
7	Genome and RNA Sequencing	3
8	Cornexistin Biosynthetic Gene Cluster	4
9	Biosynthetic Gene Cluster Comparisons	5
10	Gene Disruption Procedures	8
11	Transformation of <i>P. variotii</i> K5013	11
12	Genetic Characterisation of Gene Knock-Outs	11
12.1	<i>PCR Analysis of PVΔpks1 Strains</i>	12
12.2	<i>PCR analysis of PV AgnΔpks strains</i>	13
12.3	<i>PCR analysis of AgnΔpks-PVΔL1 strains</i>	14
12.4	<i>PCR analysis of AgnΔpks-PVΔL6 strains</i>	15
12.5	<i>PCR analysis of AgnΔpks-PVΔR1 strains</i>	16
12.6	<i>PCR analysis of AgnΔpks-PVΔL3 strains</i>	17
12.7	<i>PCR analysis of AgnΔpks-PVΔL11 strains</i>	18
12.8	<i>PCR analysis of AgnΔpks-PVΔL7 strains</i>	19
12.9	<i>PCR analysis of AgnΔpks-PVΔL9 strains</i>	20
12.10	<i>PCR analysis of AgnΔpks-PVΔL14 strains</i>	21
12.11	<i>PCR analysis of PVΔL13 strains</i>	22
13	Metabolite Extraction and LCMS Analysis of <i>P. variotii</i>	23
14	Quantification of Cornexistin Production	23

15	Comparison of Maleidride Production Between AgnΔpks and AgnΔpks-PVΔ11 Strains	24
16	LCMS Analysis of Other AgnΔpks Knock-Out Strains	24
17	Structure Elucidation	25
17.1	<i>Cornexistin 1</i>	25
17.2	<i>Analysis of the PV AgnΔpks Strain</i>	28
17.2.1	Dihydrocornexistin diastereomers 10A and 10B	28
17.2.2	6-dehydroxy-2,2'-dihydro-cornexistin 11	32
17.2.3	2,2-dihydro-2-hydroxycornexistin 15, isolated as its hemiacetal 9	33
17.3	<i>Analysis of isolated metabolites</i>	37
18	Feeding Byssochlamic Acid 4 to the PVΔpks Strain	38
19	Detection of Byssochlamic Acid 4 in <i>P. variotii</i>	40
20	Cornexistin Mid-Pathway Hypothesis	41
21	LCMS analysis of compounds 5, 5' and 13	42
22	Hydrogenation of Cornexistin	42
23	NMR Experimental Details	43
23.1	<i>Compound 9</i>	43
23.2	<i>Compound 10</i>	43
24	Structural Calculations for 9, 10A and 10B	44
24.1	<i>Conformational search for 9 and 10</i>	44
24.2	<i>Calculation of chemical shifts for 9</i>	45
24.3	<i>Calculation of distances for NOE comparison for 10</i>	46
24.4	<i>Calculation of scalar coupling constants for 10</i>	47
24.5	<i>Chemical shift analysis for 9</i>	47
24.6	<i>Analysis for 10</i>	51
25	Crystallisation of Cornexistin and X-ray Analysis	67
26	References	69

1 General Procedures

Analytical grade chemicals and reagents were supplied from Sigma-Aldrich, Alfa Aesar, Acros Organics, Becton-Dickinson, BDH, Fisher, Fluka and Difco, unless otherwise stated. Solvents used for LC-DAD-MS analyses were HPLC grade. General molecular biology procedures were performed as standard¹ and molecular biology kits used according to manufacturer's protocols. Analytical PCR was performed using BioMix Red (Bioline) and preparative PCR was performed using Phusion polymerase (NEB) or KAPA-HiFli (Roche). Restriction endonucleases were purchased from Thermo Fisher Scientific or NEB.

2 NMR Instruments

Varian 400-MR (400MHz), Varian VNMR500 (500MHz), Bruker 500 Cryo (500MHz) or Varian VNMR5600 Cryo (600MHz).

3 HRESIMS

(1) Bruker Daltonics micrOTOF II, (2) Bruker Daltonics Apex IV FT-ICR instruments.

4 Strains

Escherichia coli strain TOP10 (Invitrogen) was used as a host for all plasmids. *Saccharomyces cerevisiae* strain YPH499 (Stratagene) was used a host for plasmid assembly by homologous recombination. *Paecilomyces variotii* K5103 was obtained as a gift from Syngenta and is a derivative of *Paecilomyces variotii* SANK 21086.²⁴

5 Growth and Fermentation Conditions

P. variotii K5013 was maintained on PDA at 25 °C. Spores were inoculated into 100ml PDB in 500ml Erlenmeyer flasks and grown at 25 °C with shaking at 200 rpm. For cornexistin and related metabolite production, cultures were grown for 11 days. For transformation, the culture was grown overnight, and subsequently protoplasted.

6 Fungal Nucleic Acid Preparation

P. variotii was cultured in PDB, which was then pelleted, lyophilized and ground under liquid nitrogen. Genomic DNA for both sequencing and PCR analysis was prepared using the GenElute Plant Genomic DNA Miniprep kit (Sigma). RNA was prepared using the RNeasy Plant Mini Kit (Qiagen) for sequencing.

7 Genome and RNA Sequencing

Paired-end and mate-pair Illumina sequencing runs were performed on gDNA extracted from fungal mycelia of *P. variotii*. The reads from both sequencing runs were assembled using the ABySS-pe² algorithm with a Kmer of 71 and scaffolded using SSPACE.³ GapCloser was used to produce the final assembly. A total of 41 scaffolds were assembled with over 34 million bases and an N50 of 3.3 million. For the RNAseq, paired-end Illumina sequencing was conducted after TruSeq RNAseq library preparation. The sequencing reads were mapped to the genome assembly using Tophat.⁴

8 Cornexistin Biosynthetic Gene Cluster

Softberry FGENESH⁵ was utilized for predictions of the intron and exon positions for coding sequences within the BGC, which were manually adjusted by comparison with the transcriptomics data. Coding sequences were then annotated using BLAST⁶ and InterPro⁷ (Table S1).

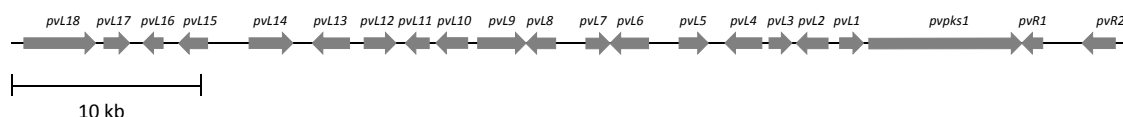


Figure S1: Cornexistin BGC

Table S1: Analysis of the putative cornexistin BGC from *P. variotii*. *Closest characterized homologue in the Swissprot database

Gene	Putative function	Homologue*	Identity (%)	E value	Query coverage	Score
<i>pvpk1</i>	Polyketide synthase	FUB1 ⁸	36%	0	98%	1380
<i>pvL1</i>	Hydrolase	FUB4 ⁸	33%	1e-21	78%	92.8
<i>pvL2</i>	2-methylcitrate dehydratase	yahT ⁹	42%	1e-130	97%	390
<i>pvL3</i>	Ketosteroid isomerase-like	-	-	-	-	-
<i>pvL4</i>	MFS transporter	QDR1 ¹⁰	31%	2e-65	86%	224
<i>pvL5</i>	Dioxygenase	GA3ox2-3 ¹¹	31%	7e-10	42%	63.2
<i>pvL6</i>	Citrate synthase-like	GltA ¹²	33%	1e-80	95%	261
<i>pvL7</i>	Six-bladed beta-propeller protein	-	-	-	-	-
<i>pvL8</i>	C6 transcription factor	gliZ ¹³	51%	5e-07	51%	55.8
<i>pvL9</i>	Serine carboxypeptidase	SCPA ¹⁴	44%	2e-177	98%	520
<i>pvL10</i>	MFS transporter	Qdr2p ¹⁵	32%	7e-76	93%	251
<i>pvL11</i>	Dienelactone hydrolase	CMBL ¹⁶	22%	2e-08	93%	57
<i>pvL12</i>	MFS transporter	FUBT ¹⁷	34%	2e-78	97%	259
<i>pvL13</i>	Cytochrome P450	PbP450-2 ¹⁸	33%	4e-72	89%	241
<i>pvL14</i>	Transketolase	TK ¹⁹	25%	9e-21	78%	100
<i>pvL15</i>	Aldo/keto reductase	CPR ²⁰	36%	5e-54	89%	181
<i>pvL16</i>	Hypothetical protein	-	-	-	-	-
<i>pvL17</i>	Fumarylacetoacetate hydrolase	-	-	-	-	-
<i>pvL18</i>	NRPS-like enzyme	FUB8 ⁸	32%	1e-153	96%	486
<i>pvR1</i>	Phosphatidylethanolamine-binding protein (PEBP)	CEN ²¹	27%	0.56	71%	33.9
<i>pvR2</i>	Phosphotransferase	-	-	-	-	-

9 Biosynthetic Gene Cluster Comparisons

BGCs were compared using Artemis Comparison Tool (ACT)²²

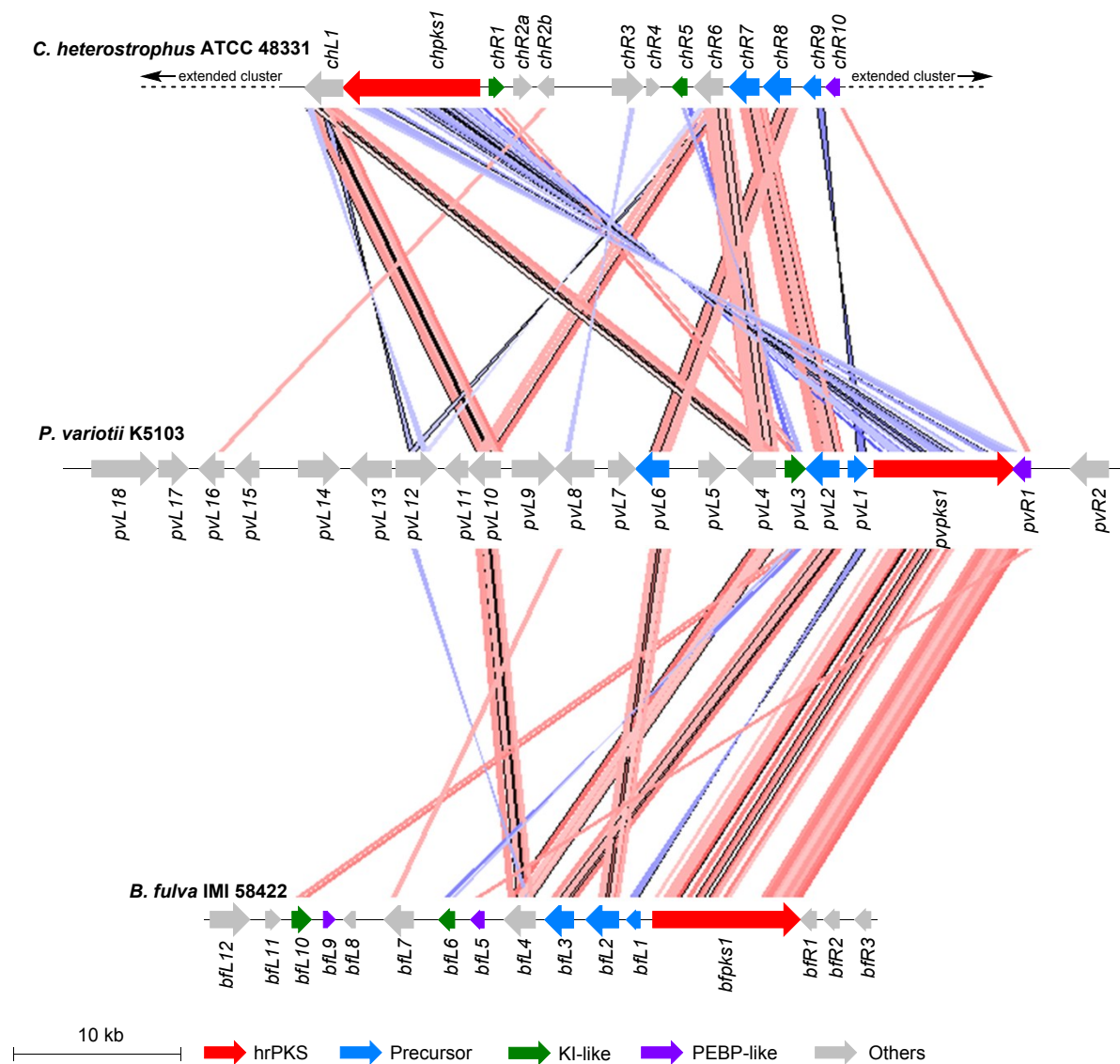


Figure S2: Comparison of the cornexistin 1 cluster (middle), to the putative maleidride cluster from *Cochliobolus* (top) and the byssochlamic acid 4 cluster using ACT. Regions of homology are identified by pink and blue lines. Pink lines denote homology on the same strand, and blue strands denote homology on the opposite strand.

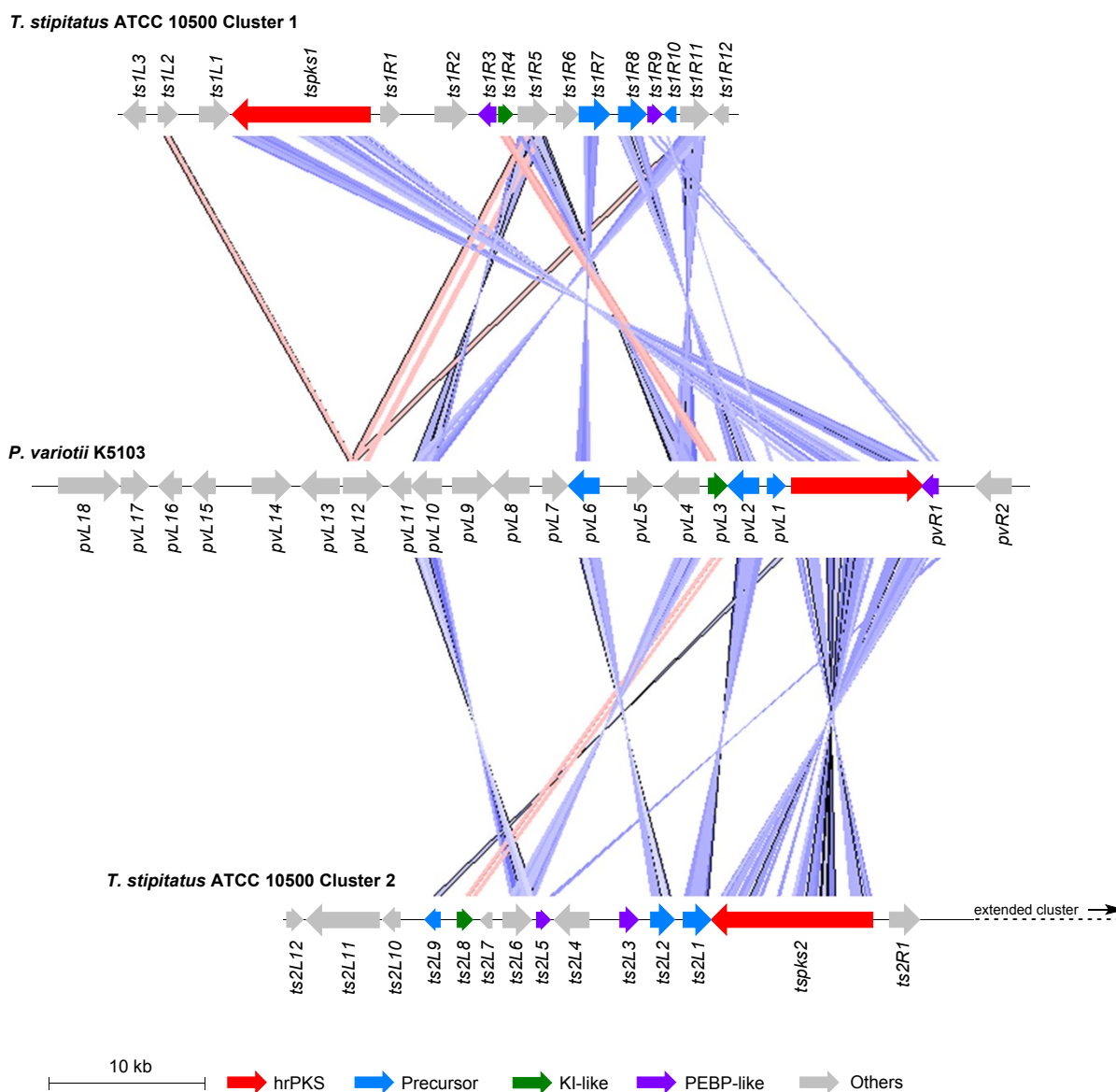


Figure S3: Comparison of the cornexistin 1 cluster (middle), to the two putative maleidride clusters from *Talaromyces* (top and bottom) using ACT. Regions of homology are identified by pink and blue lines. Pink lines denote homology on the same strand, and blue strands denote homology on the opposite strand.

Table S2: Percentage identity matrix calculated using clustal Ω of PKS sequences from the cornexistin 1 cluster, the *C. heterostrophus* cluster, the two *T. stipitatus* clusters and the byssochlamic acid 4 cluster.

PKSs	pvpks1	chpks1	tspks1	tspks2	bfpks1
pvpks1	100	47.77	48.91	50.42	50.29
chpks1	47.77	100	45.65	45.29	50.79
tspks1	48.91	45.65	100	56.51	45.8
tspks2	50.42	45.29	56.51	100	46.93
bfpks1	50.29	50.79	45.8	46.93	100

Table S3: Percentage identity matrix calculated using clustal Ω of hydrolase 341 sequences from the cornexistin 1 cluster, the *C. heterostrophus* cluster, the two *T. stipitatus* clusters and the byssochlamic acid 4 cluster.

Hyd 341	pvL1	chR9	ts1R10	ts2L9	bfl1
pvL1	100	49.54	42.79	53.18	58.64
chR9	49.54	100	40.64	51.6	54.34
ts1R10	42.79	40.64	100	45.7	44.34
ts2L9	53.18	51.6	45.7	100	53.85
bfl1	58.64	54.34	44.34	53.85	100

Table S4: Percentage identity matrix calculated using clustal Ω of citrate synthase sequences from the cornexistin 1 cluster, the *C. heterostrophus* cluster, the two *T. stipitatus* clusters and the byssochlamic acid 4 cluster.

CSs	pvL6	chR8	ts1R7	ts2L2	bfl2
pvL6	100	59.86	45.69	65.69	58.28
chR8	59.86	100	43.76	58.28	63.95
ts1R7	45.69	43.76	100	44.96	50.35
ts2L2	65.69	58.28	44.96	100	55.33
bfl2	58.28	63.95	50.35	55.33	100

Table S5: Percentage identity matrix calculated using clustal Ω of 2-methyl citrate dehydratase sequences from the cornexistin 1 cluster, the *C. heterostrophus* cluster, the two *T. stipitatus* clusters and the byssochlamic acid 4 cluster.

2MCDs	pvL2	chR7	ts1R8	ts2L1	bfl3
pvL2	100	61.94	52.59	67.23	63.66
chR7	61.94	100	50.21	58.81	61.07
ts1R8	52.59	50.21	100	54.12	52.26
ts2L1	67.23	58.81	54.12	100	63.52
bfl3	63.66	61.07	52.26	63.52	100

Table S6: Percentage identity matrix calculated using clustal Ω of ketosteroid isomerase-like sequences from the cornexistin 1 cluster, the *C. heterostrophus* cluster, the two *T. stipitatus* clusters and the byssochlamic acid 4 cluster.

KI-like	pvL3	chR5	chR1	ts1R4	ts2L8	bfl6	bfl10
pvL3	100	44.6	42.49	36.32	51.9	47.3	44
chR5	44.6	100	49.06	37.62	44.55	48.13	60.29
chR1	42.49	49.06	100	34.56	41.52	51.28	46.08
ts1R4	36.32	37.62	34.56	100	35.21	39.37	40.58
ts2L8	51.9	44.55	41.52	35.21	100	39.66	43.06
bfl6	47.3	48.13	51.28	39.37	39.66	100	49.33
bfl10	44	60.29	46.08	40.58	43.06	49.33	100

Table S7: Percentage identity matrix calculated using clustal Ω of PEBP-like sequences from the cornexistin 1 cluster, the *C. heterostrophus* cluster, the two *T. stipitatus* clusters and the byssochlamic acid 4 cluster.

PEBP-like	pvR1	chR10	ts1R3	ts1R9	ts2L3	ts2L5	bfl5	bfl9
pvR1	100	33.99	15.03	33.7	20.11	43.06	38.46	23.72
chR10	33.99	100	17.88	35.2	21.26	38.12	43.48	22.58
ts1R3	15.03	17.88	100	18.59	15.07	14.94	17.88	38.05
ts1R9	33.7	35.2	18.59	100	21.76	36.56	35.2	23.12
ts2L3	20.11	21.26	15.07	21.76	100	22.22	22.41	18.79
ts2L5	43.06	38.12	14.94	36.56	22.22	100	42.11	18.47
bfl5	38.46	43.48	17.88	35.2	22.41	42.11	100	22.73
bfl9	23.72	22.58	38.05	23.12	18.79	18.47	22.73	100

10 Gene Disruption Procedures

The genes investigated within the cornexistin cluster were knocked-out using the bipartite method.²³ This method relies on the splitting of the resistance marker (with a ~500bp overlap), which leads to the requirement for homologous recombination between the two resistance marker halves for selection to occur. This activation of the homologous recombination pathway appears to lead to higher gene disruption levels. Gene disruption in *P. variotii* using this method varied between 20-100% of transformants tested.

Two different resistance markers were utilised in the transformation of *P. variotii* K5013, the HygR gene (for hygromycin resistance) (CAA83647) and the nptII gene (for geneticin resistance) (AAL78958). In each case the resistance cassette consisted of the gpdA promoter and in some cases the trpC terminator. In some constructs no terminator was present as it does not appear to be necessary for the efficacy of the resistance marker. The gene knock-out fragments, which consisted of a region homologous (~1-2kb) to the *P. variotii* genome and one half of the resistance cassette, were amplified by several rounds of PCR. Initially, gDNA was isolated from *P. variotii* lyophilised mycelium using the GenElute Plant Genomic DNA Miniprep kit (Sigma). The left hand side homologous region was amplified using a reverse primer that contained a tail homologous to the beginning of the gpdA promoter, and the right hand side homologous region was amplified using a forward primer that contained a tail either homologous to the trpC terminator or to the end of the resistance gene. All primers used are shown in Table S8. The split fragments of the resistance cassette were amplified separately, and subsequently approximately equal amounts of the left hand side homologous region and the left hand side of the resistance cassette (and *vice versa*) were mixed and used as a template in a fusion PCR amplification. In cases where fusion PCR proved difficult, homologous recombination in the yeast, *Saccharomyces cerevisiae* was used to assemble the knock-out fragments. Approximately equal amounts of the fused PCR products were used in a transformation of *P. variotii*.

Table S8: Names and sequences of primers used

Primer Name	Sequence (5' to 3')	Notes
HygRP5-F	CATGATGGGGATCCTCTAGTG	Hygromycin resistance cassette split amplification primers (P7.1 was utilised only for the PVpks1 KO, P7.2 was used for
HygRP6.2-R	CGTCAGGACATTGTTGGAG	
HygRP7.1-F	CTGTGCGAGAAGTTTCTGATCG	

HygRP7.2-F	GCTTTCAGCTTCGATGTAGG	all other hygromycin KOs) (the two P8 primers represent the inclusion or not of the terminator)
HygRP8-R	CAGGTCGAGTGGAGATGTG	
HygRP8.2-R	CTATTCCTTTGCCCTCGGA	
nptII-P6-R	CCATGATATTCGGAAGCAG	Geneticin resistance cassette split amplification primers (the forward primer for the left hand side was HygRP5-F)
nptII-P7-F	AGAGGCTATTCGGCTATGAC	
nptII-P8-R	TCAGAAGAACTCGTCAAGAAGG	
PVs6c30-PKS-P1-F	ATACTCCTCCAACCAACTGC	Primers for the knock-out of the PKS involved in production of xanthone related compounds
PVs6c30-PKS-P2-R	CACTAGAGGATCCCCATCATGGGCGACGACA ATTATACGAC	
PVs6c30-PKS-P3.1-F	CCTTCTTGACGAGTTCTTCTGAGCATCGTTAG CAATGATCCG	
PVs6c30-PKS-P4-R	CTTTCGGGAACCTCACAACC	
PVs1c4-KI-P1-F	CGTGATGGTTAGGTTGACC	Ketosteroid isomerase-like knock-out primers
PVs1c4-KI-P2-R	CACTAGAGGATCCCCATCATGCTAGCGACTTG AAGTTGTCC	
PVs1c4-KI-P3-F	TCCGAGGGCAAAGGAATAGAGGAGCATCCC AACTACATC	
PVs1c4-KI-P4-R	ATACGGCAGTTGGGTGATG	
PVs1c4-PEBP-P1-F	GACGCGTCATATGTGCTAGTC	PEBP knock-out primers
PVs1c4-PEBP-P2-R	CACTAGAGGATCCCCATCATGAGCCCACGAC ATATCGCTTC	
PVs1c4-PEBP-P3.1-F	TCCGAGGGCAAAGGAATAGGGTAGGACTGG AACACACTG	
PVs1c4-PEBP-P4-R	GATTGATCGACTGCTCAAGC	
PVs1c4-OXR341-P1-F	ACGACCAGACACTGTCATCC	Hydrolase 341 knock-out primers
PVs1c4-OXR341-P2-R	CACTAGAGGATCCCCATCATGTGTCTACCGAG TTGGGACTG	
PVs1c4-OXR341-P3.1-F	TCCGAGGGCAAAGGAATAGAGTTGTGCGATG AGAAGTCG	
PVs1c4-OXR341-P4-R	CACAAGCATGTCCGGTGTAGTC	
PVs1c4-CS-P1-F	TCAGATGTACTCGAGTAGTGG	Citrate synthase knock-out primers
PVs1c4-CS-P2-R	CACTAGAGGATCCCCATCATGAACTGCATGC GAACGC	
PVs1c4-CS-P3-F	TCCGAGGGCAAAGGAATAGAGGTGATCGTG ATGGACG	
PVs1c4-CS-P4-R	ATGAACACGGAGGCTTCCAC	
PVs1c4-DLH-P1-F	CTACATCACCAGCTTCCAGTG	Dienelactone hydrolase knock-out primers
PVs1c4-DLH-P2-R	CACTAGAGGATCCCCATCATGAACCGATGAA GGAACCTGTC	
PVs1c4-DLH-P3.2-F	TCCGAGGGCAAAGGAATAGGACCAGTGATGT CTACATCC	
PVs1c4-DLH-P4-R	TCTATTGTTCTCCGCTGAC	
PVs1c4-P450-P1-F	CGCCAATACCTGTGCTCTAG	P450 knock-out primers
PVs1c4-P450-P2-R	CACTAGAGGATCCCCATCATGGTGCAGAAAGAG TTGGAGAAG	
PVs1c4-P450-P3-F	CACATCTCCACTCGACCTGCCTTACTGAGGAT GGTGTAGC	
PVs1c4-P450-P4-R	GGGTTATCAGTCTCGGTATGC	

PVs1c4-OXR-P1-F	GTTCCCAGGTTTCTCTGCAA	Dioxygenase knock-out primers
PVs1c4-OXR-P2-R	CACTAGAGGATCCCCATCATGGACTCAGCTTG TATGCCTTC	
PVs1c4-OXR-P3-F	CCACATCTCCACTCGACCTGATCCGTTTCCTGC ATAATCC	
PVs1c4-OXR-P4-R	CCTCAAGATAGATGCAAGCC	
PVs1c4-PKS-P1-F	GATCCGACGACAAGAGTATG	PKS knock-out primers
PVs1c4-PKS-P2-R	CACTAGAGGATCCCCATCATGCTTGACCCGTG AAGATGAAG	
PVs1c4-PKS-P3-F	CACATCTCCACTCGACCTGCAACCACGAGATT GTCTCGTC	
PVs1c4-PKS-P4-R	GCTGGGAGTCGATATTGTC	
PVs1c4-TK-P1-F	tagatcggtctctgtgctac	Transketolase knock-out primers
PVs1c4-TK-P2-R	CGAAAGATCCACTAGAGGATCCCCATCATGTT GAACTGCTTGAGGTCGAC	
PVs1c4-TK-P3-F	CCCAGCACTCGTCCGAGGGCAAAGGAATAGG TCATCGATTCTGACCTTGC	
PVs1c4-TK-P4-R	TGCCCTCCAATCATCTAAGG	
PVs1c4-GL-P1-F	gtctccgacagtaaccatc	Six-bladed beta-propeller protein knock-out primers
PVs1c4-GL-P2-R	CGAAAGATCCACTAGAGGATCCCCATCATGC GAATTGGAGGTGCTGTTGG	
PVs1c4-GL-P3-F	CCCAGCACTCGTCCGAGGGCAAAGGAATAGA CTATGGCCTCTCGTCGTCC	
PVs1c4-GL-P4-R	agcaggggatgggtactgtg	
PVs1c4-SC-P1-F	GCTGATAACAGGACTCGTG	Serine carboxypeptidase knock-out primers
PVs1c4-SC-P2-R	CGAAAGATCCACTAGAGGATCCCCATCATGA TCCCATACGTCAGCTGTC	
PVs1c4-SC-P3-F	CCCAGCACTCGTCCGAGGGCAAAGGAATAGC TATCTCAACCAACGCTGG	
PVs1c4-SC-P4-R	ACCTTGAATATGAGGCATGAC	
TrpC-Nd-F	GCTCCGTAACACCCAATACG	Primers used to test integration of KO constructs
pgpdA-Bg-R	GCTCGACGTATTTCAAGTGTC	
HygR-Nd-F	CTATCAGAGCTTGGTTGACG	
HygR-Bg-F	GCTTTCAGCTTCGATGTAGG	
s1c4-F1	CTTCTCCCATCTGTGAATGG	
s1c4-R1	TGCCGTCATCTGATGTGAAC	
s6c30-F1	CTGTGGAGACTCCTTGTGTC	
S6c30-R1	CTTCAACACGGGATCTTGAG	
s1c4-F2	CAGGCCATTCCCACCAAC	
S1c4-R2	CGAGCACCAAGTACACGATG	
s1c4-F3	AGTACCGAACGTTCTGGATC	
s1c4-R3	CGTATCTGGTAACGTAGGACC	
s1c4-F4	GTCAGTTGCTCATCTGGTTG	

s1c4-R4	GTTGGTGCATTGGTACATG
s1c4-F5	ACAATCGTCCAGGTCTGTTG
s1c4-R5	ACAACCCAGTCTGTATCACG
s1c4-F7	ATCAGGAACTGTCTCGAGAGC
s1c4-R7	ATTCTATGCCACCTCGTTCG
s1c4-F9	GCAGTCCAGACACAACAAAC
s1c4-R9	GCAGTGGATGACAATTGACC
s1c4-F10	GCTCTCTACAACATGGTAAG
s1c4-R10	GGTCAAGTAGGTATGATTGC
s1c4-F11	CAGTAGTCCAAGGAGCCAC
s1c4-R11	GGTAAAGACTGGATTGGAAG
s1c4-F12	AACAGCACCTCCAATTCGAC
s1c4-R12	ATCACATCACGAGAACTCCC

11 Transformation of *P. variotii* K5013

Transformation was performed using the PEG mediated protoplast method. *P. variotii* was grown on PDA plates for 1-2 weeks. Spores from a single plate were inoculated into 100ml PDB and cultured overnight at 25°C with shaking at 200rpm. Germinated spores were pelleted and washed with sterile H₂O and then 0.7 M KCl. The pellet was then resuspended in 10ml filter sterilised protoplasting solution (0.7M KCl, 5mg/ml driselase, 5mg/ml Trichoderma lysing enzyme), and mixed gently at 25°C for 90 minutes. Protoplasts were separated from the mycelium through sterile miracloth and centrifuged at 1000 x g for 3 minutes. The pellet was washed with solution 1 (0.7M KCl, 50mM CaCl₂ 10mM Tris-HCl [pH 7.5]), and then resuspended in at least 400µl of solution 1. Aliquots of 200µl were taken for each transformation and added to 50µl of PEG solution (25% (w/v) PEG 3350, 0.7M KCl, 50mM CaCl₂ 10mM Tris-HCl [pH 7.5]) along with ~50ng DNA of each knock-out fragment. The protoplasts were gently mixed and placed on ice for 20 minutes. Subsequently, 500µl of PEG solution was added and incubated at room temperature for 5 minutes. Aliquots of 175µl were spread onto plates containing PDA + 1M sorbitol, and the plates incubated at 25°C overnight. Overlays of ~10ml PDA containing either hygromycin/geneticin/both drugs at a final concentration of 100µg/ml were added the next day. Transformants appeared approximately 3-5 days later, and were subcultured to secondary plates containing the appropriate drug(s). After sporulation had occurred, the spores were streaked to single colonies on tertiary plates, and finally single colonies were transferred to quaternary plates to ensure genetic purity.

12 Genetic Characterisation of Gene Knock-Outs

Transformants from the gene knock-out experiments were inoculated from a single plate into 100ml PDB and cultured at 25°C, with 200rpm shaking. After 2-3 days, 10ml of the culture was removed, centrifuged and lyophilised for gDNA extraction. Integration of the knock-out constructs were tested *via* primers designed outside the homologous regions, and within the resistance cassettes. Transformants that had been determined to be knock-outs were then subjected to metabolite extraction using the remaining 90ml of culture.

12.1 PCR Analysis of PV Δ pks1 Strains

Primers TrpC-Nd-F and s1c4-R1 were used to test for 3' integration of the PVpks1 knock-out construct which should amplify a product of 2535 bp. Two putative transformants were analysed as shown in Figure S4. An amplicon of the correct size was apparent for T2.

Primers s1c4-F1 and PgpdA-Bg-R were used to test for 5' integration of the PVpks1 knock-out construct which should amplify a product of 2172 bp. Two putative transformants were analysed as shown in Figure S5. No amplicons of the correct size were apparent for either transformant.

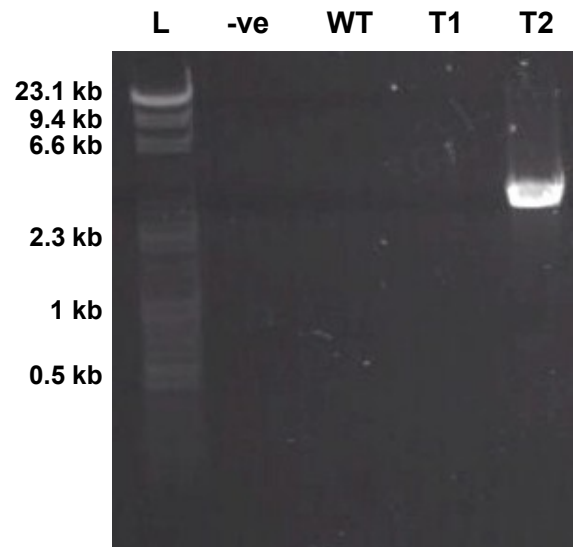


Figure S4: Gel electrophoresis of PCR analysis for integration of the 3' end of the PVpks1 knock-out construct. *P. variotii* WT was compared to two transformants, T1 and T2. -ve lane contained H₂O instead of DNA template as a negative control.

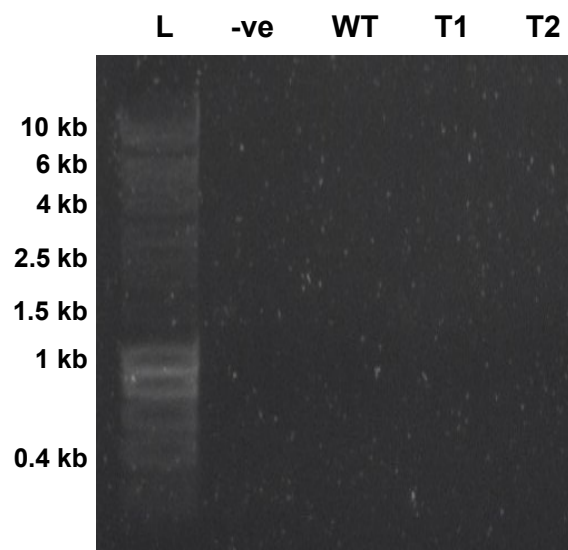


Figure S5: Gel electrophoresis of PCR analysis for integration of the 5' end of the PVpks1 knock-out construct. *P. variotii* WT was compared to two transformants, T1 and T2. -ve lane contained H₂O instead of DNA template as a negative control.

Although PCR analysis did not demonstrate that both the 5' and 3' ends of the knock-out construct had integrated correctly, T2 (PV Δ pks1-T2) was taken forward for metabolite analysis, as only 3' integration should still disrupt the PKS and prevent full gene transcription and translation.

12.2 PCR analysis of PV Agn Δ pks strains

Primers s6c30-F1 and PgpdA-Bg-R were used to test for 5' integration of the Agnpks knock-out construct which should amplify a product of 2057 bp. Seven putative transformants were analysed as shown in Figure S6. Amplicons of the correct size were apparent for four transformants.

Primers nptII-P7-F and s6c30-R1 were used to test for 3' integration of the Agnpks knock-out construct which should amplify a product of 2640 bp. Seven putative transformants were analysed as shown in Figure S7. Amplicons of the correct size were apparent for six transformants.

Transformants T1, T2, T4 and T7 showed correct integration of both sides of the Agnpks knock-out construct, and therefore were analysed for their metabolite profile.

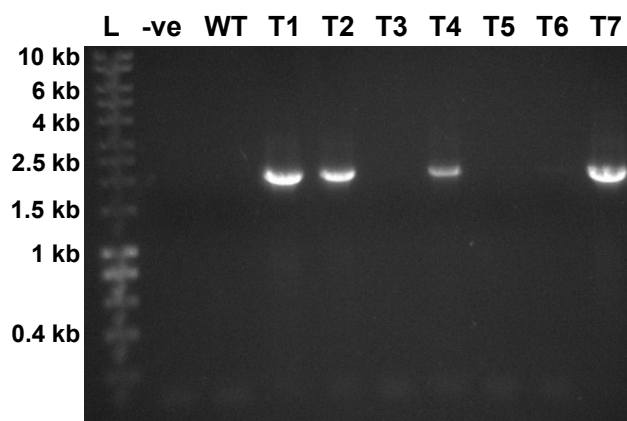


Figure S6: Gel electrophoresis of PCR analysis for integration of the 5' end of the Agnpks knock-out construct. *P. variotii* WT was compared to seven transformants, T1 to T7. -ve lane contained H₂O instead of DNA template as a negative control.

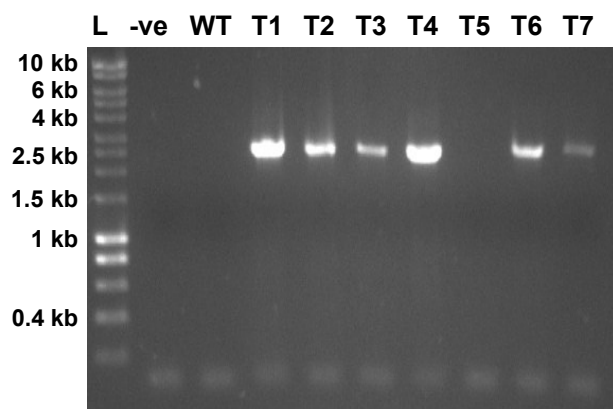


Figure S7: Gel electrophoresis of PCR analysis for integration of the 3' end of the Agnpks knock-out construct. *P. variotii* WT was compared to seven transformants, T1 to T7. -ve lane contained H₂O instead of DNA template as a negative control.

12.3 PCR analysis of AgnΔpks-PVΔL1 strains

Primers s1c4-F4 and PgpdA-Bg-R were used to test for 5' integration of the Hyd341 knock-out construct which should amplify a product of 1923 bp. Six putative transformants were analysed as shown in Figure S8. Amplicons of the correct size were apparent for four transformants.

Primers HygR-Nd-F and s1c4-R4 were used to test for 3' integration of the Hyd341 knock-out construct which should amplify a product of 1787 bp. Six putative transformants were analysed as shown in Figure S9. Amplicons of the correct size were apparent for five transformants.

Transformants T1, T4, T5 and T6 showed correct integration of both sides of the Hyd341 knock-out construct, and therefore were analysed for their metabolite profile.

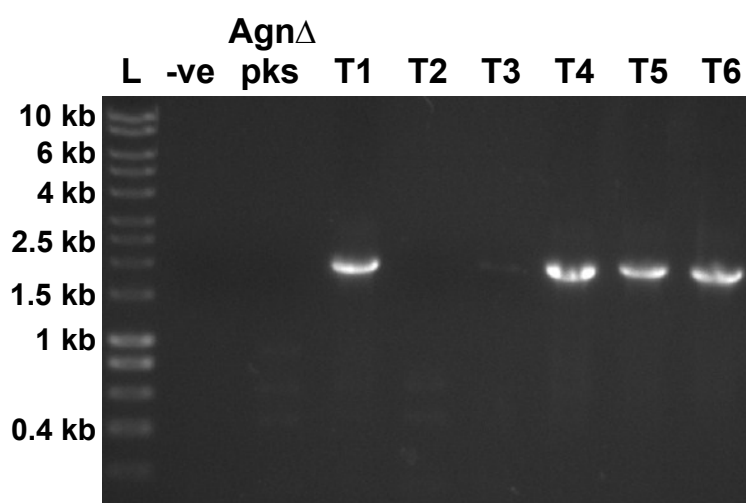


Figure S8: Gel electrophoresis of PCR analysis for integration of the 5' end of the Hyd341 knock-out construct. *P. variotii* AgnΔpks is compared to six transformants, T1 to T6. –ve lane contained H₂O instead of DNA template as a negative control.

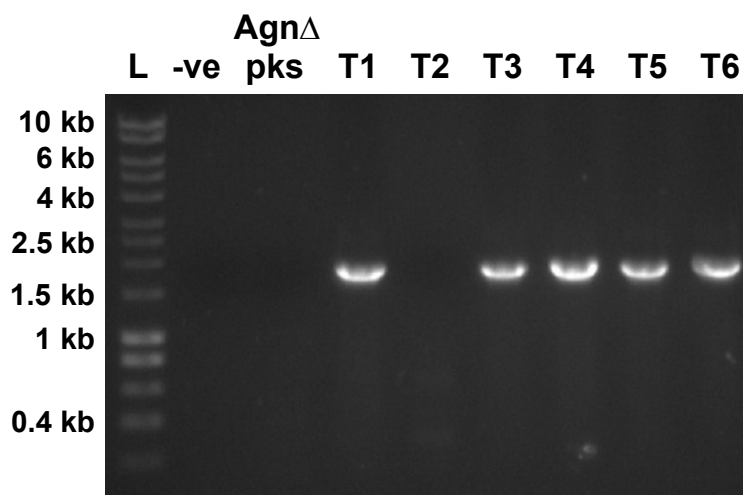


Figure S9: Gel electrophoresis of PCR analysis for integration of the 3' end of the Hyd341 knock-out construct. *P. variotii* AgnΔpks is compared to six transformants, T1 to T6. –ve lane contained H₂O instead of DNA template as a negative control.

12.4 PCR analysis of AgnΔpks-PVΔL6 strains

Primers s1c4-F12 and PgpdA-Bg-R were used to test for 5' integration of the citrate synthase knock-out construct which should amplify a product of 1825 bp. Four putative transformants were analysed as shown in Figure S10. Amplicons of the correct size were apparent for two transformants.

Primers HygR-Bg-F and s1c4-R12 were used to test for 3' integration of the citrate synthase knock-out construct which should amplify a product of 2411 bp. Four putative transformants were analysed as shown in Figure S11. Amplicons of the correct size were apparent for two transformants.

Transformants T1 and T3 showed correct integration of both sides of the citrate synthase knock-out construct, and therefore were analysed for their metabolite profile.

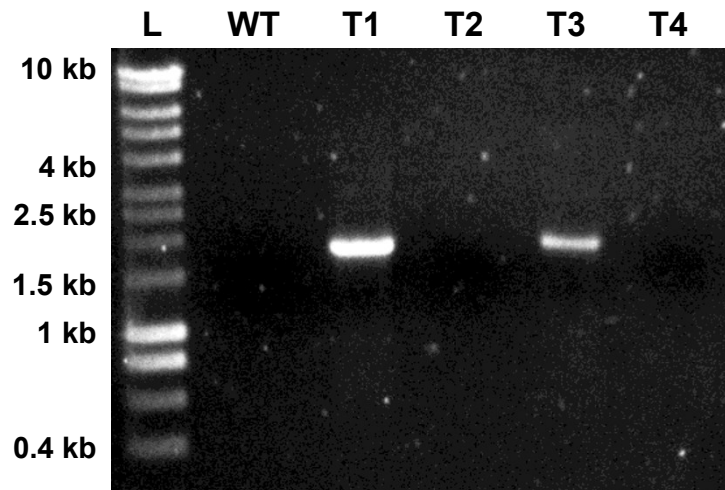


Figure S10: Gel electrophoresis of PCR analysis for integration of the 5' end of the citrate synthase knock-out construct. *P. variotii* WT was compared to four transformants, T1 to T4.

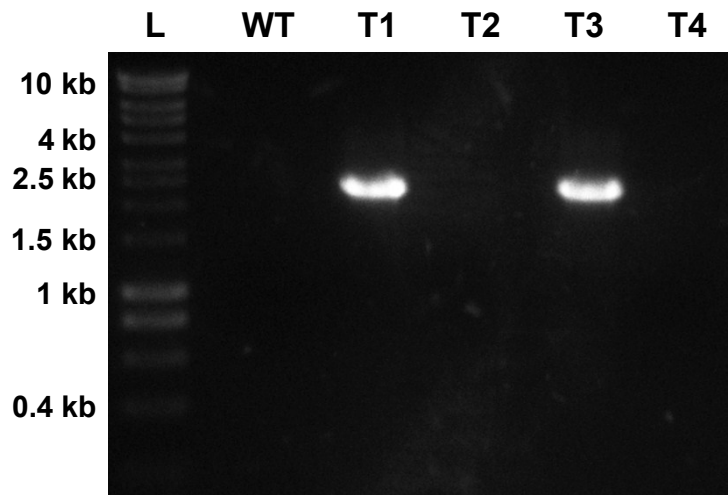


Figure S11: Gel electrophoresis of PCR analysis for integration of the 3' end of the citrate synthase knock-out construct. *P. variotii* WT was compared to four transformants, T1 to T4.

12.5 PCR analysis of AgnΔpks-PVΔR1 strains

Primers s1c4-F5 and PgpdA-Bg-R were used to test for 5' integration of the PEBP knock-out construct which should amplify a product of 1953 bp. Six putative transformants were analysed as shown in Figure S12. Amplicons of the correct size were apparent for five transformants.

Primers HygR-Nd-F and s1c4-R5 were used to test for 3' integration of the PEBP knock-out construct which should amplify a product of 2304 bp. Six putative transformants were analysed as shown in Figure S13. Amplicons of the correct size were apparent for five transformants.

Transformants T1, T2, T3, T5 and T6 showed correct integration of both sides of the PEPB knock-out construct, and therefore were analysed for their metabolite profile.

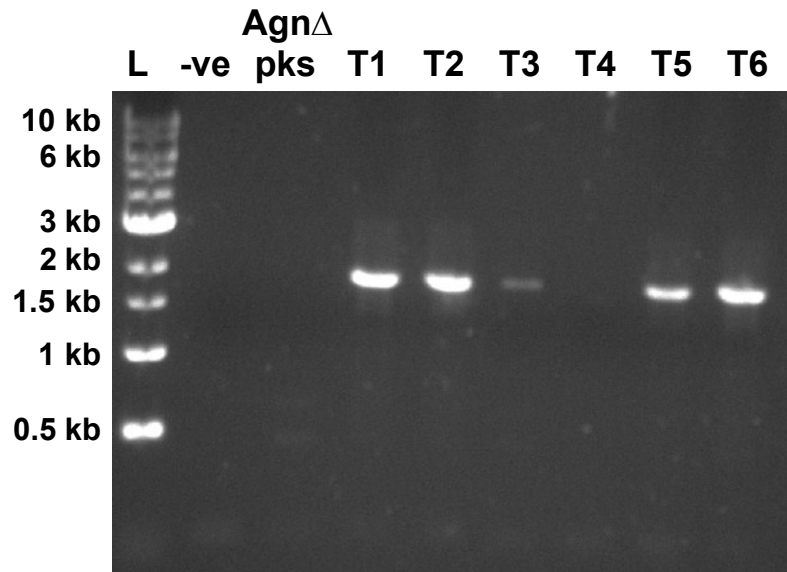


Figure S12: Gel electrophoresis of PCR analysis for integration of the 5' end of the PEBP knock-out construct. *P. variotii* AgnΔpks is compared to six transformants, T1 to T6—ve lane contained H₂O instead of DNA template as a negative control.

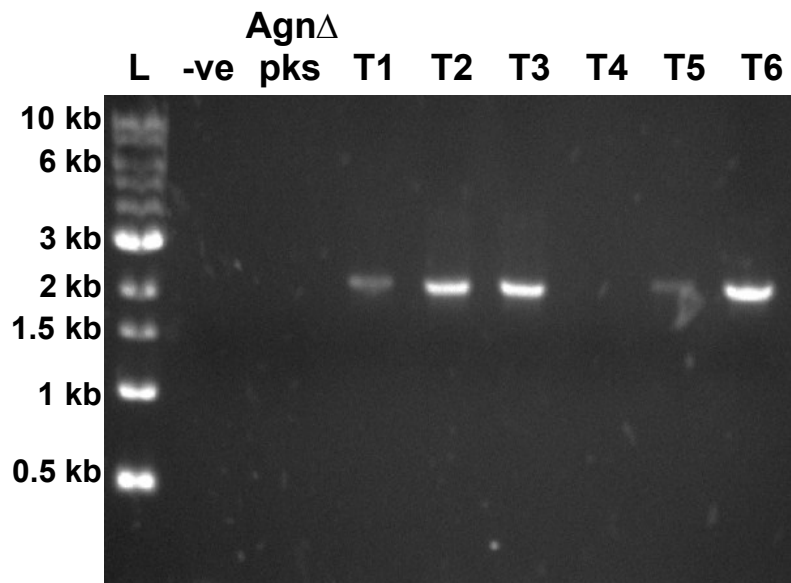


Figure S13: Gel electrophoresis of PCR analysis for integration of the 3' end of the PEBP knock-out construct. *P. variotii* AgnΔpks is compared to six transformants, T1 to T6. —ve lane contained H₂O instead of DNA template as a negative control.

12.6 PCR analysis of AgnΔpks-PVΔL3 strains

Primers s1c4-F7 and pgpdA-Bg-R were used to test for 5' integration of the KI knock-out construct which should amplify a product of 1059 bp. Five putative transformants were analysed as shown in Figure S14. Amplicons of the correct size were apparent for two transformants.

Primers HygR-Nd-F and s1c4-R7 were used to test for 3' integration of the KI knock-out construct which should amplify a product of 1723 bp. Five putative transformants were analysed as shown in Figure S15. Amplicons of the correct size were apparent for two transformants.

Transformants T1 and T5 showed correct integration of both sides of the KI knock-out construct, and therefore were analysed for their metabolite profile.

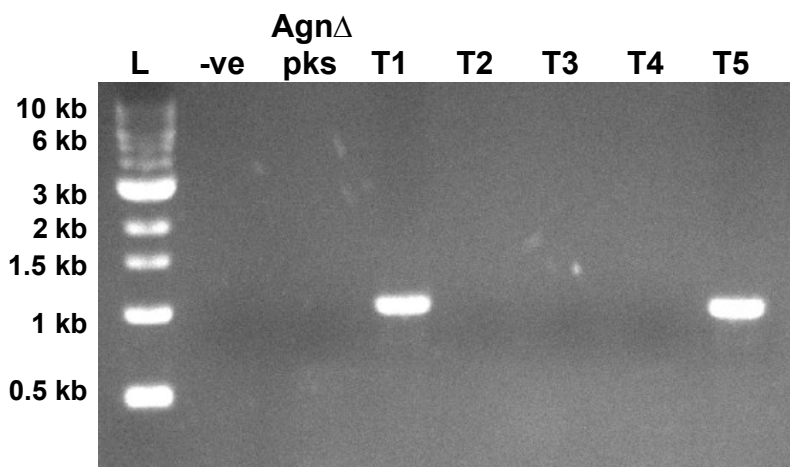


Figure S14: Gel electrophoresis of PCR analysis for integration of the 5' end of the KI knock-out construct. *P. variotii* AgnΔpks is compared to five transformants, T1 to T5. -ve lane contained H₂O instead of DNA template as a negative control.

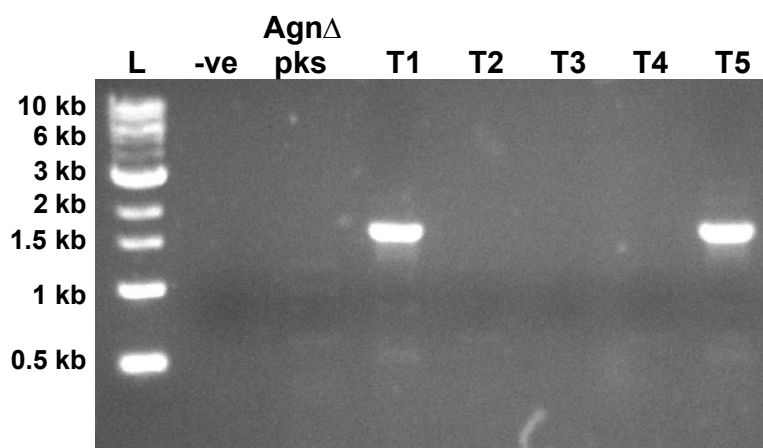


Figure S15: Gel electrophoresis of PCR analysis for integration of the 3' end of the KI knock-out construct. *P. variotii* AgnΔpks is compared to five transformants, T1 to T5. -ve lane contained H₂O instead of DNA template as a negative control.

12.7 PCR analysis of AgnΔpks-PVΔL11 strains

Primers s1c4-F3 and PgpdA-Bg-R were used to test for 5' integration of the DLH knock-out construct which should amplify a product of 2099 bp. Six putative transformants were analysed as shown in Figure S16. Amplicons of the correct size were apparent for three transformants.

Primers HygR-Nd-F and s1c4-R3 were used to test for 3' integration of the DLH knock-out construct which should amplify a product of 2029 bp. Six putative transformants were analysed as shown in Figure S17. Amplicons of the correct size were apparent for three transformants.

Transformants T1, T3 and T4 showed correct integration of both sides of the DLH knock-out construct, and therefore were analysed for their metabolite profile.

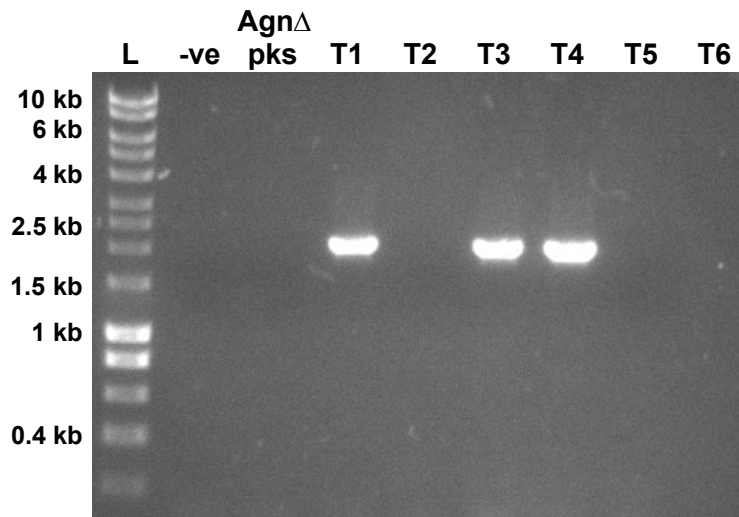


Figure S16: Gel electrophoresis of PCR analysis for integration of the 5' end of the DLH knock-out construct. *P. variotii* AgnΔpks is compared to six transformants, T1 to T6. –ve lane contained H₂O instead of DNA template as a negative control.

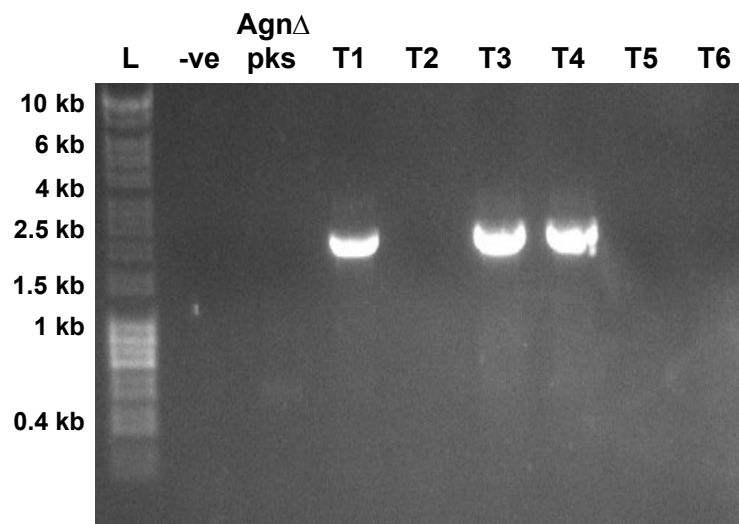


Figure S17: Gel electrophoresis of PCR analysis for integration of the 3' end of the DLH knock-out construct. *P. variotii* AgnΔpks is compared to six transformants, T1 to T6. –ve lane contained H₂O instead of DNA template as a negative control.

12.8 PCR analysis of AgnΔpks-PVΔL7 strains

Primers s1c4-F9 and Pgpda-Bg-R were used to test for 5' integration of the 6-bladed beta propeller knock-out construct which should amplify a product of 1467 bp. Five putative transformants were analysed as shown in Figure S18. Amplicons of the correct size were apparent for four transformants.

Primers HygR-Nd-F and s1c4-R9 were used to test for 3' integration of the 6-bladed beta propeller knock-out construct which should amplify a product of 1396 bp. Five putative transformants were analysed as shown in Figure S19. Amplicons of the correct size were apparent for all transformants, however some products were clearer than others.

Transformants T1, T2, T3 and T5 showed correct integration of both sides of the 6-bladed beta propeller knock-out construct, and therefore were analysed for their metabolite profile.

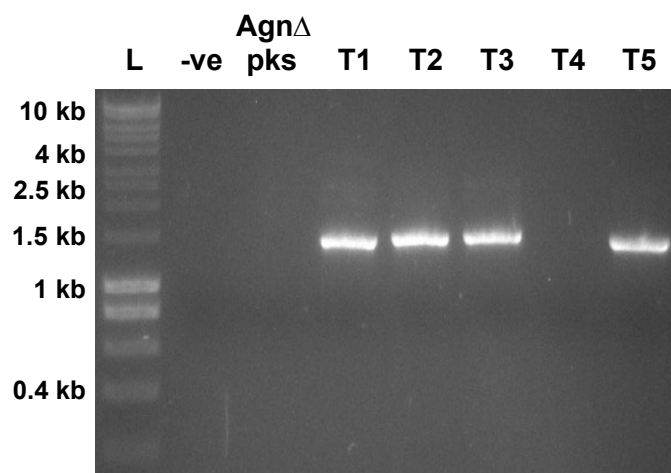


Figure S18: Gel electrophoresis of PCR analysis for integration of the 5' end of the 6-bladed beta propeller knock-out construct. *P. variotii* AgnΔpks is compared to five transformants, T1 to T5. –ve lane contained H₂O instead of DNA template as a negative control.

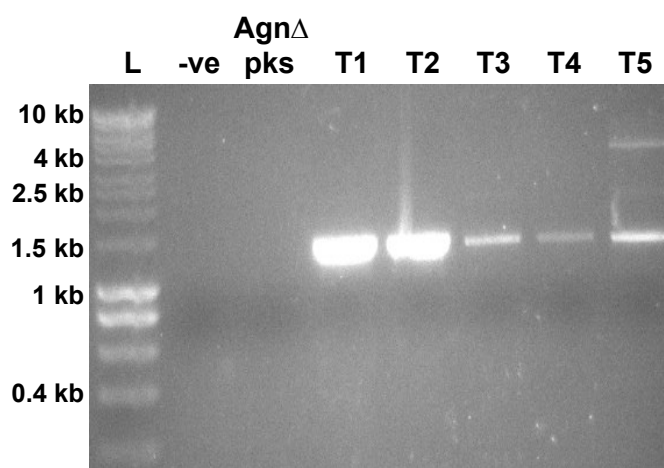


Figure S19: Gel electrophoresis of PCR analysis for integration of the 3' end of the 6-bladed beta propeller knock-out construct. *P. variotii* AgnΔpks is compared to five transformants, T1 to T5. –ve lane contained H₂O instead of DNA template as a negative control. Some non-specific binding is apparent.

12.9 PCR analysis of AgnΔpks-PVΔL9 strains

Primers s1c4-F11 and PgpdA-Bg-R were used to test for 5' integration of the serine carboxypeptidase knock-out construct which should amplify a product of 1282 bp. Five putative transformants were analysed as shown in Figure S20. An amplicon of the correct size was apparent for one transformant.

Primers HygR-Nd-F and s1c4-R11 were used to test for 3' integration of the serine carboxypeptidase knock-out construct which should amplify a product of 1213 bp. Five putative transformants were analysed as shown in Figure S21. No amplicons of the correct size were apparent for any transformants.

Although PCR analysis does not demonstrate that both the 5' and 3' ends of the knock-out construct have integrated correctly, T1 (AgnΔpks-PVΔL9-T1) was taken forward for metabolite analysis, as only 5' integration should still disrupt the serine carboxypeptidase and prevent full gene transcription and translation.

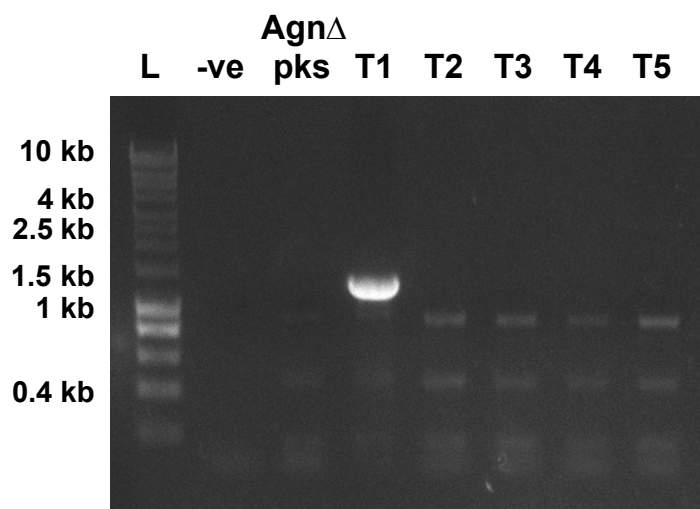


Figure S20: Gel electrophoresis of PCR analysis for integration of the 5' end of the serine carboxypeptidase knock-out construct. *P. variotii* Agn Δ pks is compared to five transformants, T1 to T5. –ve lane contained H₂O instead of DNA template as a negative control. Some non-specific binding is apparent.

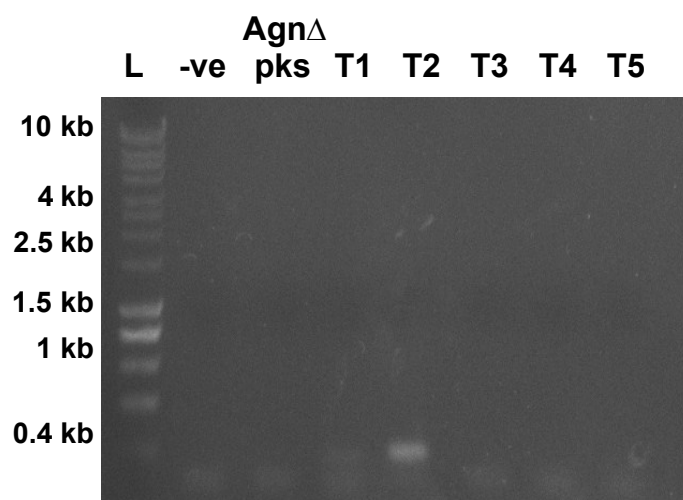


Figure S21: Gel electrophoresis of PCR analysis for integration of the 3' end of the serine carboxypeptidase knock-out construct. *P. variotii* Agn Δ pks is compared to five transformants, T1 to T5. –ve lane contained H₂O instead of DNA template as a negative control.

12.10 PCR analysis of Agn Δ pks-PV Δ L14 strains

Primers s1c4-F10 and PgpdA-Bg-R were used to test for 5' integration of the transketolase knock-out construct which should amplify a product of 1253 bp. Two putative transformants were analysed as shown in Figure S22. Amplicons of the correct size were apparent for both transformants.

Primers HygR-Bg-F and s1c4-R10 were used to test for 3' integration of the transketolase knock-out construct which should amplify a product of 2236 bp. Two putative transformants were analysed as shown in Figure S23. Amplicons of the correct size were apparent for both transformants.

Transformants T1 and T2 showed correct integration of both sides of the transketolase knock-out construct, and therefore were analysed for their metabolite profile.

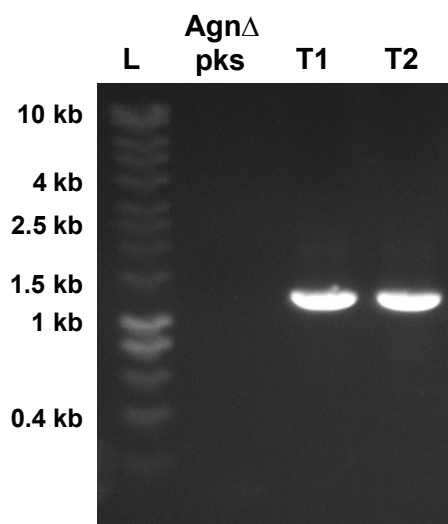


Figure S22: Gel electrophoresis of PCR analysis for integration of the 5' end of the transketolase knock-out construct. *P. variotii* AgnΔpks is compared to two transformants, T1 and T2.

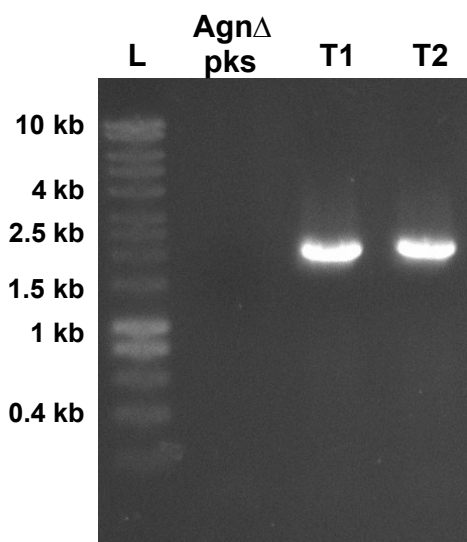


Figure S23: Gel electrophoresis of PCR analysis for integration of the 3' end of the transketolase knock-out construct. *P. variotii* AgnΔpks is compared to two transformants, T1 and T2.

12.11 PCR analysis of PVΔL13 strains

Primers TrpC-Nd-F and s1c4-R2 were used to test for 3' integration of the P450 knock-out construct which should amplify a product of 2266 bp. Seven putative transformants were analysed as shown in Figure S24. Amplicons of the correct size were apparent for four transformants.

Primers s1c4-F2 and PgpdA-Bg-R were used to test for 5' integration of the P450 knock-out construct which should amplify a product of 1954 bp. Four putative transformants were analysed as shown in Figure S25 (those that had amplified products for 3' integration). Amplicons of the correct size were apparent for three transformants.

Transformants T1, T3 and T5 showed correct integration of both sides of the P450 knock-out construct, and therefore were analysed for their metabolite profile.

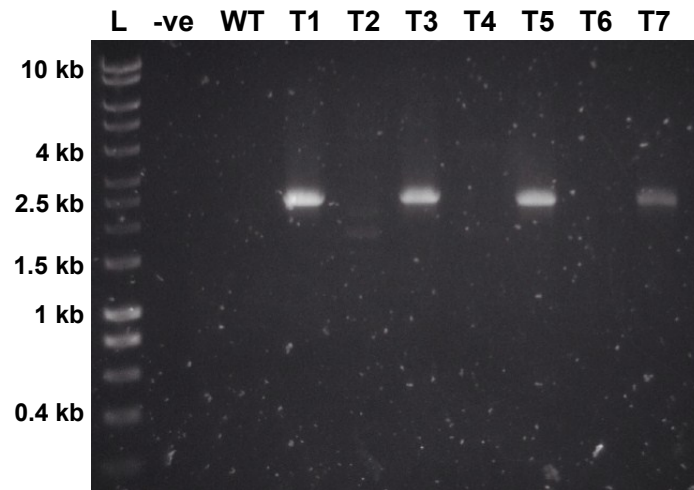


Figure S24: Gel electrophoresis of PCR analysis for integration of the 3' end of the P450 knock-out construct. *P. variotii* WT was compared to seven transformants, T1 to T7. -ve lane contained H₂O instead of DNA template as a negative control.

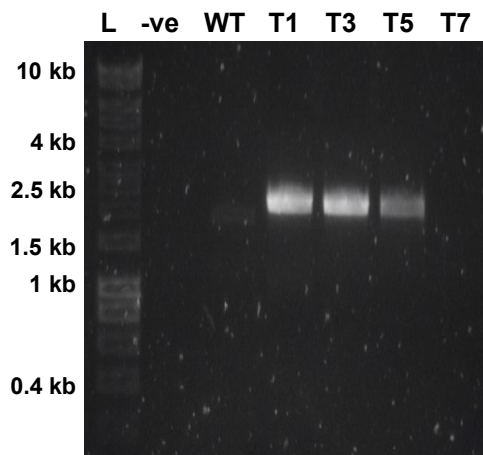


Figure S25: Gel electrophoresis of PCR analysis for integration of the 5' end of the P450 knock-out construct. *P. variotii* WT was compared to four transformants, T1, T3, T5 and T7. -ve lane contained H₂O instead of DNA template as a negative control.

13 Metabolite Extraction and LCMS Analysis of *P. variotii*

Metabolite extraction was performed at 11 days. The culture liquid was separated from the mycelium, and an equal volume of ethyl acetate was added. The mixture was acidified with HCl to pH 4.0 and mixed. The ethyl acetate phase was taken and dried, then resuspended in acetonitrile at 5mg/ml. Nonadrides do not appear to accumulate in the mycelium, although where appropriate, the mycelium was also extracted by blending in acetone, and then re-extracted using ethyl acetate as before. The extracts were analysed using a Waters LCMS system comprising of a Waters 2767 autosampler, Waters 2545 pump system, a Phenomenex Kinetex column (2.6 μ , C18, 100 \AA , 4.6 \times 100 mm) equipped with a Phenomenex Security Guard precolumn (Luna C5 300 \AA) eluted at 1 mL/min. Detection was by Waters 2998 Diode Array detector between 200 and 600 nm; Waters 2424 ELSD and Waters SQD-2 mass detector operating simultaneously in ES+ and ES- modes between 100 m/z and 800 m/z . Solvents were: A, HPLC grade H₂O containing 0.05% formic acid; and B, HPLC grade CH₃CN containing 0.045% formic acid. Most samples were run on a 15%-60% CH₃CN gradient over 30 min, unless otherwise specified.

14 Quantification of Cornexistin Production

A UV-based method for quantifying cornexistin **1** content in fungal extracts was established in the following manner. A calibration curve was created by running a fixed volume of a series of dilutions of cornexistin **1** solution and integrating the corresponding signal for extracted wavelength at 250 nm. Integrated values were then plotted against a known sample concentration (Figure S26) and fitted into a straight line described by **Equation 1** $y = 210099C + 4792$, where y is the dimensionless integration value of the UV peak (UV_{int}) and C is the corresponding concentration of **1** in $\text{mg}\cdot\text{ml}^{-1}$. The relationship was linear within the 0.03 – 4.00 $\text{mg}\cdot\text{ml}^{-1}$ concentration range and the lower limit of detection was 0.02 $\text{mg}\cdot\text{ml}^{-1}$. **Equation 1** in a form of $C = (UV_{int} - 4792.7) / 210099$ was then applied to quantify cornexistin **1**. The method was validated by analysing crude extract from *P. variotii* using LCMS and quantifying the concentration of cornexistin **1** and using the UV-signal (**Equation 1**), and then comparing the calculated value with the actual, weighted amount of cornexistin **1**, which had been HPLC-purified from the same extract.

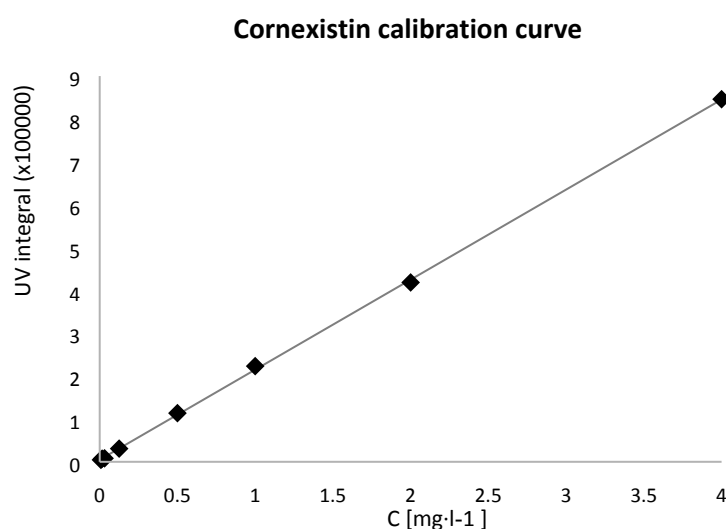


Figure S26: Calibration curve for cornexistin **1** quantification.

15 Comparison of Maleidride Production Between AgnΔpks and AgnΔpks-PVΔ11 Strains

Cornexistin production was not abolished, but was significantly reduced in AgnΔpks-PVΔ11 strains (Figure S27).

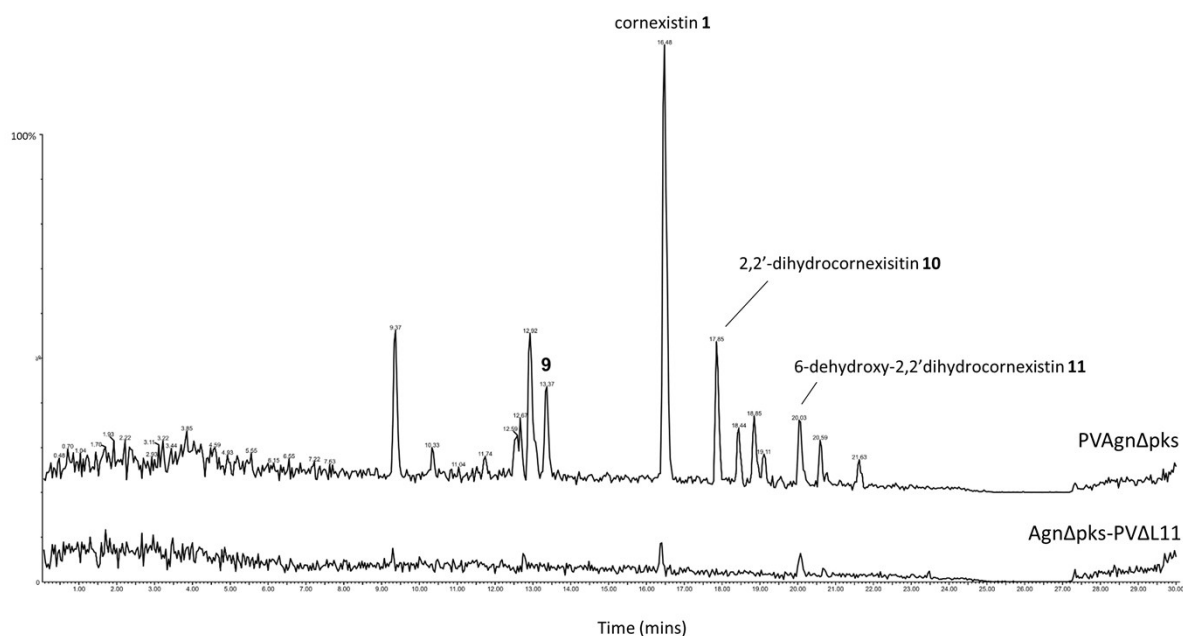


Figure S27: ES- chromatograms comparing AgnΔpks to AgnΔpks PVΔ11

Mean integrated peak area was calculated for both cornexistin and 2,2'-dihydrocornexistin production from two AgnΔpks replicates, and three AgnΔpks-PVΔ11 strains. Titres of both compounds are reduced by ~2.6 fold in the AgnΔpks-PVΔ11 strains (Figure S28).

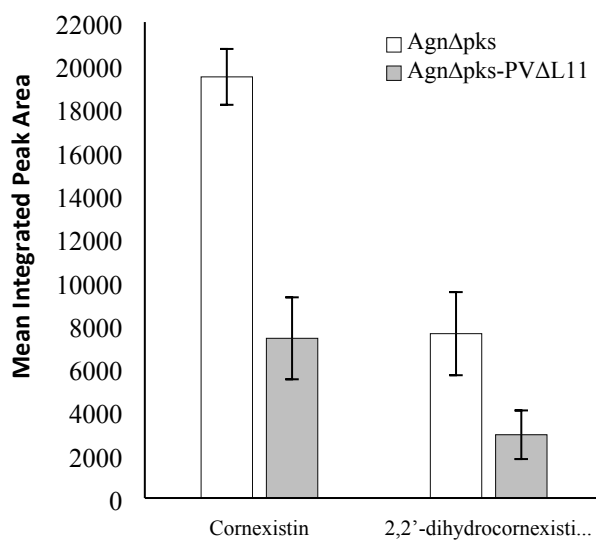


Figure S28: Comparison of maleidride production between AgnΔpks and AgnΔpks-PVΔ11 strains

16 LCMS Analysis of Other AgnΔpks Knock-Out Strains

Other knock-out strains were compared to AgnΔpks using LCMS analysis (Figure S28). No cornexistin **1** or related intermediates were identified in any of the strains.

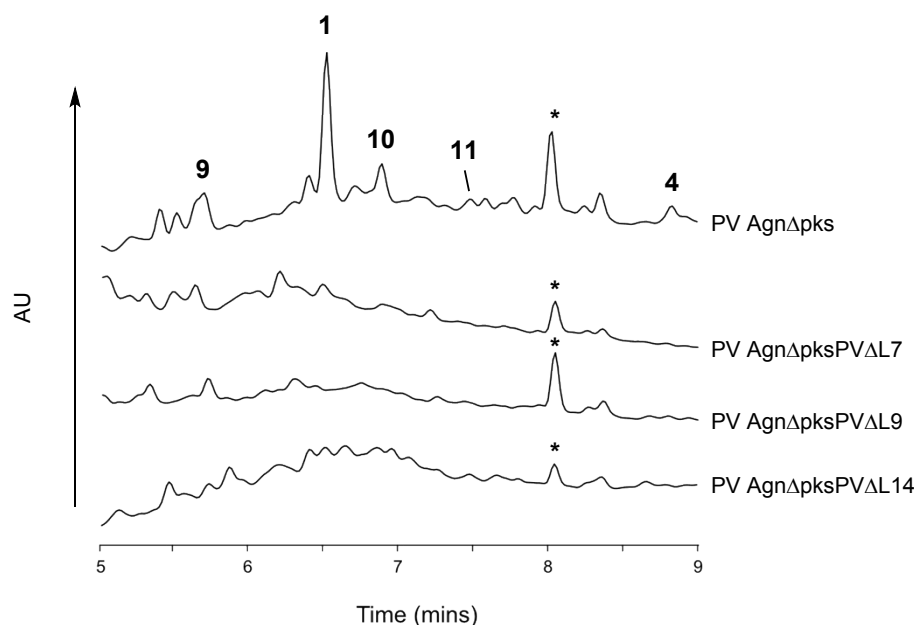


Figure S28A: HPLC analysis (10-90% ACN programme, 15 min) of AgnΔpks compared to AgnΔpks PVΔL7, AgnΔpks PVΔL9 and AgnΔpks PVΔL14. *: unrelated metabolite

17 Structure Elucidation

17.1 Cornexistin **1**

Cornexistin **1** gives a UV spectrum characteristic for nonadrides with λ_{\max} at 210 and 251 nm (Figure S29, a) and it also ionizes well in $^{-}$ ESIMS, showing a molecular ion of m/z 307.6 [M-H] $^{-}$, a possible dimer of m/z 616.0 [2M-H] $^{-}$ and putative fragment peaks of m/z 289.6 [M-H $_2$ O-H] $^{-}$, 263.5 [M-CO $_2$ -H] $^{-}$ and 222.9 [M-2CO $_2$ -H] $^{-}$ (Figure S29, b).

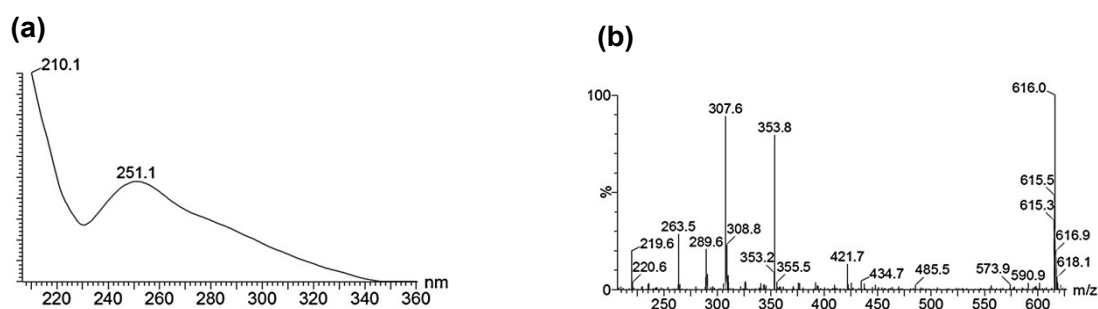


Figure S29: (a) UV and (b) $^{-}$ ESIMS spectra of cornexistin **1**.

NMR spectra for both ^1H and ^{13}C matched the available literature data (Figure S30), and analysis of the 2D data enabled assignment of all peaks for the first time. The doublet of 1'-CH $_3$ was apparent in

the ^1H NMR spectrum (δ_{H} 1.69), as was the $2'\text{-CH}$ appearing at δ_{H} 5.81, characteristic for olefinic protons. The $3'\text{-CH}_3$ was quickly identified as the triplet (δ_{H} 0.92) integrating as three protons and COSY correlations were utilized to identify peaks of the pendant propyl group (4-CH_2 and $5'\text{-CH}_2$) as well as of the 1-CH_2 showing long-range coupling to $2'\text{-CH}$ (Figure S31). The obvious peak identified by its ^{13}C NMR chemical shifts was the C-5 carbonyl (δ_{C} 212.6). Other than the $2'\text{-CH}$, there were three other methine signals apparent from the HSQC spectrum, two of which had chemical shifts characteristic for the oxygen-bound carbons $3/6\text{-CH}$ (δ_{C} 68.5/80.7). The third signal was assigned as the 7-CH (δ_{C} 41.8). Resonances of 3-CH (δ_{C} 68.5) and 6-CH (δ_{C} 80.7) were differentiated based on the observed COSY correlations to $2'\text{-CH}$ and 7-CH respectively (Figure S31). The HMBC spectrum (Figure S32) served to assign the quaternary carbons of the anhydride moiety. The 8-C (δ_{C} 142.4) was identified by correlations from 6-CH and 5-CH_2 , while 9-C (δ_{C} 145.9) from $1'\text{-CH}_3$ and $2'\text{-CH}$. Similarly, the anhydride carbonyls C-10 (δ_{C}) and C-11 were distinguished by correlations from 1-CH_2 and 7-CH respectively. The remaining quaternary carbon 2-C was assigned the chemical shift of δ_{C} 134.0, which was confirmed by the observed HMBC correlations from $2'\text{-CH}$, 4-CH_2 , $1'\text{-CH}_3$, 1-CH_2 and 3-CH_2 .

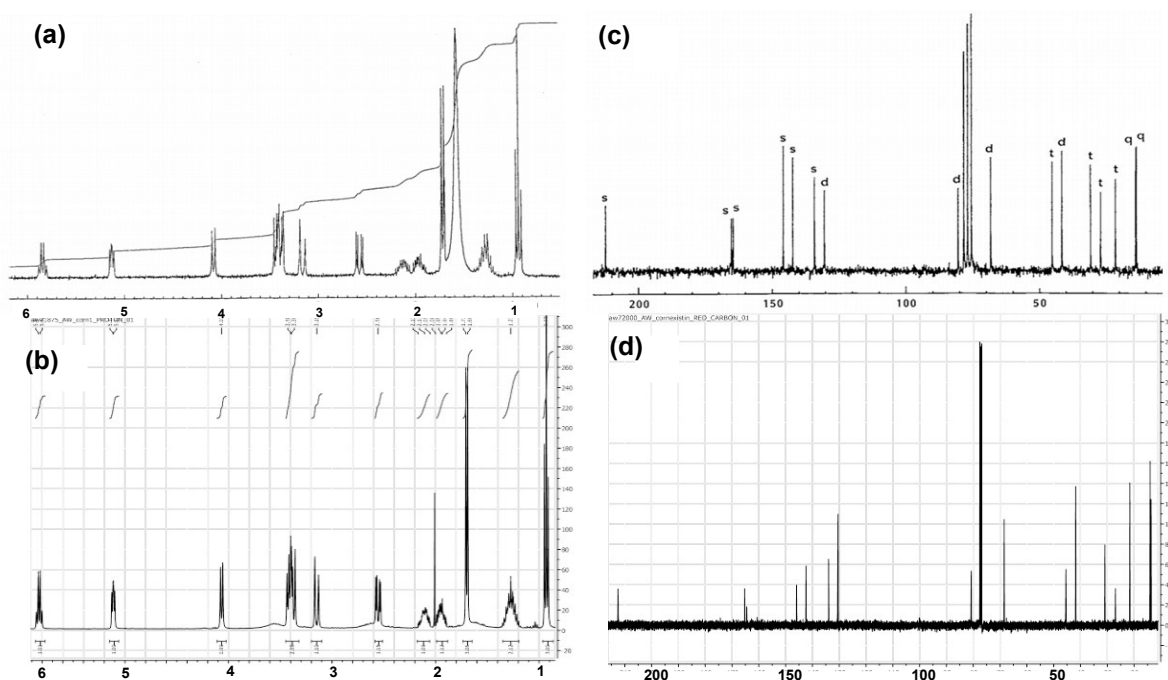


Figure S30: Reference (top) and experimental (bottom) ^1H (a, b) and ^{13}C (c, d) NMR spectra of **1**. Spectra a and c are reproduced from Nakajima *et al.*²⁴

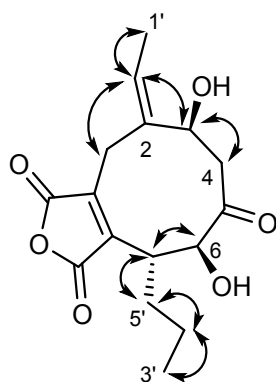


Figure S31: Important COSY correlations of cornexistin 1.

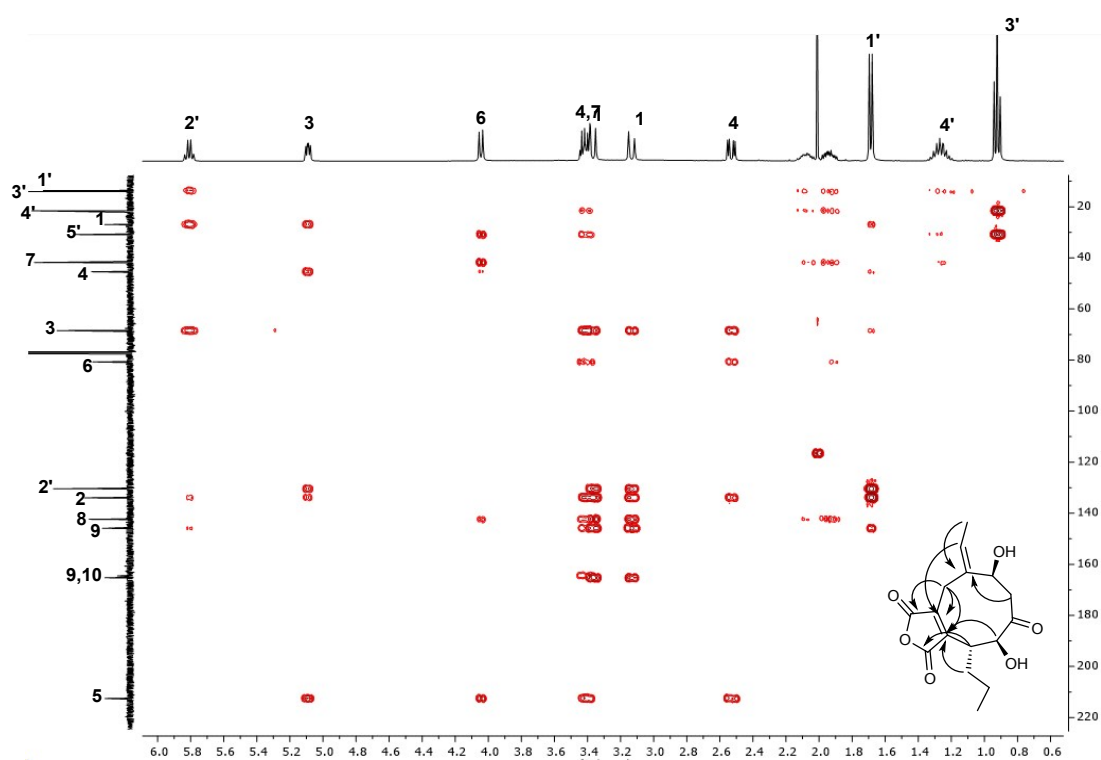


Figure S32: The HMBC spectrum of 1 with key correlations highlighted in the right bottom corner.

17.2 Analysis of the PV AgnΔpks Strain

Three peaks were targeted for purification and structural elucidation from the PV AgnΔpks strain (Figure S33, t_R 14.9, 20.4 and 22.9 min).

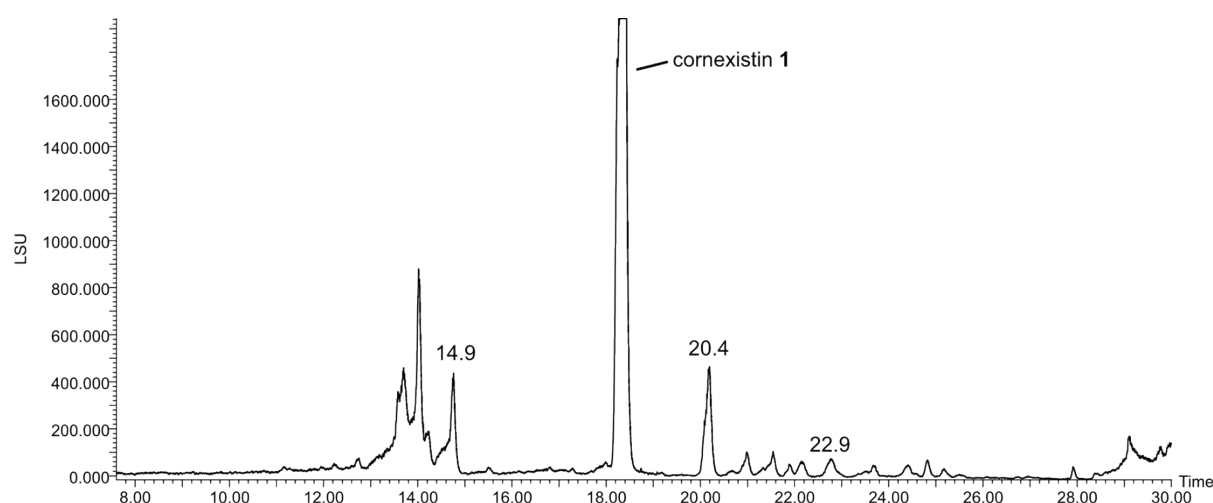


Figure S33: ELSD chromatogram showing the crude extract from 11 day old cultures of *P. variotii* AgnΔpks strain. Cornexistin **1** is highlighted, along with three further peaks targeted for purification at 14.9, 20.4 and 22.9 minutes.

17.2.1 Dihydrocornexistin diastereomers 10A and 10B

The compound eluting at 20.4 min had a UV spectrum with λ_{max} 210 and 257 nm resembling the spectrum of cornexistin **1** (Figure S34, a). It gave a molecular ion of m/z 309.3 [M-H]⁻ and dimer of m/z 619.5 [2M-H]⁻ in the ⁻ESIMS spectrum and putative fragment ions of m/z 265.3 [M-CO₂-H]⁻, 221.3 [M-2CO₂-H]⁻, which indicated a reduced analogue of cornexistin **1** (Figure S34, b).

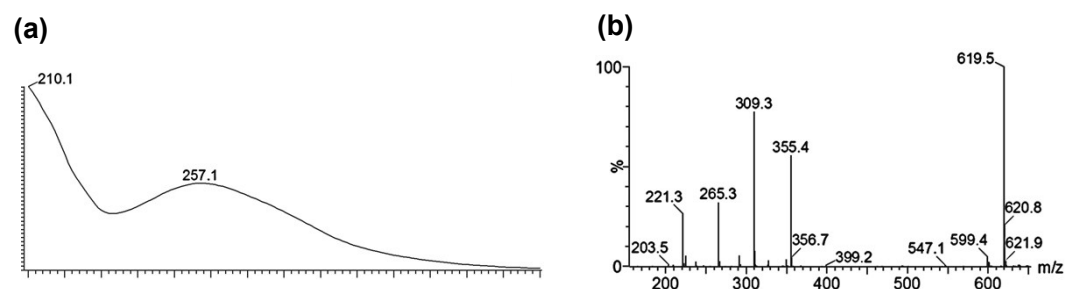


Figure S34: (a) UV and (b) ⁻ESIMS spectra of the 20.4 min peak.

HRMS analysis of the HPLC-purified 20.4 min peak confirmed the formula to be C₁₆H₂₂O₆, confirming the presence of two additional protons in comparison with **1**. NMR analysis showed key differences in comparison with the NMR spectra of cornexistin **1**. In the ¹H NMR spectrum (Figure S35), the two methyl groups (1'-CH₃ and 3'-CH₃) both appeared as triplets (δ_H 0.92 and 1.04), indicating coupling with two neighbouring protons, which was a new feature for 1'-CH₃ and suggested that there was a methylene present at 2'-C position. This was further corroborated by the observed COSY coupling of 1'-CH₃ with 2'-CH₂ of chemical shift (δ_H 1.74) characteristic for an alkene. Analysis of the ¹³C NMR spectrum (Figure S36) showed that, in comparison with the spectrum of cornexistin **1**, both olefinic

resonances of 2-C (δ_c 134.0) and 2'-CH (δ_c 130.4) in **1** disappeared, and new aliphatic peaks (substitutions also confirmed by HSQC data) of 2-CH and 2'-CH₂ appeared at δ_c 45.9 and δ_c 27.5 respectively. This change also affected the chemical shift of 3-CH₂ which moved *ca.* 0.9 ppm upfield with respect to the corresponding peak in cornexistin **1**. The chemical shifts of the four quaternary carbons of anhydride moiety (δ_c 143.4, 148.3, 164.6, 165.3) were practically unchanged (assigned by HMBC correlations, Figure S37) further confirming the 8, 9-bond remained unmodified. All data suggested the saturation of the 2, 2'-ethylidene bond (in comparison with cornexistin **1**) and therefore the compound was named 2, 2'-dihydrocornexistin **10**.

Table S9: Experimental ¹H and ¹³C chemical shifts for **10A** and **10B** obtained by hydrogenation of **1** (see section 22) referenced to internal chloroform at 7.258 ppm at 600 MHz (¹H) and 76.990 ppm at 500 MHz (¹³C).

10A		10B	
Exp. Label	δ _{exp} /ppm	Exp. Label	δ _{exp} /ppm
H01a	2.527	H01a	2.435
H01b	2.267	H01b	2.435
H02	2.002	H02	1.735
H03	4.166	H03	4.235
H04a	2.561	H04a	2.653
H04b	3.273	H04b	3.138
H06	4.305	H06	4.140
H07	3.414	H07	3.259
H01'	1.047	H01'	1.039
H02'a	1.460	H02'a	1.622/1.592
H02'b	1.689	H02'b	1.592/1.622
H03'	0.924	H03'	0.916
H04'a	1.270	H04'a	1.229/1.283
H04'b	1.361	H04'b	1.229/1.283
H05'a	1.817	H05'a	2.029
H05'b	1.562	H05'b	1.955
C1	26.400	C1	22.730
C2	47.430	C2	45.780
C3	72.800	C3	70.550
C4	45.380	C4	44.800
C5	213.370	C5	212.330
C6	78.230	C6	78.610
C7	41.400	C7	41.070
C8	142.310	C8	143.250
C9	146.190	C9	148.190
C10	165.600	C10	165.130
C11	166.470	C11	164.380
C1'	11.290	C1'	11.990
C2'	26.040	C2'	27.380
C3'	13.780	C3'	13.860
C4'	21.040	C4'	21.260
C5'	31.450	C5'	30.180

The relative stereochemistry at the 2-CH was assigned based on comparison to the two diastereomers of 2,2'-dihydrocornexistin obtained by hydrogenation of cornexistin itself (Section 22).

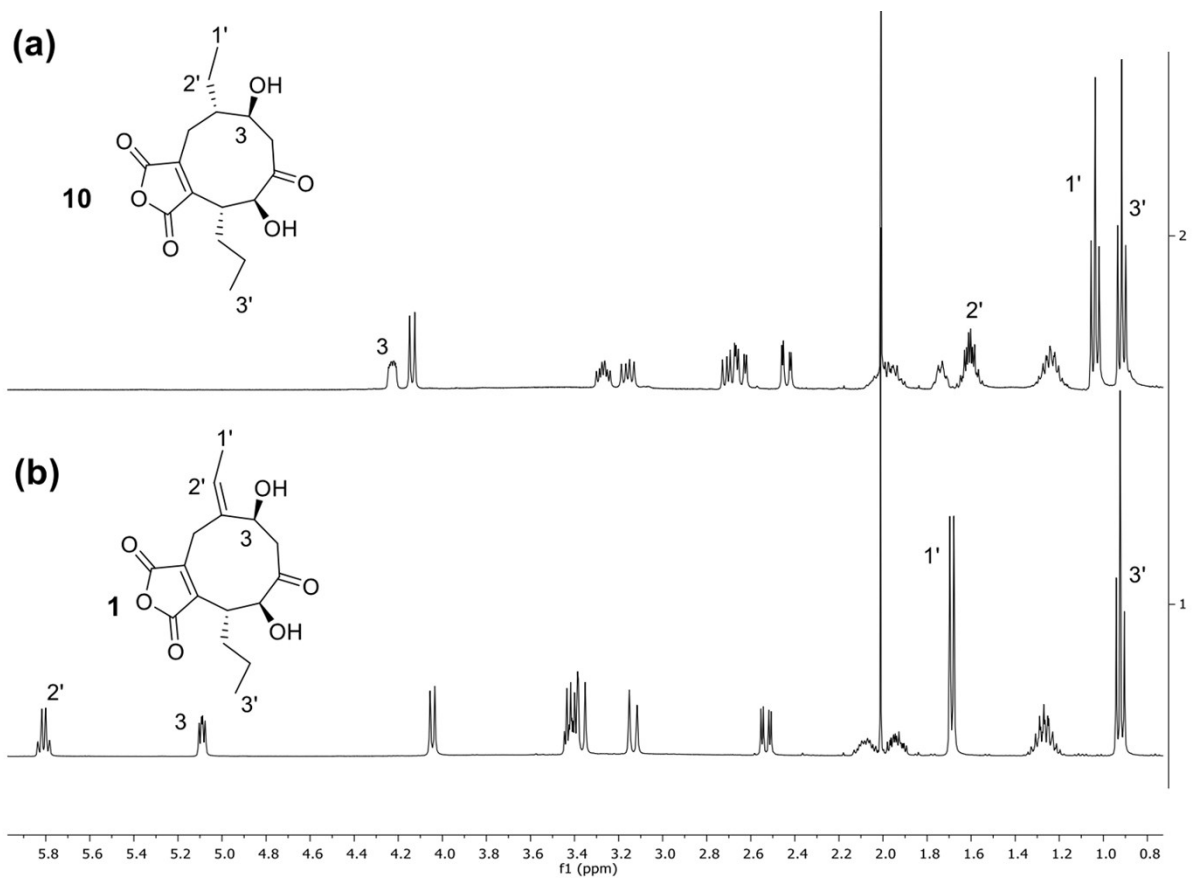


Figure S35: Comparison of the ^1H NMR spectra of (a) 2, 2'-dihydrocornexistin **10a** and (b) cornexistin **1**.

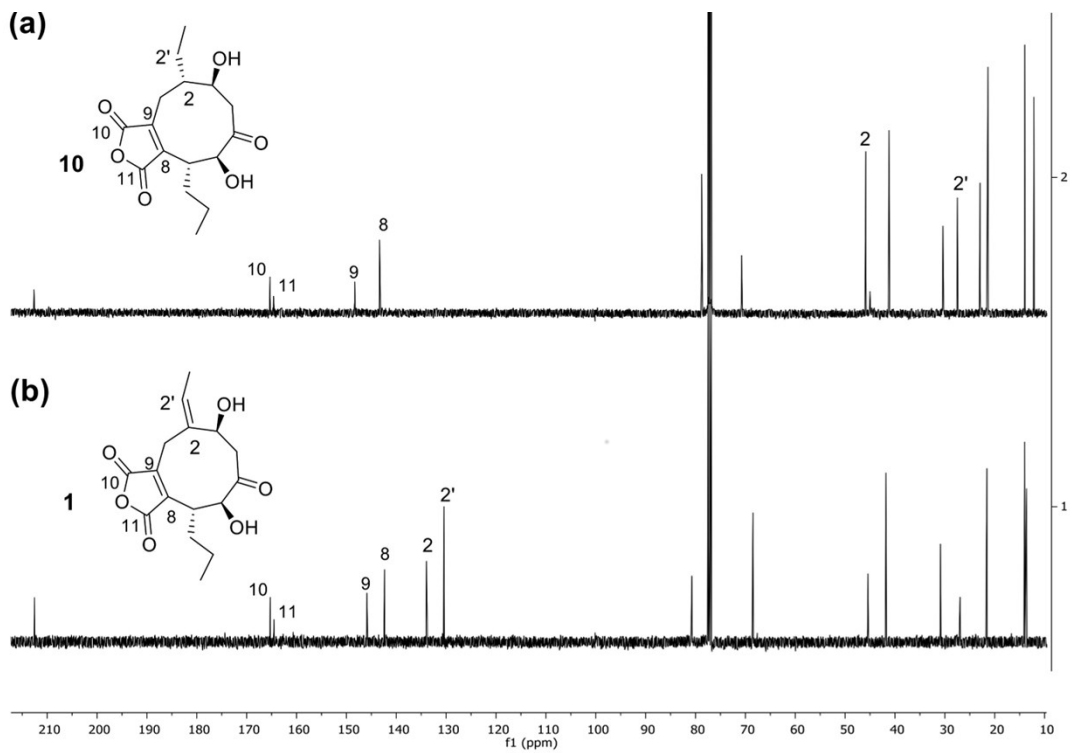


Figure S36: Comparison of the ^{13}C NMR spectra of (a) 2, 2'-dihydrocornexistin **10a** and (b) cornexistin **1**.

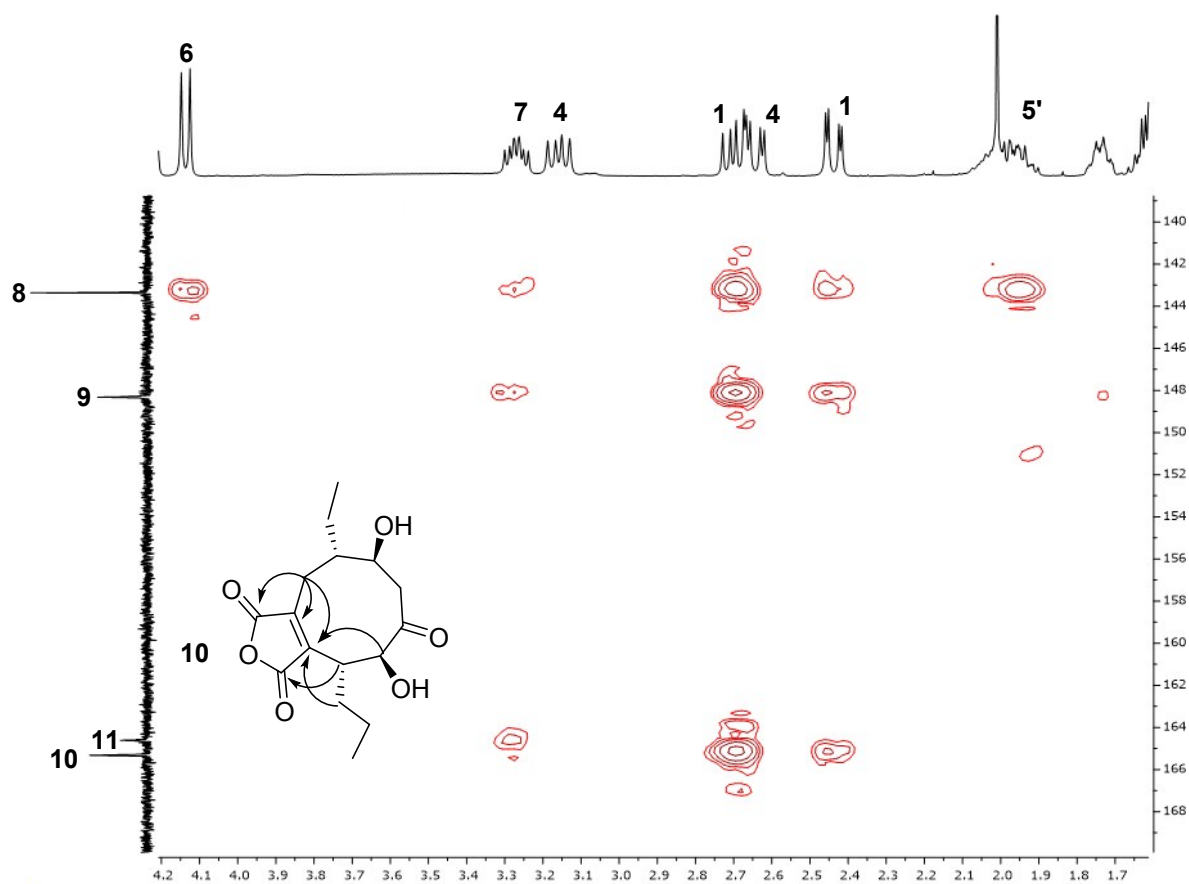
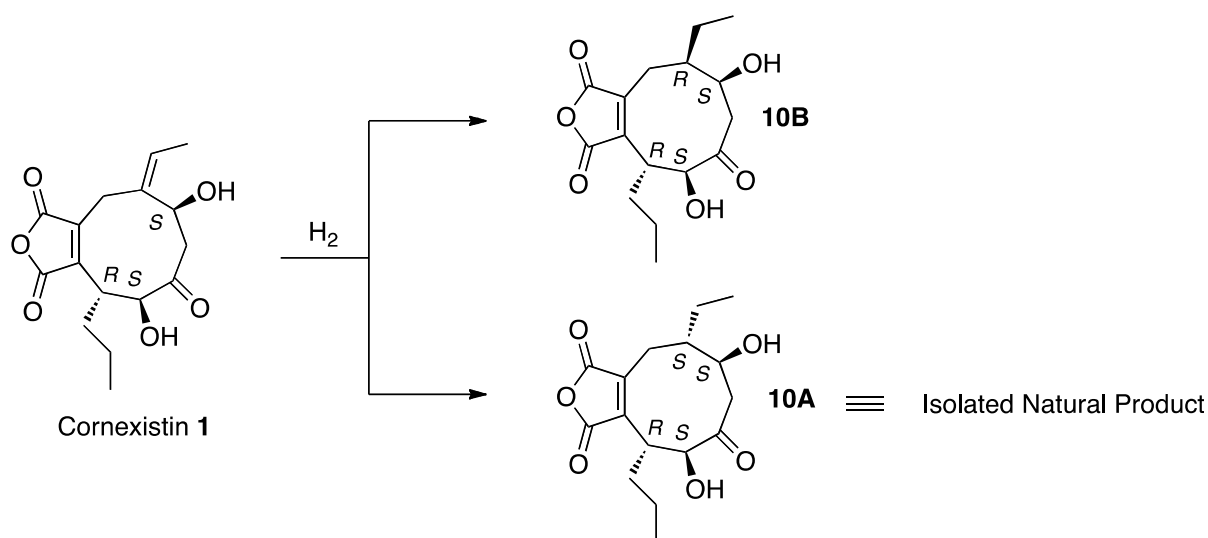


Figure S37: HMBC spectrum of **10a**, showing key correlations of quaternary carbons.



Scheme S1: The relative stereochemistry of a natural product 2,2-dihydrocornexistin **10** was determined by comparison of the NMR data with synthetic epimers **10A/10B** obtained by hydrogenation of **1** (see section 22). The relative configurations of **10A** and **10B** were determined computationally (see section 24).

17.2.2 6-dehydroxy-2,2'-dihydro-cornexistin **11**

The peak eluting at 22.9 min had a UV spectrum indicating similarity to cornexistin **1** (Figure S38, a). The ESIMS spectrum indicated the nominal mass of the compound to be 294 (m/z 293.6 [M-H]⁻), equivalent to the mass of 2, 2'-dihydrocornexistin **10**, but lacking one oxygen (Figure S38, b).

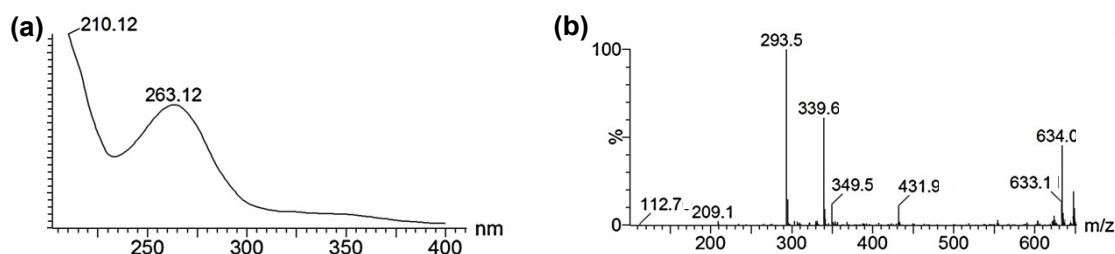


Figure S38: (a) UV and (b) ESIMS spectra of the 22.9 min peak.

The HRMS analysis of the HPLC-purified compound confirmed the molecular formula of the compound to be $C_{15}H_{22}O_5$. Analysis of the 1H NMR data revealed the presence of two triplets (δ_H 1.05 and 0.93) (Figure S39), corresponding to two methyl groups (1'-CH₃ and 3'-CH₃ respectively), which confirmed that it was a derivative of 2,2'-dihydrocornexistin **10** and not cornexistin **1**, which shows a triplet for 3'-CH₃ and a doublet for the 1'-CH₃. In comparison with the ^{13}C spectrum of **10**, the obvious difference was the presence of only one peak within the 70-80 ppm range, where usually the oxygen-linked carbons appear (3-CH and 6-CH in cornexistin). Additionally, the HSQC spectrum showed that there were only three methine groups present in the molecule (four in **10**). These data suggested that the compound is lacking one of the -OH groups. Analysis of the methine signal at δ_H 4.23, which appeared as a doublet of triplets and showed COSY coupling to 4-CH₂ (δ_H 2.78, 2.61) and 2-CH (δ_H 1.85), indicating that the 3-OH is retained, suggesting structure **11** (Figure S40). The 6-CH₂ (δ_H 2.79) showed HMBC correlations (Figure S40, b) to 5-C, 7-CH and 8-C, which further corroborated structure **11** and was therefore named 6-dehydroxy-2, 2'-dihydrocornexistin **11**.

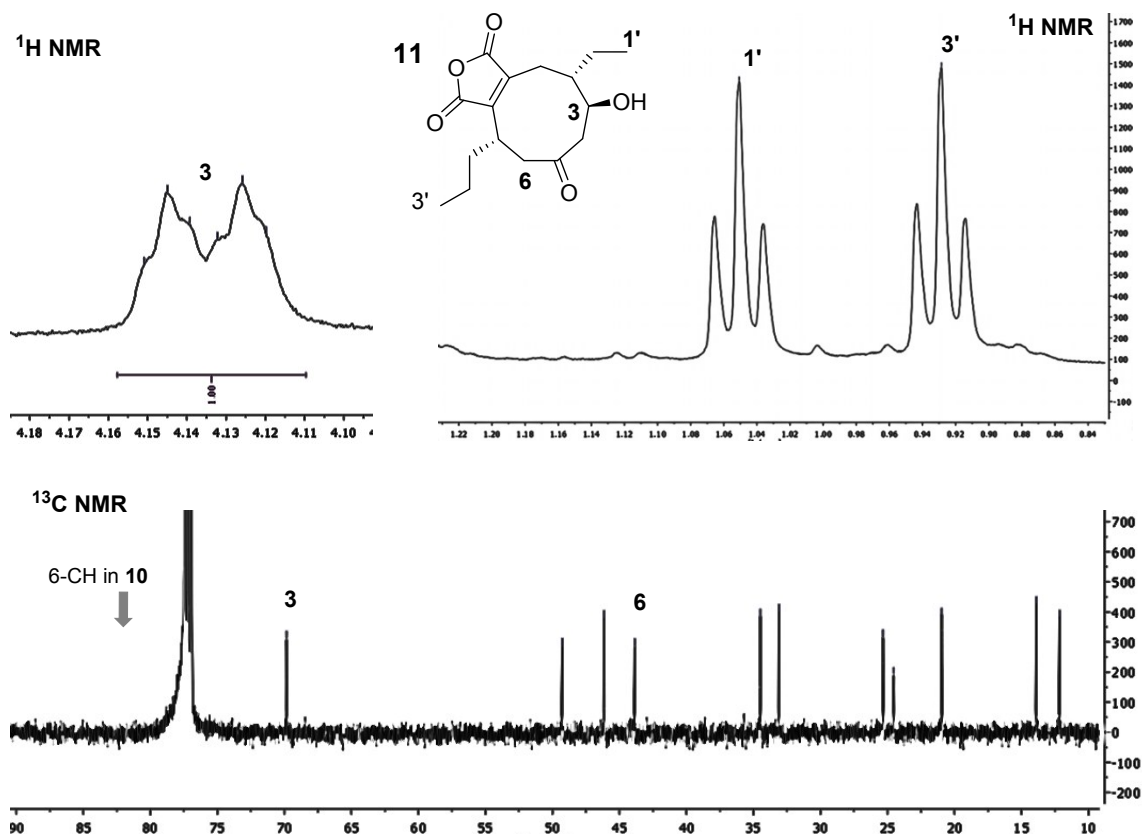


Figure S39: Key fragments of ^1H and ^{13}C NMR spectra of the 22.9 min compound.

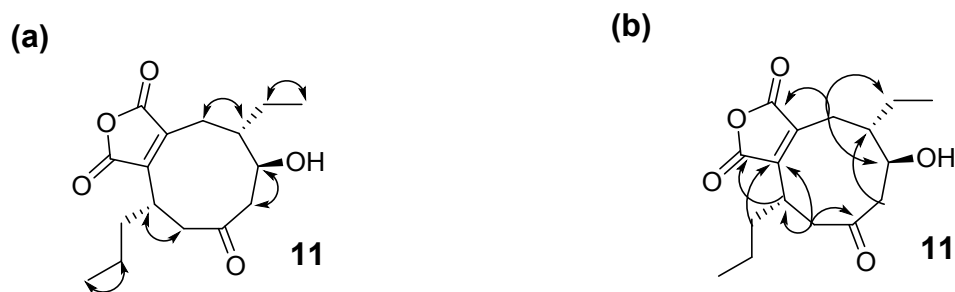


Figure S40: (a) COSY and (b) HMBC correlations of 6-dehydroxy-2,2'-dihydrocornexistin **11**.

17.2.3 2,2-dihydro-2-hydroxycornexistin **15**, isolated as its hemiacetal **9**

The peak eluting at 14.9 min had a UV spectrum indicating similarity to cornexistin **1** (Figure S41, a). MS analysis suggested the mass of the compound eluting at 14.9 min to be 326 (m/z 325.5 in the low resolution $^-$ ESIMS spectrum), indicating either a hydrated derivative of cornexistin **1** ($308 + 18$) or a hydroxyl-derivative of dihydrocornexistin ($310 + 16$).

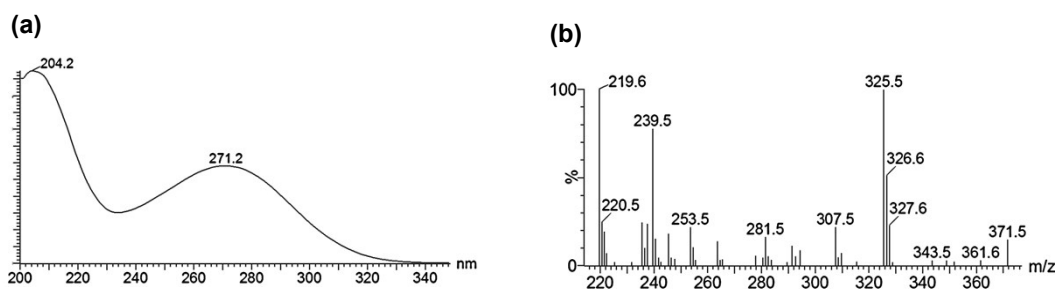


Figure S41: (a) UV and (b) ESIMS spectra of the 14.9 min peak.

The molecular formula was confirmed by HRMS analysis as $C_{16}H_{22}O_7$. All 22 protons were visible in the 1H NMR spectrum (Figure S42, a). The 1H NMR spectrum in DMSO- d_6 showed broad peaks, so variable temperature (VT) experiments up to 70 °C were run to collect good quality NMR data (Figure S42, b). Inspection of the HSQC spectrum showed resonances at δ_H 5.86 and 5.20 that had no carbon attached, which indicated a presence of $-OH$ groups and this was further confirmed by a deuterium exchange experiment (Figure S42, c). The δ_H 5.20 peak was split at the top, which was further confirmed to be an overlap of two singlets by the observed three peaks in the 1H NMR spectrum at 60 °C (Figure S42, b - δ_H 5.72, 5.09 and 5.01). The presence of two triplets arising from the methyl groups suggested that the compound was another derivative of 2, 2'-dihydrocornexistin **10** and not cornexistin **1** (a triplet and a doublet). Analysis of the ^{13}C NMR spectrum, where no signals were visible above the anhydride carbonyls (*ca.* δ_C 160-165), indicated a lack of the 5-C ketone (*ca.* δ_C 200). Instead, a quaternary carbon at δ_C 106.2 was present, showing HMBC correlation from 4- CH_2 . This suggested that the 5-C carbonyl present in cornexistin **1** was replaced by a hydroxyl, and to keep the formula correct, the additional oxygen must have been introduced elsewhere. Another significant difference, in comparison with cornexistin **1**, was the lack of one of the methine groups (2-CH or 7-CH) and a presence of an additional quaternary centre, identified as 2-C. Due to its much higher chemical shift (δ_C 89.8, when compared with 2- CH δ_C 45.9 in 2, 2'-dihydrocornexistin **10**), it was evident that this carbon has been linked with a more electronegative substituent, such as an oxygen atom. The HMBC data acquired at 70 °C revealed some new correlations (with regard to the spectrum acquired at 25 °C), and information from both spectra was combined to aid elucidation of the structure of the 14.9 min compound, which was proposed as **9** (Figure S43).

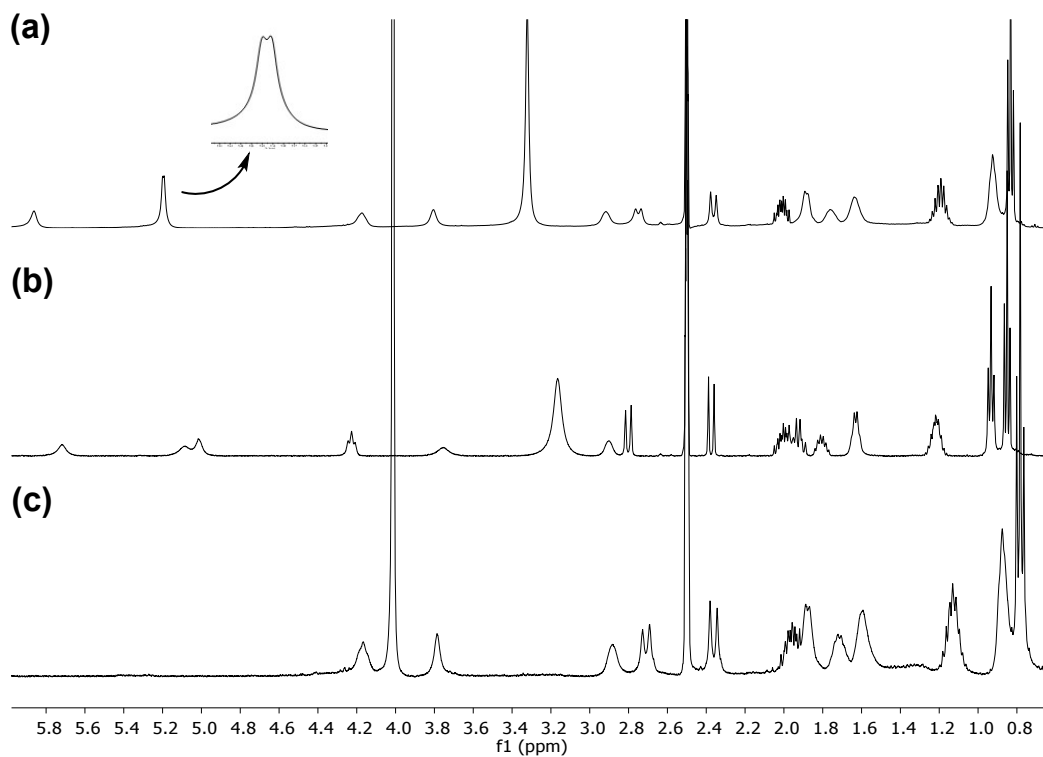


Figure S42: (a) ^1H NMR spectrum of the 14.9 min compound in DMSO-d_6 ; (b) ^1H NMR spectrum of the 14.9 min compound in DMSO-d_6 at 60°C ; (c) ^1H NMR spectrum of the 14.9 min compound in DMSO-d_6 mixed with a drop of D_2O .

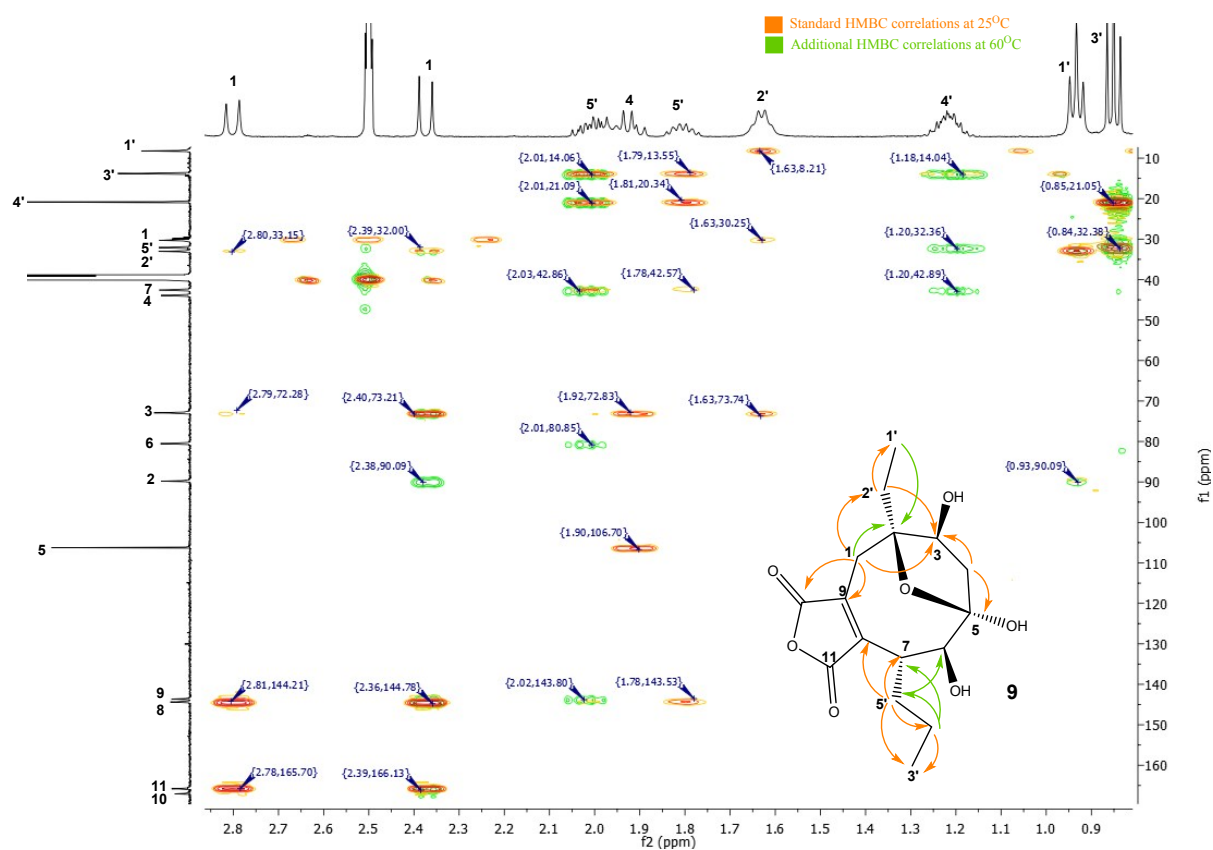


Figure S43: Superimposed HMBC spectra of **9** acquired at 25 °C (orange) and 70 °C (green).

Table S10: Experimental ^1H and ^{13}C chemical shifts for **9** referenced to internal DMSO at 2.508 ppm (^1H) and 39.520 ppm (^{13}C) at 500 MHz.

9			
Exp. Label	^1H δ_{exp} /ppm	Exp. Label	^{13}C δ_{exp} /ppm
H1a/b	2.363	C1	30.319
H1a/b	2.747	C2	89.817
H3	4.172	C3	72.949
H4	1.891	C4	43.940
H6	3.807	C5	106.241
H7	2.917	C6	80.540
H1'	0.925	C7	42.593
H2'	1.636	C8/C9	144.387
H3'	0.832	C8/C9	143.664
H4'a/b	1.271 - 1.141	C10	165.831
H5'a/b	1.756	C11	167.075
H5'a/b	2.012	C1'	8.214
OH3	5.196	C2'	33.038
OH5	5.196	C3'	13.778
OH6	5.862	C4'	20.791
		C5'	32.083

17.3 Analysis of isolated metabolites

Cornexistin **1** - whitish solid; λ_{\max} (UV) 210, 251 nm; $^{-}$ ESIMS (LCMS) m/z 307.6 [M-H] $^{-}$, 289.6 [M-H₂O-H] $^{-}$, 263.5 [M-CO₂-H] $^{-}$, 219.6 [M-2CO₂-H] $^{-}$, 616.0 [2M-H] $^{-}$; 1 H and 13 C NMR data see: Table S11.

2, 2'-dihydrocornexistin **10a** – isolated as brown oil; λ_{\max} (UV) 210, 257 nm; $^{-}$ ESIMS (LCMS) m/z 309.3 [M-H] $^{-}$, 265.3 [M-H-CO₂] $^{-}$, 221.3 [M-H-2CO₂] $^{-}$, 619.5 [2M-H] $^{-}$; 1 H and 13 C NMR data see: Table S11.

6-dehydroxy-2, 2'-dihydrocornexistin **11** – isolated as whitish residue; λ_{\max} (UV) 210, 263 nm; $^{-}$ ESIMS (LCMS) m/z 293.5 [M-H] $^{-}$, 339.6 [M-H]HCOOH $^{-}$; HRESIMS m/z 317.1360 [M]Na $^{+}$ (C₁₆H₂₂NaO₅ requires 317.1365); 1 H and 13 C NMR data see: Table S12

Hemiacetal **9** – isolated as whitish residue; λ_{\max} (UV) 204, 271 nm; $^{-}$ ESIMS (LCMS) m/z 325.5 [M-H] $^{-}$, 307.5 [M-H-H₂O] $^{-}$; HRESIMS m/z 349.1258 [M]Na $^{+}$ (C₁₆H₂₂NaO₇ requires 349.1263); 1 H and 13 C NMR data see: Table S12.

Table S11: 1 H, 13 C and HMBC NMR data for **1** and **10a** (CDCl₃). ^a 400 MHz, ^b 101 MHz, ^c 500 MHz, ^d126 MHz..



	cornexistin 1			2, 2'-dihydrocornexistin 10a		
Position	δ_{H} (J in Hz) ^a	δ_{C} ^b	HMBC ^c	δ_{H} (J in Hz) ^c	δ_{C} ^d	HMBC ^e
1	3.37 (d, 13.7), 3.13 (d, 14.3)	26.9	2, 2', 3, 8, 9, 10	2.43 (dd, 14.0, 3.0); 2.67 (dd, 14.4, 4.1)	22.9	2, 2', 3, 8, 9, 10
2	-	134.0	-	1.74 (m)	45.9	none
3	5.09 (dd, 6.8, 4.4)	68.5	1, 2, 2', 4, 5	4.22 (m)	70.8	1, 5
4	2.53 (dd, 14.1, 4.3), 3.42 (m)	45.4	2, 3, 5, 6	3.1 (dd, 14.7, 8.4), 2.62 (m)	45.0	2, 3, 5
5	-	212.6	-	-	212.6	-
6	4.04 (d, 8.6)	80.7	4, 5, 5', 7, 8	4.14, d (9.2)	78.8	5, 5', 7, 8
7	3.42 (m)	41.8	4', 5, 5', 6, 8, 9, 11	3.27 (td, 10.0, 5.3)	41.2	5', 6, 8, 9, 11
8	-	142.4	-	-	143.4	-
9	-	145.9	-	-	148.3	-
10	-	165.3	-	-	165.3	-
11	-	164.4	-	-	164.6	-
1'	1.69 (d, 7.1)	13.6	1, 2, 2', 3, 4, 9	1.04 (t, 7.3)	12.1	2, 2'
2'	5.81 (q, 7.1)	130.4	1, 1', 2, 3, 9	1.60 (m)	27.5	1, 1', 2, 3
3'	0.92 (t, 7.3)	14.0	4', 5'	0.92 (t, 7.3)	14.0	4', 5'
4'	1.27 (m)	21.6	3', 5', 7	1.24 (m)	21.4	none
5'	1.94 (m), 2.07 (m)	30.9	3', 4', 6, 7, 8	1.95 (m)	30.4	3', 4', 7, 8

Table S12: ^1H , ^{13}C and HMBC NMR data for **11** (CDCl_3) and **9** (DMSO-d_6). ^a 500 MHz, ^b 126 MHz. * at 60 °C, otherwise bs - broad singlet; bm- broad multiplet.



Position	6-dehydroxy-2, 2'-dihydrocornexistin 11			hemiacetal 9		
	δ_{H} (J in Hz) ^a	δ_{C} ^b	HMBC ^a	δ_{H} (J in Hz) ^a	δ_{C} ^b	HMBC ^a
1	2.51 (m)	25.3	2', 2, 3, 10, 8, 9	2.37 (d, 14.2), 2.80 (d, 14.2)	30.3	2', 3, 2, 9, 10
2	1.85 (m)	46.1	none	-	89.8	-
3	4.14 (dt, 9.7, 2.9)	69.8	none	4.23 (t, 9.1)*	72.85	-
4	2.78 (m), 2.61 (dd, 14.3, 2.7)	49.3	2, 5, 3	1.93 (m)	43.9	-
5	-	211.5	-	-	106.2	-
6	2.79 (m)	43.9	5, 8, 7	3.75 (bs)	80.5	-
7	3.30 (m)	33.1	5', 6, 5, 11, 9, 8	2.91 (bs)	42.6	-
8	-	146.2	-	-	143.6	-
9	-	144.5	-	-	144.4	-
10	-	165.5	-	-	165.8	-
11	-	165.7	-	-	167.1	-
1'	1.05 (t, 7.3)	12.1	2', 2	0.93 (t, 7.3)	8.2	2, 2'
2'	1.78 (m), 1.46 (m)	24.5	1', 1, 2, 3	1.63 (bs)	33.0	-
3'	0.93 (t, 7.3)	13.9	4', 5'	0.85 (t, 7.3)	13.8	4', 5', 7
4'	1.42 (m), 1.27 (m)	20.95	none	1.21 (m)	20.8	3', 5', 7
5'	1.70 (m)	34.5	4', 7, 8	2.00 (m), 1.80 (m)	32.1	3', 4', 7, 6, 8

18 Feeding Byssochlamic Acid **4** to the PV Δ pks Strain

The *P. variotii* PV Δ pks strain was used in feeding studies with (+)-byssochlamic acid **4** (purified from *B. fulva* cultures), which is a potential precursor to cornexistin **1**. 10 mg of pure byssochlamic acid **4** (in aqueous ethanol) was fed to *P. variotii* PV Δ pks cultured in PDB medium and extracted after 10 days. The production of cornexistin **1** was not restored in the mutant, however the conversion of byssochlamic acid **4** into dihydrobyssochlamic acid **12** (tR 13.3 min) was observed (Figure S44, a). The compound accumulating in the PV Δ pks mutant culture was identified as dihydrobyssochlamic acid **12** based on the LCMS data (similar UV spectrum and –ESIMS spectrum with molecular ion m/z

333.6, indicating the nominal mass of the compound to be 334, Figure S44, cd), compared with data for 10-dihydrobyssochlamic acid previously isolated from *B. fulva*.²⁵

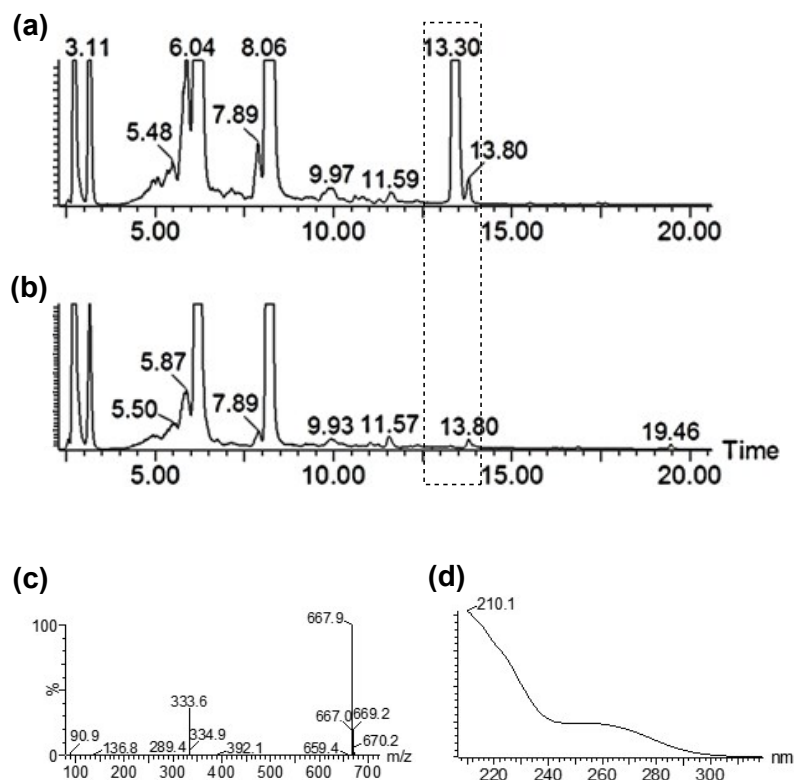


Figure S44: (a) ELSD chromatogram (30-80% ACN programme) of the extract from the PV Δ pks culture fed with byssochlamic acid **4**; (b) ELSD chromatogram of the extract from the control PV Δ pks culture not fed with byssochlamic acid **4**; (c) -ESIMS spectrum of the 13.3 min peak; (d) UV spectrum of the 13.3 min peak.

When **12** was analysed by NMR, similarly to 10-dihydrobyssochlamic acid isolated from *B. fulva*,²⁵ there appeared to be a mixture of isomeric compounds (Figure S45). There were four -CH-OH signals visible, indicating a mixture of isomers. The 13.3 min compound from *P. variotii* however showed a different ratio of those methine peaks (two compounds, δ H 5.93 and 5.85 appeared to be dominating) and the rest of the signals were an overlapping mixture, which greatly complicated structural elucidation.

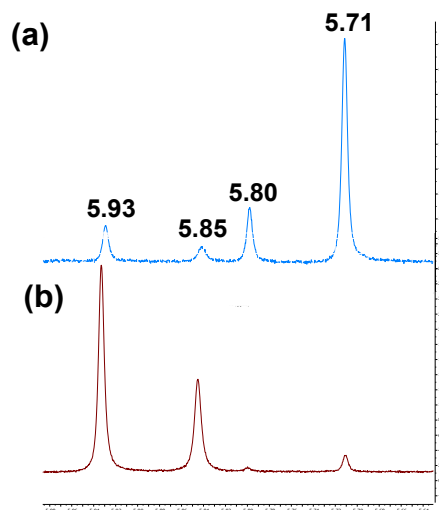


Figure S45: Methine region of the ^1H NMR spectrum of (a) 10-dihydrobyssochlamic acid isolated from *B. fulva*;²⁵ (b) dihydrobyssochlamic acid **12** isolated from *P. variotii* fed with (+)-byssochlamic acid **4**.

19 Detection of Byssochlamic Acid 4 in *P. variotii*

Extracts of *P. variotii* Agn Δ pks and wild type *B. fulva* were analysed by HR-LCMS. Byssochlamic acid elutes at 15.6 min (Figure S46).

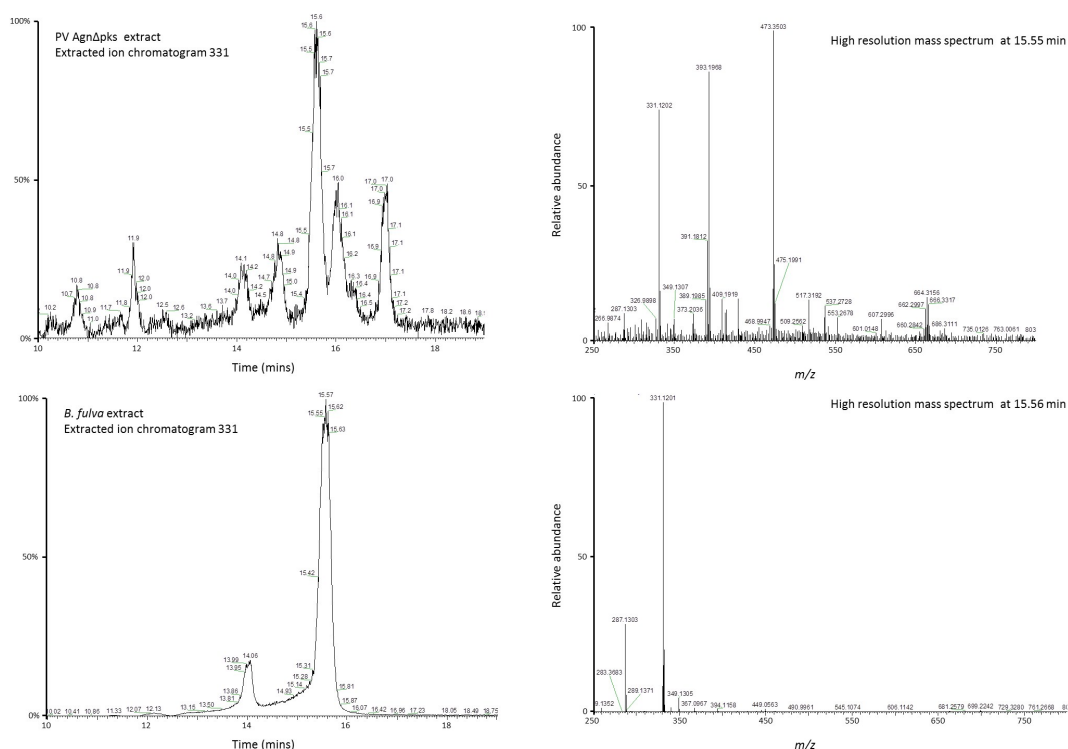


Figure S46: HR-LCMS analysis of byssochlamic acid (15.6 min) production in *P. variotii* Agn Δ pks (top) and *B. fulva* WT (bottom). Left-hand panels show the extracted ion chromatogram (ES-) at 331 Da; right-hand panel shows HRMS of the 15.6 min peak in each case. Byssochlamic acid, $\text{C}_{18}\text{H}_{19}\text{O}_6$ [M-H]⁻ calc 331.1182; found 331.1201.

20 Cornexistin Mid-Pathway Hypothesis

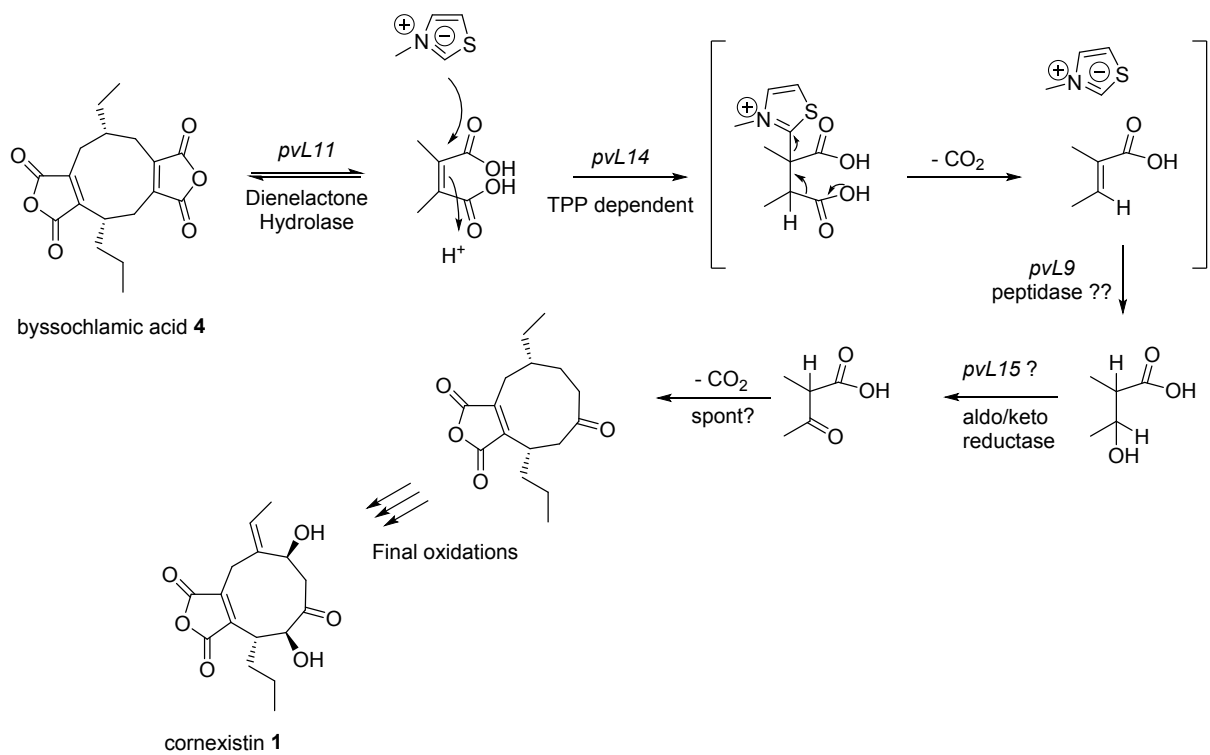


Figure S47: Hypothesis for the biosynthesis of the central section of the cornexistin **1** pathway

21 LCMS analysis of compounds 5, 5' and 13

Various forms of the anhydride monomer were observed in *P. variotii* extracts (Figure S48). The monomer **5** has been previously shown to undergo spontaneous decarboxylation, as well as interconversion between the ring closed and the diacid forms.

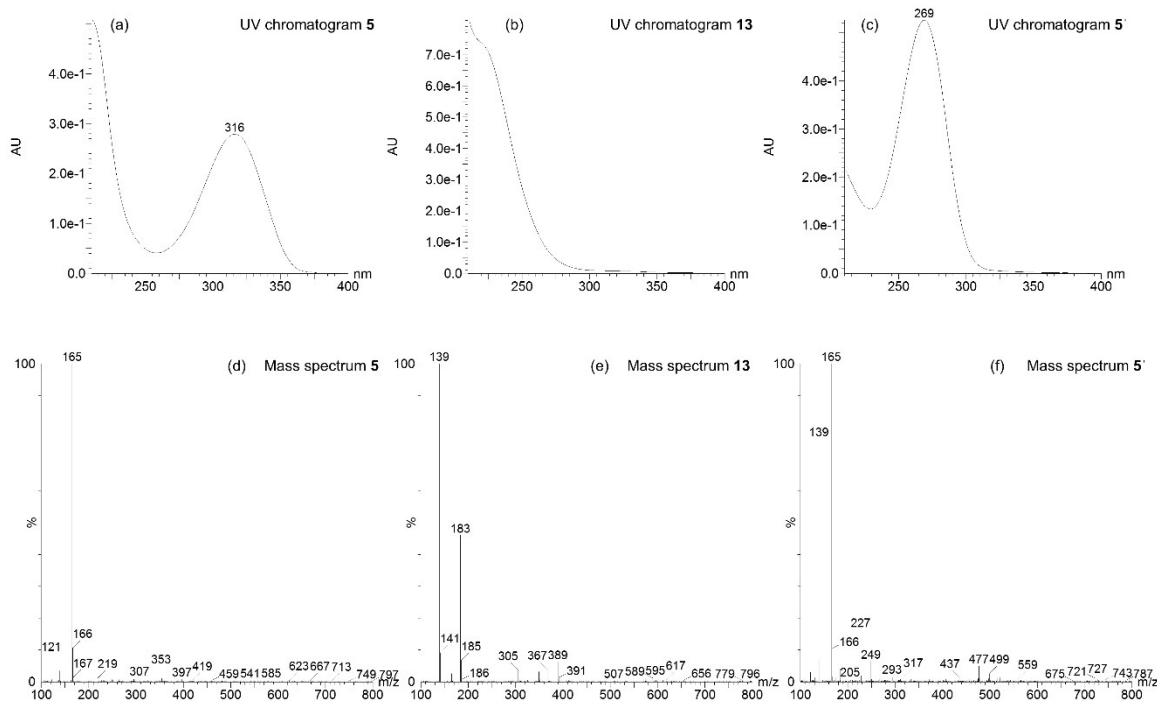


Figure S48: LCMS analysis of compounds **5**, **13** and **5'**. (a) UV chromatogram of **5**. (b) UV chromatogram of **13**. (c) UV chromatogram of **5'**. (d) Mass fragmentation of **5**. (e) Mass fragmentation of **13**. (f) Mass fragmentation of **5'**.

22 Hydrogenation of Cornexistin

5% Pt on C (Aldrich, 8 mg) was pre-washed with ethyl acetate (3 x 3 ml). A solution of cornexistin (10 mg) in ethyl acetate (1.5 ml) was carefully added, the vessel was purged three times with nitrogen and three times with hydrogen, and the reaction mixture was then stirred at room temperature under 0.5 bar of hydrogen. After 130 minutes, analytical reverse phase LCMS showed that the cornexistin had been completely consumed, and showed a new peak (two stereoisomers co-eluting). The reaction mixture was filtered and concentrated under reduced pressure to give a colourless gum (10 mg). Proton NMR showed two stereoisomeric products, and normal phase TLC on silica gel (50% EtOAc in isohexane) also showed two spots corresponding to the two stereoisomers.

The crude product was purified by normal phase chromatography on silica gel, eluting with a 0-30% gradient of ethyl acetate in isohexane. Good separation of the stereoisomers was achieved. First eluting stereoisomer (3mg, gum) called **10A**. Second eluting stereoisomer (3mg, gum/solid) called **10B**. Analytical reverse phase LCMS of each sample showed $[M]H^+$ 311, $[M]Na^+$ 333 in ESI⁺, supporting MWt 310.

23 NMR Experimental Details

Data were processed in MestReNova 9.0.1.²⁶

23.1 Compound 9

Spectra were recorded using *ca* 2 mg of **9** in 0.7 ml deuterated dimethyl sulfoxide on a Bruker AVANCE III HD 500 MHz NMR Spectrometer with 5 mm DCH ¹³C-¹H/D Cryo Probe at 298 K.

¹³C spectra were collected with a spectrum width of 31,250 Hz centred on 110 ppm with an acquired size of 59,522 data points and 2,000 scans. The data were baseline corrected with the Bernstein polynomial fit, zero-filled to a spectral size of 131,072 and apodized with a 1.0 Hz exponential function.

¹H spectra were collected with a spectrum width of 15,015 Hz centred on 6.0 ppm with an acquired size of 65,536 data points and 16 scans. The data were baseline corrected with a Bernstein polynomial fit, zero-filled to a spectral size of 262,144.

23.2 Compound 10

¹³C spectra were recorded for the two diastereomers of **10** (**10A** and **10B**) on a Bruker AVANCE III HD 500 MHz NMR Spectrometer with 5 mm DCH ¹³C-¹H/D Cryo Probe at 298 K using *ca* 2 mg of **10** in 0.7 ml deuterated chloroform. ¹³C spectra were collected with a spectrum width of 29762 Hz centred on 110 ppm with an acquired size of 32,768 data points and 4,128 scans. The data were baseline corrected with the Bernstein polynomial fit, zero-filled to a spectral size of 65,536 and apodized with a 1.0 Hz exponential function.

Subsequent spectra were recorded for the two diastereomers of **10** on Varian VNMRS 600 MHz with HCN Cryo probe at 298K using 2.0mg in 0.7ml deuterated chloroform in 5mm tubes under air without degassing.

¹H spectra were collected with a spectrum width of 9,615 Hz centred on 6.0 ppm with an acquired size of 32,768 data points and 8 scans. The data were baseline corrected with a Bernstein polynomial fit, zero-filled to a spectral size of 65,536. The spin simulation tool in available in MestReNova 9.0.1²⁶ was used to extract ¹H chemical shifts and ¹H-¹H scalar couplings (ⁿJ_{HH}), the fitting between experimental and simulated spectra was assessed by eye.

2D NOESY spectra were collected with a mixing time of 500ms, a relaxation delay of 5s and selective saturation of the residual H₂O resonance during the relaxation delay. F1 and F2 spectral widths of 5,411 Hz centred on 4.0 ppm with an acquired size of 400 increments in F1, 1,624 data points and 16 scans in F2 were used. The data were baseline corrected with a Bernstein polynomial fit, zero-filled to a spectral size of 4096 in both dimensions and apodized with 90° sine square in F1 and a 90° sine bell in F2.

2D NOESY data were converted into interproton distances with the PANIC (peak amplitude normalization for improved cross-relaxation) approach where the NOE intensity was taken to be the ratio between cross peaks and diagonal peaks (this allows longer mixing times to be used while assuming the initial rate approximation is still valid).^{27,28,29} This was achieved by using F2 traces for each proton of interest, and setting the integral of each diagonal peak to have an integral of 1,000. Equation 2, as derived using this approximation in Chapter 4 of Neuhaus and Williamson³⁰ and

applied to distance determination by Butts *et al.*³¹ and Jones *et al.*,³² was used to convert the measured intensities ($\eta^{x,y}$) for the cross peaks into distances ($r^{x,y}$) using the H1a-H1b correlation as a reference distance (r^{ref}) and intensity (η^{ref}) for each diastereomer (**10A** and **10B**).

$$\frac{\eta^{x,y}}{\eta^{ref}} = \frac{(r^{x,y})^{-6}}{(r^{ref})^{-6}} \quad (2)$$

Where, $\eta^{x,y}$ is experimentally measured NOE intensity between nuclei x and y ; η^{ref} is experimentally measured NOE intensity between two reference nuclei; $r^{x,y}$ is experimentally determined distance between nuclei x and y ; r^{ref} is a reference distance.

In cases of cross peaks arising from NOE correlations to methyl groups, the PANIC-corrected intensity is divided by a factor of 3 to account for the 3 ^1H contributing to the signal (Equation 3).

$$\frac{\eta^{x,y}}{3 \times \eta^{ref}} = \frac{(r^{x,y})^{-6}}{(r^{ref})^{-6}} \quad (3)$$

24 Structural Calculations for **9**, **10A** and **10B**

MATLAB R2016a (9.0.0341360) was used to calculate Boltzmann-averaged DFT-derived values for chemical shift, scalar couplings and ^1H - ^1H distances for the diastereomers of **9** and **10**. Microsoft Excel 2013 (15.0.4885.1000) was used to calculate the statistics used to compare experimental and calculated datasets.

24.1 Conformational search for **9** and **10**

An MCM (Monte Carlo Multiple Minimum) conformational search was performed for the four diastereomers of **9** and two diastereomers of **10** (Figure S49) with MacroModel³³ using MMFFs (Merk Molecular Force Field) with 1,000,000 steps, molecules within 50.0 kJ/mol of the lowest energy molecule found were retained. The calculations were conducted in gaseous phase for **9** and with chloroform for **10**. Structures were minimised using the TNCG (truncated Newton Conjugate Gradient) method with 500 iterations with a gradient convergence criteria of 0.05.

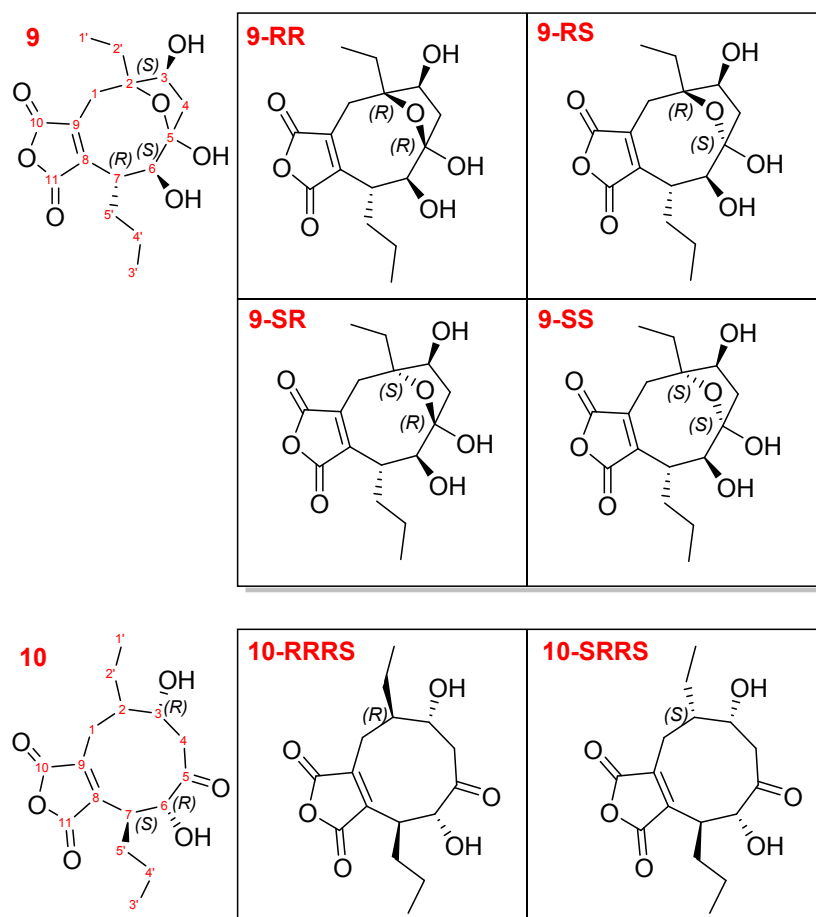


Figure S49: Labelling systems for **9** and **10** (for diastereotopic ^1H *Pro-R* labelled as Ha and *Pro-S* as Hb) and the six diastereomers under investigation.

24.2 Calculation of chemical shifts for **9**

All subsequent DFT (density functional theory) calculations were performed using Gaussian 09.³⁴

According to the method of Goodman *et al.*³⁵ molecules within 10.0 kJ/mol of the lowest energy conformer found by the conformational search were subjected to single point energy and NMR shielding tensor calculations using B3LYP/6-31G(d,p) and the GIAO method for the NMR calculations. The isotropic magnetic shielding tensors for each nucleus across the conformers were then weighted according to the Boltzmann distribution (Equation 4) determined by the potential energy for single point energy calculations.

$$\sigma^x = \frac{\sum_i \sigma_i^x e^{-E_i/RT}}{\sum_i e^{-E_i/RT}} \quad (4)$$

Where, σ^x is the Boltzmann-averaged shielding for nucleus x ; σ^x is the shielding for nucleus x in conformer i ; E_i is the relative potential energy of conformer i ; R is the molar gas constant and T the temperature (298K).

Calculated shieldings for the ^1H and ^{13}C of TMS (tetramethylsilane) were then used to calculate chemical shifts from the weighted shielding (Equation 5).

$$\delta_{calc}^x = \frac{\sigma^{TMS} - \sigma^x}{1 - \sigma^{TMS} \times 10^{-6}} \quad (5)$$

Where, δ_{calc}^x is the Boltzmann-averaged calculated chemical shift for nucleus x and σ^{TMS} is the shielding for the ^1H (31.755) or ^{13}C (191.800) of TMS.

TMS geometry optimisation and NMR calculations performed using DFT B3LYP/6-31G(d,p) with the GIAO method. These calculated chemical shifts were then scaled according to the gradient and intercept between calculated and experimental data (Equation 6).

$$\delta_{scaled}^x = \frac{\delta_{calc}^x - c}{m} \quad (6)$$

Where, δ_{scaled}^x is the scaled Boltzmann-averaged chemical shift for nucleus x ; c is the intercept of a plot of δ_{calc} against the experimental chemical shift and m is the gradient.

These scaled and experimental chemical shifts were then analysed by calculating the mean absolute deviation (MAD), standard deviation in the deviations (SD) and root mean squared deviation (RMSD) as defined in Equations 7 to 9 and with the DP4 method described by Goodman *et al.*³⁵

$$MAD = \frac{1}{n} \sum_{j=1}^n |a_j - b_j| \quad (7)$$

Where, a_j is the experimental value (such as chemical shift); b_j is the calculated value; n is the total number of values for a molecule.

$$SD = \sqrt{\frac{\sum_{j=1}^n (\bar{z} - z_j)^2}{n - 1}} \quad (8)$$

Where, $z_j = a_j - b_j$ and $\bar{z} = \frac{1}{n} \sum_{j=1}^n z_j$

$$RMSD = \sqrt{\frac{\sum_{j=1}^n (z_j)^2}{n}} \quad (9)$$

24.3 Calculation of distances for NOE comparison for 10

Molecules found by the conformational search were subjected to single point energy calculations using B3LYP/6-31g(d,p) with the IEFPCM solvent model for chloroform. Molecules within 21.0 kJ/mol of the lowest energy found were subjected to optimisation and frequency calculations (mPW1PW91/6-311g(d,p) with the IEFPCM solvent model for chloroform). Conformers which converged to the same geometry following optimisation were eliminated.

The ^1H - ^1H distances across the different conformers were then weighted according to the Boltzmann distribution (Equation 10) determined by the frequency calculations which provided the Gibbs free energy.

$$r_{effective}^{x,y} = \left(\frac{\sum_i (r_i^{x,y})^{-6} e^{-G_i/RT}}{\sum_i e^{-G_i/RT}} \right)^{-1/6} \quad (10)$$

Where, $r_{effective}^{x,y}$ is the Boltzmann-averaged effective distance between nuclei x and y ; $r_i^{x,y}$ is the calculated distance for conformer i .

Methyl ^1H distances were averaged according to equation 11.

$$r_{effective}^{x,y(Me)} = \left(\frac{\sum_i 1/3((r_i^{x,y1})^{-6} + (r_i^{x,y2})^{-6} + (r_i^{x,y3})^{-6}) e^{-G_i/RT}}{\sum_i e^{-G_i/RT}} \right)^{-1/6} \quad (11)$$

Where, $r_{effective}^{x,y(Me)}$ is the Boltzmann-averaged effective distance between nuclei x and methyl ^1H y ; $r_i^{x,y1}$, $r_i^{x,y2}$, $r_i^{x,y3}$ are the calculated distances between x and y for the three ^1H for conformer i .

The calculated ^1H - ^1H coupling constants were compared to the experimentally determined values by calculating the MAD, SD (Equations 7-8) and the mean absolute percentage deviation (MA%D) (Equation 12).

$$MA\%D = \frac{1}{n} \sum_{j=1}^n \frac{|a_j - b_j|}{a_j} \quad (12)$$

The reference distance (r^{ref}), required by equations 2-3, was determined by minimising the RMSD (Equation 9) using the Datasolver tool in Microsoft Excel 2013 from a starting value of 1.78Å for each combination of experimental and calculated datasets.

24.4 Calculation of scalar coupling constants for 10

The structures found by geometry optimisation and frequency calculations were subjected NMR calculations using the GIAO method with mPW1PW91/6-311g(d,p) and the IEFPCM solvent model for chloroform giving the total spin-spin couplings (J).

The scalar couplings across the different conformers were then weighted according to the Boltzmann distribution (Equation 13) determined by the frequency calculations which provided the Gibbs free energy.

$$J^{x,y} = \frac{\sum_i J_i^{x,y} e^{-G_i/RT}}{\sum_i e^{-G_i/RT}} \quad (13)$$

Where, $J^{x,y}$ is the Boltzmann-averaged scalar coupling constant between nuclei x and y ; $J_i^{x,y}$ scalar coupling constant between nuclei x and y for conformer i and G_i the relative Gibbs free energy of conformer i .

The calculated ^1H - ^1H coupling constants were compared to the experimentally determined values by calculating the MAD and SD (Equations 7-8).

24.5 Chemical shift analysis for 9

Conformational searching using MCMM with MMFFs for the four diastereomers of **9** found between 18 and 58 conformers below 10kJ/mol relative to the global minimum found. Table S13 to Table S16 show the populations calculated from the relative potential energies from single point calculations using DFT.

Table S13: 9-RR - relative potential energies (DFT B3LYP/6-31g (d,p)) and populations at 289K, Cartesian co-ordinates for these conformers are attached.

Label	Relative Energy (E) /kJ.mol ⁻¹	Population	Label	Relative Energy (E) /kJ.mol ⁻¹	Population
1	0.00	32.77%	10	4.61	5.09%
2	3.43	8.20%	11	4.60	5.11%
3	4.57	5.18%	12	5.97	2.94%
4	7.69	1.47%	13	11.62	0.30%
5	2.38	12.55%	14	11.18	0.36%
6	3.41	8.26%	15	11.43	0.32%
7	6.88	2.04%	16	5.38	3.73%
8	5.28	3.88%	17	14.10	0.11%
9	7.78	1.42%	18	4.09	6.28%

Table S14: 9-RS - relative potential energies (DFT B3LYP/6-31g (d,p)) and populations at 289K, Cartesian co-ordinates for these conformers are attached.

Label	Relative Energy (E) /kJ.mol ⁻¹	Population	Label	Relative Energy (E) /kJ.mol ⁻¹	Population
1	7.71	1.41%	25	16.22	0.05%
2	1.69	16.06%	26	14.08	0.11%
3	0.00	31.77%	27	19.84	0.01%
4	5.02	4.18%	28	15.17	0.07%
5	10.77	0.41%	29	13.52	0.13%
6	8.20	1.16%	30	7.62	1.46%
7	13.73	0.12%	31	9.40	0.72%
8	6.09	2.71%	32	15.43	0.06%
9	14.77	0.08%	33	9.65	0.65%
10	11.20	0.35%	34	7.18	1.75%
11	9.93	0.58%	35	14.89	0.08%
12	5.26	3.81%	36	19.67	0.01%
13	3.97	6.40%	37	9.72	0.63%
14	3.49	7.77%	38	6.80	2.04%
15	20.87	0.01%	39	18.54	0.02%
16	9.24	0.76%	40	10.76	0.41%
17	10.84	0.40%	41	15.89	0.05%
18	5.44	3.54%	42	18.43	0.02%
19	5.22	3.86%	43	24.46	0.00%
20	15.02	0.07%	44	14.97	0.08%
21	18.54	0.02%	45	5.84	3.01%
22	12.24	0.23%	46	8.95	0.85%
23	10.91	0.39%	47	19.03	0.01%
24	16.17	0.05%	48	7.31	1.66%

Table S15: 9-SR - relative potential energies (DFT B3LYP/6-31g (d,p)) and populations at 289K, Cartesian co-ordinates for these conformers are attached.

Label	Relative Energy (E) /kJ.mol ⁻¹	Population	Label	Relative Energy (E) /kJ.mol ⁻¹	Population
1	9.98	0.33%	28	7.10	1.07%
2	5.29	2.22%	29	6.81	1.20%
3	5.29	2.22%	30	10.38	0.28%
4	3.41	4.75%	31	13.65	0.08%
5	8.05	0.73%	32	13.15	0.09%
6	10.75	0.25%	33	6.31	1.47%
7	8.98	0.50%	34	10.66	0.25%
8	4.04	3.69%	35	10.58	0.26%
9	4.05	3.67%	36	2.38	7.19%
10	10.44	0.28%	37	5.68	1.90%
11	6.36	1.44%	38	0.00	18.82%
12	11.46	0.18%	39	10.44	0.28%
13	9.83	0.36%	40	14.38	0.06%
14	9.86	0.35%	41	7.14	1.05%
15	7.83	0.80%	42	4.16	3.51%
16	6.13	1.58%	43	8.94	0.51%
17	14.61	0.05%	44	5.90	1.74%
18	9.99	0.33%	45	1.74	9.32%
19	8.57	0.59%	46	5.43	2.10%
20	10.26	0.30%	47	16.18	0.03%
21	17.95	0.01%	48	7.10	1.07%
22	6.91	1.16%	49	8.53	0.60%
23	11.76	0.16%	50	11.59	0.17%
24	1.19	11.63%	51	13.77	0.07%
25	8.39	0.64%	52	5.10	2.40%
26	3.17	5.22%	53	8.59	0.59%
27	9.35	0.43%			

Table S16: 9-SS - relative potential energies (DFT B3LYP/6-31g (d,p)) and populations at 289K, Cartesian co-ordinates for these conformers are attached.

Label	Relative Energy (E) /kJ.mol ⁻¹	Population	Label	Relative Energy (E) /kJ.mol ⁻¹	Population
1	7.24	0.97%	30	9.17	0.44%
2	5.44	2.01%	31	4.03	3.55%
3	6.19	1.48%	32	10.38	0.27%
4	3.05	5.27%	33	11.32	0.19%
5	8.83	0.51%	34	12.85	0.10%
6	7.42	0.90%	35	3.57	4.28%
7	7.40	0.91%	36	6.56	1.28%
8	2.43	6.76%	37	6.60	1.26%
9	19.30	0.01%	38	21.88	0.00%
10	1.69	9.11%	39	18.56	0.01%
11	7.88	0.75%	40	23.52	0.00%
12	17.10	0.02%	41	14.82	0.05%
13	9.41	0.40%	42	14.82	0.05%
14	10.96	0.22%	43	14.81	0.05%
15	4.56	2.87%	44	10.73	0.24%
16	4.55	2.87%	45	19.78	0.01%
17	8.14	0.68%	46	9.92	0.33%
18	9.39	0.41%	47	17.40	0.02%
19	9.39	0.41%	48	4.53	2.90%
20	24.60	0.00%	49	4.54	2.89%
21	17.89	0.01%	50	13.33	0.08%
22	0.00	18.06%	51	22.67	0.00%
23	7.70	0.81%	52	26.82	0.00%
24	0.15	16.98%	53	6.29	1.43%
25	24.51	0.00%	54	20.33	0.00%
26	6.88	1.12%	55	12.43	0.12%
27	10.25	0.29%	56	20.31	0.00%
28	10.24	0.29%	57	2.92	5.56%
29	9.00	0.48%	58	10.10	0.31%

The populations were used to weight the calculated σ for the different conformers (Equation 4) which were used to calculate δ_{scaled} for the four diastereomers (Equations 5-6). δ_{scaled} were then compared to the δ_{exp} and used to calculate MAD, SD and DP4 for ¹H (Table S17) and ¹³C (Table S18). The chemical shifts of H4'a and H4'b, for which the experimental measurement of chemical shift was ambiguous, and the chemical shifts of ¹H in OH groups were not included in the calculation of MAD, SD or DP4.

Table S17: Experimental ^1H chemical shifts for **9** referenced to internal DMSO at 2.508 ppm and δ_{scaled} is the corresponding scaled chemical shift for the different diastereomers (Equation 6).

Exp. Label	$\delta_{\text{exp}}/\text{ppm}$	Calc. Label	9-RR $\delta_{\text{scaled}}/\text{ppm}$	9-RS $\delta_{\text{scaled}}/\text{ppm}$	9-SR $\delta_{\text{scaled}}/\text{ppm}$	9-SS $\delta_{\text{scaled}}/\text{ppm}$
H1a/b	2.363	H1b	2.572	2.7750	2.711	2.321
H1a/b	2.747	H1a	2.331	2.9639	3.172	2.739
H3	4.172	H3	3.881	4.4151	4.149	4.387
H4	1.891	H4	2.012	1.8646	1.779	2.138
H6	3.807	H6	3.869	3.3671	3.692	3.380
H7	2.917	H7	3.364	3.1264	2.935	3.022
H1'	0.925	H1'	0.856	0.8739	0.921	0.899
H2'	1.636	H2'	1.797	1.4683	1.471	1.555
H3'	0.832	H3'	0.728	0.9571	0.893	0.809
H4'a/b	1.271 - 1.141	H5'b	1.575	1.4234	1.623	1.523
H5'a/b	1.756	H5'a	2.291	1.4734	1.428	2.422
H5'a/b	2.012					
OH3	5.196					
OH5	5.196					
OH6	5.862					
MAD /ppm			0.22	0.31	0.25	0.22
SD /ppm			0.18	0.26	0.19	0.16
DP4			40.0%	0.1%	23.7%	36.1%

Table S18: Experimental ^{13}C chemical shifts for **9** referenced to internal DMSO at 39.520 ppm and δ_{scaled} is the corresponding scaled chemical shift for the different diastereomers (Equation 6).

Exp. Label	$\delta_{\text{exp}}/\text{ppm}$	Calc. Label	9-RR $\delta_{\text{scaled}}/\text{ppm}$	9-RS $\delta_{\text{scaled}}/\text{ppm}$	9-SR $\delta_{\text{scaled}}/\text{ppm}$	9-SS $\delta_{\text{scaled}}/\text{ppm}$
C1	30.319	C1	29.383	38.055	36.612	29.113
C2	89.817	C2	94.233	74.985	76.620	90.342
C3	72.949	C3	74.549	85.477	81.677	73.482
C4	43.940	C4	43.131	44.412	41.102	41.193
C5	106.241	C5	108.605	103.851	107.503	109.949
C6	80.540	C6	83.086	76.717	75.055	85.272
C7	42.593	C7	43.441	57.488	58.388	40.451
C8/C9	144.387	C8	140.733	150.031	146.960	141.217
C8/C9	143.664	C9	142.603	137.541	141.073	141.285
C10	165.831	C10	165.827	167.337	166.693	166.792
C11	167.075	C11	166.130	168.278	167.816	166.962
C1'	8.214	C1'	7.490	2.489	2.656	7.975
C2'	33.038	C2'	30.706	25.136	30.227	33.829
C3'	13.778	C3'	12.233	8.783	9.206	13.203
C4'	20.791	C4'	21.364	18.730	18.370	21.872
C5'	32.083	C5'	31.746	35.951	35.303	32.323
MAD /ppm			1.96	7.71	6.68	2.15
SD /ppm			1.54	5.98	4.93	1.57
DP4			65.5%	0.0%	0.0%	34.5%

It was found that either the **9-RR** or **9-SS** diastereomers were the most probable match to the experimental data, however the results for DP4 (Figure S50) show that distinguishing the **9-RR** (67.7% using ^1H and ^{13}C) from the **9-SS** (32.3% using ^1H and ^{13}C) was more difficult.

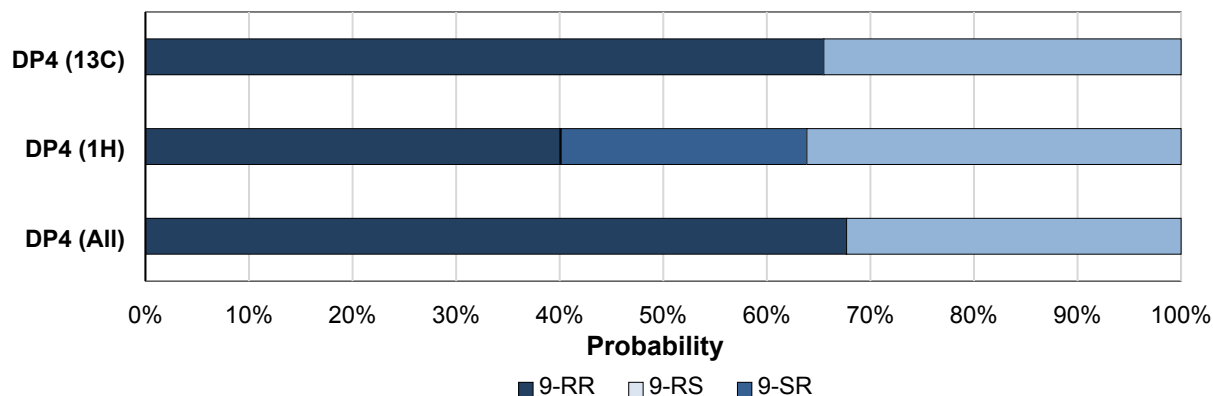


Figure S50: Summary of DP4 results for the different diastereomers of 9.

24.6 Analysis for 10

Conformational searching using MCMC with MMFFs for the two diastereomers of **10** found 538 conformers below 50kJ/mol for **10-RRRS** and 1423 for **10-SRRS** relative to the global minima. Following single point energy calculations (using DFT B3LYP 6-31g(d,p)) to obtain the relative potential energies, 158 conformers were found below 21 kJ/mol for **10-RRRS** and 202 for **10-SRRS**. The conformers were then further geometry optimised and frequency calculations were performed to obtain the relative Gibbs free energy which was used to calculate the population of each conformer using the Boltzmann distribution (Table S19, Table S20). Conformers which converged to the same geometry following optimisation were eliminated, resulting in 136 conformers for **10-RRRS** and 132 for **10-SRRS**.

Table S19: **10-RRRS** - relative Gibb's free energies (DFT mPW1PW91/6-311g(d,p)) and populations at 289K, Cartesian coordinates for these conformers are attached.

Label	Relative Energy (G) /kJ.mol ⁻¹	Population	Label	Relative Energy (G) /kJ.mol ⁻¹	Population
1	2.418	5.305%	102	15.895	0.023%
2	0.000	14.086%	104	7.911	0.577%
3	1.864	6.635%	108	6.800	0.904%
4	1.397	8.014%	110	15.819	0.024%
5	5.674	1.425%	112	8.488	0.457%
6	4.035	2.761%	114	7.567	0.663%
7	5.700	1.410%	115	11.841	0.118%
9	11.135	0.157%	118	3.810	3.025%
10	6.863	0.881%	119	5.301	1.656%
11	5.109	1.790%	121	18.465	0.008%
12	12.371	0.095%	126	1.665	7.192%
13	8.932	0.382%	129	11.250	0.150%
14	6.858	0.883%	130	12.545	0.089%
15	13.569	0.059%	132	5.692	1.414%
16	5.419	1.579%	133	10.481	0.204%
17	4.802	2.026%	134	9.231	0.339%
18	16.165	0.021%	135	12.786	0.081%
19	12.064	0.108%	143	7.934	0.572%
20	10.229	0.226%	144	13.293	0.066%
21	8.344	0.485%	148	12.437	0.093%
22	12.991	0.074%	149	6.301	1.106%
23	7.312	0.735%	150	10.323	0.218%
24	6.866	0.880%	155	9.024	0.368%
26	17.512	0.012%	156	7.774	0.610%
27	11.917	0.115%	158	7.015	0.829%
28	11.605	0.130%	162	11.991	0.111%
29	9.948	0.254%	165	15.070	0.032%
30	9.612	0.290%	167	11.497	0.136%
31	15.157	0.031%	169	3.613	3.275%
32	10.200	0.229%	170	7.317	0.734%
33	15.210	0.030%	173	12.017	0.110%

35	11.376	0.142%	175	8.134	0.528%
39	13.114	0.071%	176	11.424	0.140%
41	11.610	0.130%	182	11.783	0.121%
42	17.163	0.014%	184	4.560	2.234%
43	12.458	0.092%	188	12.936	0.076%
44	10.371	0.214%	190	13.976	0.050%
45	14.587	0.039%	191	11.059	0.162%
47	13.884	0.052%	201	15.383	0.028%
49	9.964	0.252%	209	4.910	1.940%
50	13.461	0.061%	214	14.393	0.042%
51	9.334	0.325%	215	6.805	0.902%
55	19.274	0.006%	218	15.034	0.033%
57	7.186	0.774%	221	7.165	0.780%
58	11.836	0.118%	223	14.608	0.039%
61	16.992	0.015%	230	9.237	0.338%
64	17.677	0.011%	234	15.464	0.027%
66	21.479	0.002%	243	16.023	0.022%
68	8.055	0.545%	244	11.093	0.160%
70	7.596	0.656%	252	3.497	3.431%
71	9.953	0.253%	254	14.595	0.039%
72	14.052	0.048%	264	6.826	0.895%
74	12.878	0.078%	268	7.228	0.761%
75	7.958	0.566%	277	17.184	0.014%
76	14.926	0.034%	288	11.718	0.124%
78	18.701	0.007%	302	15.262	0.030%
80	16.131	0.021%	306	8.683	0.423%
81	7.196	0.770%	315	12.776	0.081%
83	19.043	0.006%	339	13.983	0.050%
85	14.073	0.048%	342	18.759	0.007%
87	10.534	0.200%	359	9.307	0.328%
89	6.322	1.097%	363	13.813	0.053%
90	20.474	0.004%	419	12.621	0.086%
93	17.520	0.012%	422	15.595	0.026%
94	8.063	0.543%	428	11.143	0.157%
95	7.123	0.794%	432	18.754	0.007%
96	11.242	0.150%	444	11.208	0.152%
99	6.075	1.211%	504	13.432	0.062%

Table S20: 10-SRRS - relative Gibb's free energies (DFT mPW1PW91/6-311g(d,p)) and populations at 289K, Cartesian coordinates for these conformers are attached.

Label	Relative Energy (G) /kJ.mol ⁻¹	Population	Label	Relative Energy (G) /kJ.mol ⁻¹	Population
1	9.181	1.123%	145	23.905	0.003%
2	9.373	1.040%	147	11.676	0.410%
3	9.583	0.955%	148	14.081	0.155%
4	8.953	1.232%	150	3.445	11.391%
7	15.630	0.083%	155	24.170	0.003%
8	13.826	0.172%	170	18.371	0.027%
9	11.715	0.404%	172	21.393	0.008%
10	18.896	0.022%	173	20.287	0.013%
11	17.210	0.044%	176	5.574	4.821%
12	16.121	0.068%	177	19.802	0.015%
13	11.035	0.531%	188	18.526	0.026%
14	13.763	0.177%	206	15.504	0.087%
15	14.984	0.108%	210	16.401	0.061%
16	14.616	0.125%	212	21.316	0.008%
18	8.677	1.377%	214	8.402	1.539%
19	14.107	0.154%	224	4.104	8.730%
20	7.588	2.138%	232	24.966	0.002%
21	14.401	0.136%	249	23.879	0.003%
22	15.464	0.089%	250	9.005	1.206%
23	13.608	0.188%	270	27.476	0.001%
24	17.255	0.043%	271	10.912	0.559%
26	20.048	0.014%	278	19.809	0.015%
27	13.965	0.163%	287	22.146	0.006%
29	23.070	0.004%	292	19.555	0.017%
35	16.638	0.055%	303	18.323	0.028%
36	17.856	0.034%	305	19.836	0.015%
37	11.471	0.446%	312	10.898	0.562%
38	21.009	0.009%	314	24.821	0.002%
39	17.349	0.041%	329	5.894	4.236%
40	20.337	0.012%	339	23.104	0.004%
44	28.516	0.000%	347	24.128	0.003%
45	18.688	0.024%	359	23.430	0.004%
46	22.955	0.004%	365	19.689	0.016%

47	21.151	0.009%	371	18.019	0.032%
48	12.072	0.350%	379	13.978	0.162%
49	12.833	0.257%	388	13.834	0.172%
51	19.731	0.016%	427	22.648	0.005%
54	21.177	0.009%	435	21.818	0.007%
57	21.529	0.008%	505	19.261	0.019%
58	19.886	0.015%	517	20.608	0.011%
65	20.962	0.010%	522	18.541	0.026%
67	0.000	45.779%	538	23.637	0.003%
68	30.044	0.000%	541	25.588	0.001%
69	19.972	0.014%	562	13.810	0.173%
70	21.537	0.008%	567	23.527	0.003%
74	16.373	0.062%	571	15.010	0.107%
75	17.756	0.035%	611	23.026	0.004%
78	23.207	0.004%	642	24.462	0.002%
79	14.682	0.122%	764	16.207	0.066%
81	17.137	0.045%	823	17.903	0.033%
83	16.441	0.060%	866	18.919	0.022%
84	14.640	0.124%	878	23.307	0.004%
91	25.383	0.002%	999	22.269	0.006%
100	19.135	0.020%	1008	12.384	0.308%
101	6.519	3.291%	1018	24.905	0.002%
105	14.283	0.143%	1153	21.676	0.007%
109	16.444	0.060%	1172	15.816	0.077%
111	17.762	0.035%	1188	13.227	0.219%
116	13.443	0.201%	1219	21.684	0.007%
117	20.489	0.012%	1228	23.057	0.004%
123	13.419	0.203%	1262	27.381	0.001%
124	18.376	0.027%	1266	17.486	0.039%
128	16.795	0.052%	1268	7.745	2.006%
138	11.762	0.396%	1287	20.823	0.010%
141	15.378	0.092%	1319	25.354	0.002%
144	23.401	0.004%	1378	24.084	0.003%

The spin simulation tool available in MestReNova 9.0.1²⁶ was used to extract ^1H chemical shifts and $^nJ_{\text{HH}}$ where possible (Figure S51-Figure S52). Due to overlap and complex, broad peak shapes not all $^nJ_{\text{HH}}$ involving H4'a/b could be measured for **10A** or **10B** (Table S21, Table S22). Assignment of diastereotopic (a/b) ^1H was achieved using distinguishing experimental and computational $^nJ_{\text{HH}}$ such as the couplings between H1a/b and H2, which differ by between 5.3 and 8.8 Hz. Where this was not possible, such as H4'a/b and H5'a/b in **10A**, these were assigned by comparison of experimentally determined ^1H - ^1H distances and DFT-derived $r_{\text{effective}}$ ^1H - ^1H distances (Table S23, Table S24). In the case of H2'a/b and H4'a/b in **10B** the issues of overlap (in NOE-intensity measurements) and non-distinguishing $^nJ_{\text{HH}}$ meant that was not possible to assign the chemical shifts.

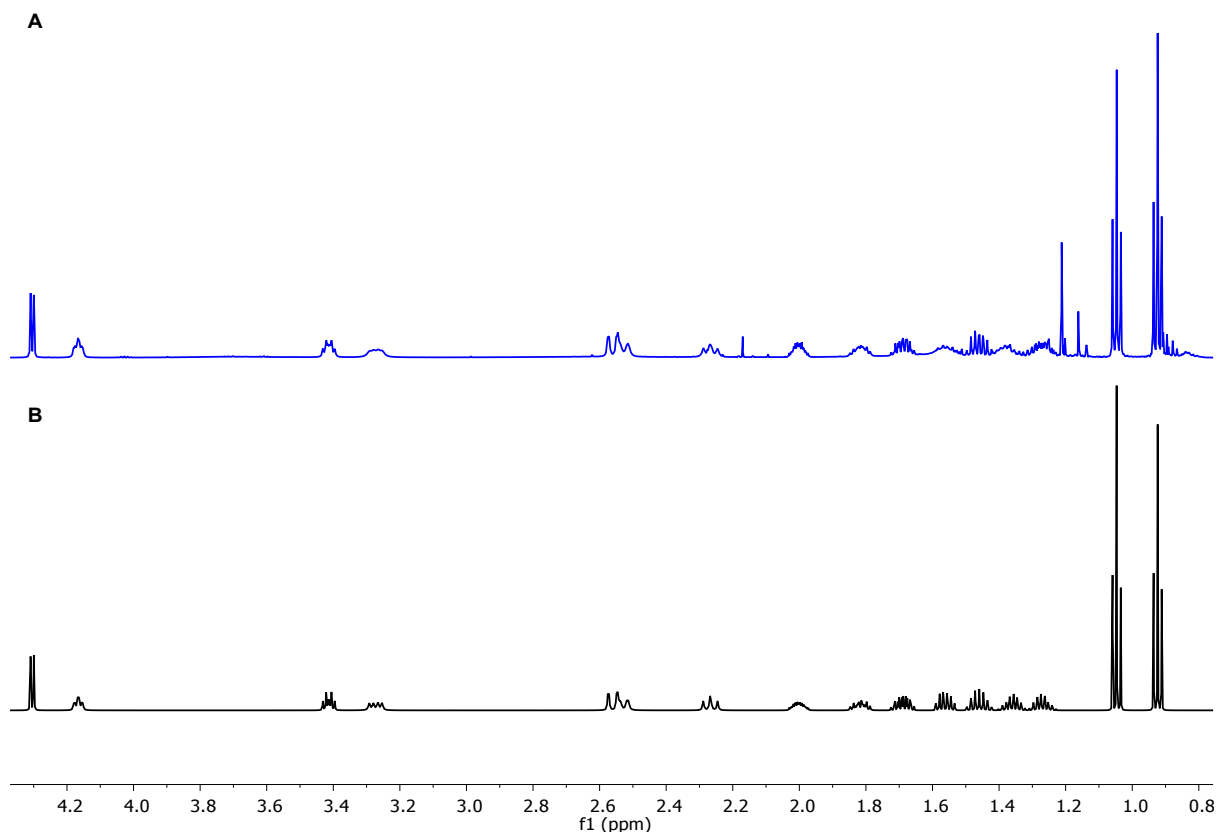


Figure S51: ^1H spectrum for **10A** in deuterated chloroform at 600 MHz A) experimental data, B) spin simulation.

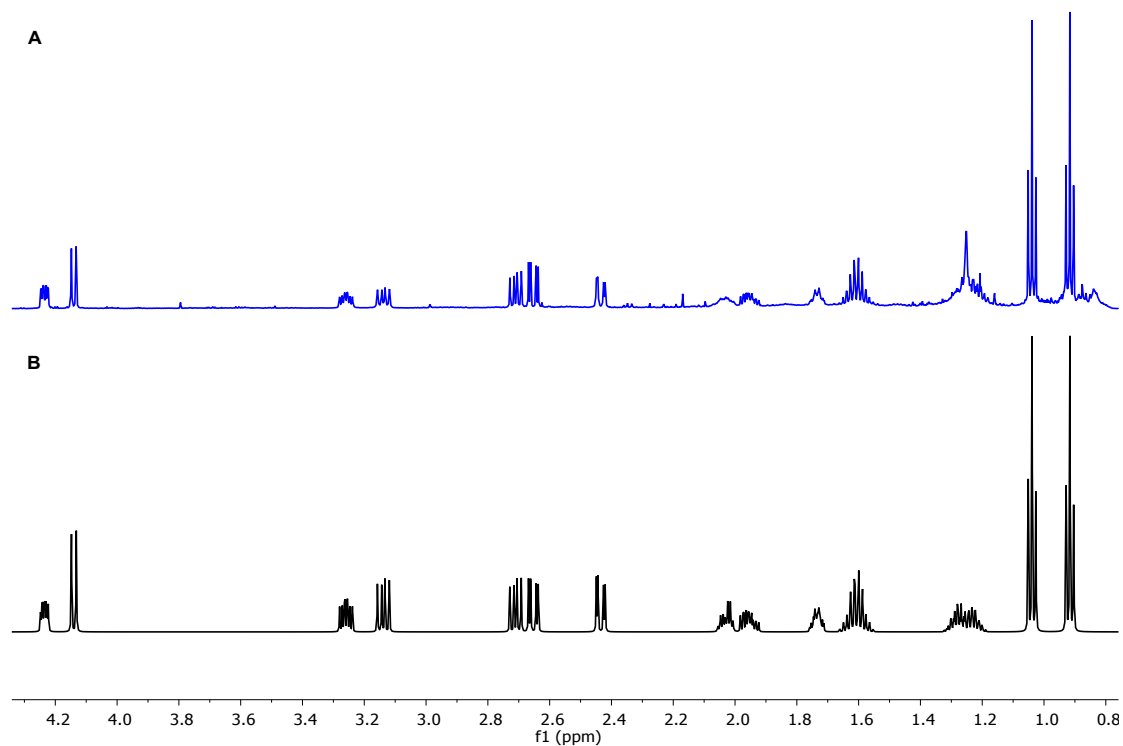


Figure S52: ^1H spectrum for **10B** in deuterated chloroform at 600 MHz A) experimental data, B) spin simulation.

Table S21: $^nJ_{\text{HH}}$ measured experimentally for **10A** compared to DFT-derived values for **10-RRRS** and **10-SRRS**. Experimental ^1H chemical shifts for **10A** referenced to internal chloroform at 7.258 ppm at 600 MHz. $^{\dagger}J_{\text{HH}} > 0.5\text{Hz}$ reported.

Label 1	Label 2	10-RRRS				10-SRRS			
		$\delta_{\text{exp 1}}$ /ppm	$\delta_{\text{exp 2}}$ /ppm	DFT $^nJ_{\text{HH}} / \text{Hz}^{\dagger}$	10A $^nJ_{\text{HH}} / \text{Hz}$	$\delta_{\text{exp 1}}$ /ppm	$\delta_{\text{exp 2}}$ /ppm	DFT $^nJ_{\text{HH}} / \text{Hz}^{\dagger}$	10A $^nJ_{\text{HH}} / \text{Hz}$
H1a	H1b	2.527	2.267	14.8	13.8	2.267	2.527	13.3	13.8
H1a	H2	2.527	2.002	3.4	3.2	2.267	2.002	8.9	12.0
H1a	H3	2.527	4.166	0.2		2.267	4.166	0.6	
H1b	H2	2.267	2.002	9.6	12.0	2.527	2.002	1.7	3.2
H2	H3	2.002	4.166	5.8	6.6	2.002	4.166	1.8	6.6
H2	H2'a	2.002	1.460	7.5	7.9	2.002	1.689	5.1	4.8
H2	H2'b	2.002	1.689	3.8	4.8	2.002	1.460	7.3	7.9
H3	H4a	4.166	2.561	3.2	2.4	4.166	2.561	3.0	2.4
H3	H4b	4.166	3.273	6.3	7.5	4.166	3.273	9.9	7.5
H4a	H4b	2.561	3.273	15.0	15.5	2.561	3.273	14.3	15.5
H6	H7	4.305	3.414	6.3	5.8	4.305	3.414	9.0	5.8
H7	H5'a	3.414	1.817	6.1	6.1	3.414	1.817	3.9	6.1
H7	H5'b	3.414	1.562	8.0	9.5	3.414	1.562	10.0	9.5
H1'	H2'a	1.047	1.460	6.4	7.4	1.047	1.689	6.5	7.4
H1'	H2'b	1.047	1.689	6.6	7.4	1.047	1.460	6.5	7.4
H2'a	H2'b	1.460	1.689	13.8	14.7	1.689	1.460	13.7	14.7
H3'	H4'a	0.924	1.270	6.4	7.3	0.924	1.270	6.4	7.3
H3'	H4'b	0.924	1.361	6.3	7.3	0.924	1.361	6.3	7.3
H4'a	H4'b	1.270	1.361	12.9		1.270	1.361	13.1	
H4'a	H5'a	1.270	1.817	9.8		1.270	1.817	10.0	
H4'a	H5'b	1.270	1.562	3.8		1.270	1.562	4.0	
H4'b	H5'a	1.361	1.817	4.6		1.361	1.817	5.2	
H4'b	H5'b	1.361	1.562	9.6		1.361	1.562	9.3	
H5'a	H5'b	1.817	1.562	13.6	13.9	1.817	1.562	13.7	13.9

Table S22: ${}^nJ_{\text{HH}}$ measured experimentally for **10B** compared to DFT-derived values for **10-RRRS** and **10-SRRS**. Experimental ${}^1\text{H}$ chemical shifts for **10B** referenced to internal chloroform at 7.258 ppm at 600 MHz. ${}^{\dagger}\text{DFT } {}^nJ_{\text{HH}} > 0.5\text{Hz}$ reported.

Label 1	Label 2	10-RRRS				10-SRRS			
		$\delta_{\text{exp 1}}$ /ppm	$\delta_{\text{exp 2}}$ /ppm	DFT ${}^nJ_{\text{HH}}$ / Hz †	10B ${}^nJ_{\text{HH}}$ / Hz	$\delta_{\text{exp 1}}$ /ppm	$\delta_{\text{exp 2}}$ /ppm	DFT ${}^nJ_{\text{HH}}$ / Hz †	10B ${}^nJ_{\text{HH}}$ / Hz
H1a	H1b	2.435	2.710	14.8	14.0	2.710	2.435	13.3	14.0
H1a	H2	2.435	1.735	3.4	3.0	2.710	1.735	8.9	8.3
H1a	H3	2.435	4.235	0.2		2.710	4.235	0.6	
H1b	H2	2.710	1.735	9.6	8.3	2.435	1.735	1.7	3.0
H2	H3	1.735	4.235	5.8	2.2	1.735	4.235	1.8	2.2
H2	H2'a	1.735	1.622/1.592	7.5	6.9	1.735	1.622/1.592	5.1	6.9
H2	H2'b	1.735	1.622/1.592	3.8	6.9	1.735	1.622/1.592	7.3	6.9
H3	H4a	4.235	2.653	3.2	4.1	4.235	2.653	3.0	4.1
H3	H4b	4.235	3.138	6.3	8.5	4.235	3.138	9.9	8.5
H4a	H4b	2.653	3.138	15.0	14.7	2.653	3.138	14.3	14.7
H6	H7	4.140	3.259	6.3	9.4	4.140	3.259	9.0	9.4
H7	H5'a	3.259	2.029	6.1	5.0	3.259	2.029	3.9	5.0
H7	H5'b	3.259	1.955	8.0	10.5	3.259	1.955	10.0	10.5
H1'	H2'a	1.039	1.622/1.592	6.4	7.4	1.039	1.622/1.592	6.5	7.4
H1'	H2'b	1.039	1.622/1.592	6.6	7.4	1.039	1.622/1.592	6.5	7.4
H2'a	H2'b	1.622/1.592	1.622/1.592	13.8	13.6	1.622/1.592	1.622/1.592	13.7	13.6
H3'	H4'a	0.916	1.229/1.283	6.4	7.3	0.916	1.229/1.283	6.4	7.3
H3'	H4'b	0.916	1.229/1.283	6.3	7.3	0.916	1.229/1.283	6.3	7.3
H4'a	H4'b	1.229/1.283	1.229/1.283	12.9		1.229/1.283	1.229/1.283	13.1	
H4'a	H5'a	1.229/1.283	2.029	9.8		1.229/1.283	2.029	10.0	
H4'a	H5'b	1.229/1.283	1.955	3.8		1.229/1.283	1.955	4.0	
H4'b	H5'a	1.229/1.283	2.029	4.6		1.229/1.283	2.029	5.2	
H4'b	H5'b	1.229/1.283	1.955	9.6	6.6	1.229/1.283	1.955	9.3	6.6
H5'a	H5'b	2.029	1.955	13.6	13.9	2.029	1.955	13.7	13.9

Table S23: Experimental ${}^1\text{H}$ - ${}^1\text{H}$ distances **10A**. η^{ref} was 89.14 (H1a-H1b) and r^{ref} set to 1.753Å for **10-RRRS** and 1.902Å for **10-SRRS**.

F1 Label	F2 Label	10-RRRS					10-SRRS				
		$\delta_{\text{exp F1}}$ /ppm	$\delta_{\text{exp F2}}$ /ppm	$r^{\text{effective}}$ / Å	η	$r_{\text{exp 10A}}$ /Å	$\delta_{\text{exp F1}}$ /ppm	$\delta_{\text{exp F2}}$ /ppm	$r^{\text{effective}}$ / Å	η	$r_{\text{exp 10A}}$ /Å
H01a	H01b	2.527	2.267	1.75	82.17	1.78	2.267	2.527	1.76	89.11	1.90
H01a	H02	2.527	2.002	2.49	19.14	2.27	2.267	2.002	2.97		
H01a	H03	2.527	4.166	3.91			2.267	4.166	3.68	6.69	2.93
H01a	H04a	2.527	2.561	4.40			2.267	2.561	3.57		
H01a	H04b	2.527	3.273	4.62			2.267	3.273	4.06		
H01a	H06	2.527	4.305	5.33			2.267	4.305	4.65	1.39	3.80
H01a	H07	2.527	3.414	3.89			2.267	3.414	2.31		
H01a	H01'	2.527	1.047	2.70	16.97	2.78	2.267	1.047	3.76		
H01a	H02'a	2.527	1.460	2.68	8.79	2.58	2.267	1.689	3.08	1.99	3.58
H01a	H02'b	2.527	1.689	3.03			2.267	1.460	2.77	8.48	2.81
H01a	H03'	2.527	0.924	5.57			2.267	0.924	4.25		
H01a	H04'a	2.527	1.270	4.42			2.267	1.270	4.12		
H01a	H04'b	2.527	1.361	4.70			2.267	1.361	3.70		
H01a	H05'a	2.527	1.817	3.80			2.267	1.562	4.60	13.96	2.59
H01a	H05'b	2.527	1.562	3.85			2.267	1.817	4.73	7.32	2.88
H01b	H01a	2.267	2.527	1.75	89.14	1.75	2.527	2.267	1.76	82.17	1.93
H01b	H02	2.267	2.002	2.99			2.527	2.002	2.58	19.14	2.46
H01b	H03	2.267	4.166	2.91	6.69	2.70	2.527	4.166	4.19		
H01b	H04a	2.267	2.561	3.30			2.527	2.561	3.92		
H01b	H04b	2.267	3.273	3.76			2.527	3.273	4.88		
H01b	H06	2.267	4.305	4.00	1.39	3.51	2.527	4.305	5.22		
H01b	H07	2.267	3.414	4.15			2.527	3.414	3.72		
H01b	H01'	2.267	1.047	3.45			2.527	1.047	2.72	16.97	3.01
H01b	H02'a	2.267	1.460	2.65	8.48	2.59	2.527	1.689	3.07		

H01b	H02'b	2.267	1.689	3.07	1.99	3.30	2.527	1.460	2.48	8.79	2.80
H01b	H03'	2.267	0.924	5.08			2.527	0.924	5.48		
H01b	H04'a	2.267	1.270	4.14			2.527	1.270	4.63		
H01b	H04'b	2.267	1.361	4.41			2.527	1.361	4.64		
H01b	H05'a	2.267	1.817	2.61	7.32	2.66	2.527	1.562	4.05		
H01b	H05'b	2.267	1.562	2.51	13.96	2.39	2.527	1.817	3.97		
H02	H01a	2.002	2.527	2.49	15.85	2.34	2.002	2.267	2.97		
H02	H01b	2.002	2.267	2.99			2.002	2.527	2.58	15.85	2.54
H02	H03	2.002	4.166	2.59	10.44	2.51	2.002	4.166	2.46	10.44	2.72
H02	H04a	2.002	2.561	3.65			2.002	2.561	2.44		
H02	H04b	2.002	3.273	3.11	3.61	2.99	2.002	3.273	3.31	3.61	3.25
H02	H06	2.002	4.305	5.25			2.002	4.305	4.91		
H02	H07	2.002	3.414	2.87			2.002	3.414	4.40		
H02	H01'	2.002	1.047	2.93	7.34	3.19	2.002	1.047	2.89	7.34	3.46
H02	H02'a	2.002	1.460	2.72	3.61	2.99	2.002	1.689	2.65	6.14	2.97
H02	H02'b	2.002	1.689	2.57	6.14	2.74	2.002	1.460	2.70	3.61	3.25
H02	H03'	2.002	0.924	6.82			2.002	0.924	7.48		
H02	H04'a	2.002	1.270	5.86			2.002	1.270	6.20		
H02	H04'b	2.002	1.361	5.52			2.002	1.361	6.21		
H02	H05'a	2.002	1.817	5.28			2.002	1.562	6.24		
H02	H05'b	2.002	1.562	5.29			2.002	1.817	5.61		
H03	H01a	4.166	2.527	3.91			4.166	2.267	3.68	6.40	2.95
H03	H01b	4.166	2.267	2.91	6.40	2.72	4.166	2.527	4.19		
H03	H02	4.166	2.002	2.59	14.08	2.38	4.166	2.002	2.46	14.08	2.59
H03	H04a	4.166	2.561	2.43	17.07	2.31	4.166	2.561	2.71	17.07	2.50
H03	H04b	4.166	3.273	2.52	8.26	2.61	4.166	3.273	2.25	8.26	2.83
H03	H06	4.166	4.305	4.88			4.166	4.305	4.96		
H03	H07	4.166	3.414	5.42			4.166	3.414	4.48		
H03	H01'	4.166	1.047	3.09	8.76	3.10	4.166	1.047	2.89	8.76	3.36
H03	H02'a	4.166	1.460	2.92	5.62	2.78	4.166	1.689	2.36	11.40	2.68
H03	H02'b	4.166	1.689	2.57	11.40	2.47	4.166	1.460	3.13	5.62	3.01
H03	H03'	4.166	0.924	7.63			4.166	0.924	8.10		
H03	H04'a	4.166	1.270	6.75			4.166	1.270	7.17		
H03	H04'b	4.166	1.361	6.48			4.166	1.361	6.81		
H03	H05'a	4.166	1.817	5.14			4.166	1.562	6.61		
H03	H05'b	4.166	1.562	5.14			4.166	1.817	6.82		
H04a	H01a	2.561	2.527	4.40			2.561	2.267	3.57		
H04a	H01b	2.561	2.267	3.30			2.561	2.527	3.92		
H04a	H02	2.561	2.002	3.65			2.561	2.002	2.44		
H04a	H03	2.561	4.166	2.43	17.40	2.30	2.561	4.166	2.71	17.40	2.50
H04a	H04b	2.561	3.273	1.76	66.22	1.84	2.561	3.273	1.75	66.22	2.00
H04a	H06	2.561	4.305	3.30	2.05	3.29	2.561	4.305	2.67	2.05	3.57
H04a	H07	2.561	3.414	4.43			2.561	3.414	3.44		
H04a	H01'	2.561	1.047	4.09			2.561	1.047	5.01		
H04a	H02'a	2.561	1.460	2.83			2.561	1.689	4.39		
H04a	H02'b	2.561	1.689	2.85			2.561	1.460	4.64		
H04a	H03'	2.561	0.924	7.06			2.561	0.924	6.90		
H04a	H04'a	2.561	1.270	5.95			2.561	1.270	5.58		
H04a	H04'b	2.561	1.361	5.66			2.561	1.361	5.58		
H04a	H05'a	2.561	1.817	4.30			2.561	1.562	5.06		
H04a	H05'b	2.561	1.562	3.76			2.561	1.817	4.81		
H04b	H01a	3.273	2.527	4.62			3.273	2.267	4.06		
H04b	H01b	3.273	2.267	3.76			3.273	2.527	4.88		
H04b	H02	3.273	2.002	3.11	4.05	2.93	3.273	2.002	3.31	4.05	3.18
H04b	H03	3.273	4.166	2.52	14.20	2.38	3.273	4.166	2.25	14.20	2.58
H04b	H04a	3.273	2.561	1.76	110.92	1.69	3.273	2.561	1.75	110.92	1.83
H04b	H06	3.273	4.305	3.40	4.73		3.273	4.305	3.36	4.73	
H04b	H07	3.273	3.414	4.41			3.273	3.414	3.83		
H04b	H01'	3.273	1.047	5.17			3.273	1.047	5.22		
H04b	H02'a	3.273	1.460	4.35			3.273	1.689	4.45		
H04b	H02'b	3.273	1.689	4.16			3.273	1.460	4.78		

H04b	H03'	3.273	0.924	7.35			3.273	0.924	7.77		
H04b	H04'a	3.273	1.270	6.09			3.273	1.270	6.73		
H04b	H04'b	3.273	1.361	5.80			3.273	1.361	6.41		
H04b	H05'a	3.273	1.817	4.93			3.273	1.562	5.66		
H04b	H05'b	3.273	1.562	4.97			3.273	1.817	5.82		
H06	H01a	4.305	2.527	5.33			4.305	2.267	4.65	1.09	3.96
H06	H01b	4.305	2.267	4.00	1.09	3.65	4.305	2.527	5.22		
H06	H02	4.305	2.002	5.25			4.305	2.002	4.91		
H06	H03	4.305	4.166	4.88			4.305	4.166	4.96		
H06	H04a	4.305	2.561	3.30	1.59	3.43	4.305	2.561	2.67	1.59	3.72
H06	H04b	4.305	3.273	3.40	1.67	3.40	4.305	3.273	3.36	1.67	3.69
H06	H07	4.305	3.414	2.44	12.51	2.43	4.305	3.414	2.93	12.51	2.64
H06	H01'	4.305	1.047	7.32			4.305	1.047	7.50		
H06	H02'a	4.305	1.460	5.93			4.305	1.689	6.66		
H06	H02'b	4.305	1.689	6.13			4.305	1.460	6.70		
H06	H03'	4.305	0.924	4.50			4.305	0.924	5.44		
H06	H04'a	4.305	1.270	3.17	2.68	3.14	4.305	1.270	4.22	2.68	3.41
H06	H04'b	4.305	1.361	2.68	4.38	2.90	4.305	1.361	3.85	4.38	3.14
H06	H05'a	4.305	1.817	2.65	10.85	2.49	4.305	1.562	3.12	2.11	3.55
H06	H05'b	4.305	1.562	3.21	2.11	3.27	4.305	1.817	2.86	10.85	2.70
H07	H01a	3.414	2.527	3.89			3.414	2.267	2.31		
H07	H01b	3.414	2.267	4.15			3.414	2.527	3.72		
H07	H02	3.414	2.002	2.87			3.414	2.002	4.40		
H07	H03	3.414	4.166	5.42			3.414	4.166	4.48		
H07	H04a	3.414	2.561	4.43			3.414	2.561	3.44		
H07	H04b	3.414	3.273	4.41			3.414	3.273	3.83		
H07	H06	3.414	4.305	2.44	23.05	2.20	3.414	4.305	2.93	23.05	2.38
H07	H01'	3.414	1.047	6.03			3.414	1.047	6.26		
H07	H02'a	3.414	1.460	5.89			3.414	1.689	5.14		
H07	H02'b	3.414	1.689	5.77			3.414	1.460	4.90		
H07	H03'	3.414	0.924	3.46			3.414	0.924	3.36		
H07	H04'a	3.414	1.270	2.77	4.29	2.91	3.414	1.270	3.05	4.29	3.15
H07	H04'b	3.414	1.361	2.68	5.30	2.81	3.414	1.361	2.59	5.30	3.04
H07	H05'a	3.414	1.817	2.60	10.65	2.50	3.414	1.562	2.48	3.88	3.21
H07	H05'b	3.414	1.562	2.72	3.88	2.96	3.414	1.817	2.98	10.65	2.71
H01'	H01a	1.047	2.527	2.70	4.97	2.84	1.047	2.267	3.76		
H01'	H01b	1.047	2.267	3.45			1.047	2.527	2.72	4.97	3.08
H01'	H02	1.047	2.002	2.93	3.73	2.97	1.047	2.002	2.89	3.73	3.23
H01'	H03	1.047	4.166	3.09	2.42	3.20	1.047	4.166	2.89	2.42	3.47
H01'	H04a	1.047	2.561	4.09			1.047	2.561	5.01		
H01'	H04b	1.047	3.273	5.17			1.047	3.273	5.22		
H01'	H06	1.047	4.305	7.32			1.047	4.305	7.50		
H01'	H07	1.047	3.414	6.03			1.047	3.414	6.26		
H01'	H02'a	1.047	1.460	2.62			1.047	1.689	2.61		
H01'	H02'b	1.047	1.689	2.61	2.89		1.047	1.460	2.62		
H01'	H03'	1.047	0.924	7.75			1.047	0.924	9.00		
H01'	H04'a	1.047	1.270	7.10			1.047	1.270	7.66		
H01'	H04'b	1.047	1.361	6.92			1.047	1.361	7.60		
H01'	H05'a	1.047	1.817	6.44			1.047	1.562	8.43		
H01'	H05'b	1.047	1.562	6.17			1.047	1.817	8.30		
H02'a	H01a	1.460	2.527	2.68			1.689	2.267	3.08	4.49	3.13
H02'a	H01b	1.460	2.267	2.65	8.54	2.59	1.689	2.527	3.07	3.46	
H02'a	H02	1.460	2.002	2.72	6.91	2.68	1.689	2.002	2.65	10.56	2.71
H02'a	H03	1.460	4.166	2.92	4.76	2.86	1.689	4.166	2.36	9.98	2.74
H02'a	H04a	1.460	2.561	2.83			1.689	2.561	4.39	8.00	
H02'a	H04b	1.460	3.273	4.35			1.689	3.273	4.45		
H02'a	H06	1.460	4.305	5.93			1.689	4.305	6.66		
H02'a	H07	1.460	3.414	5.89			1.689	3.414	5.14		
H02'a	H01'	1.460	1.047	2.62			1.689	1.047	2.61	13.08	3.14
H02'a	H02'b	1.460	1.689	1.75			1.689	1.460	1.75	61.20	2.02
H02'a	H03'	1.460	0.924	7.39			1.689	0.924	7.60		

H02'a	H04'a	1.460	1.270	6.68			1.689	1.270	7.36		
H02'a	H04'b	1.460	1.361	6.69			1.689	1.361	6.93		
H02'a	H05'a	1.460	1.817	5.33			1.689	1.562	7.49		
H02'a	H05'b	1.460	1.562	5.15			1.689	1.817	7.65		
H02'b	H01a	1.689	2.527	3.03	3.46		1.460	2.267	2.77	8.54	2.81
H02'b	H01b	1.689	2.267	3.07	4.49	2.88	1.460	2.527	2.48		
H02'b	H02	1.689	2.002	2.57	10.56	2.50	1.460	2.002	2.70	6.91	2.91
H02'b	H03	1.689	4.166	2.57	9.98	2.52	1.460	4.166	3.13	4.76	3.10
H02'b	H04a	1.689	2.561	2.85	8.00		1.460	2.561	4.64		
H02'b	H04b	1.689	3.273	4.16			1.460	3.273	4.78		
H02'b	H06	1.689	4.305	6.13			1.460	4.305	6.70		
H02'b	H07	1.689	3.414	5.77			1.460	3.414	4.90		
H02'b	H01'	1.689	1.047	2.61	13.08	2.90	1.460	1.047	2.62		
H02'b	H02'a	1.689	1.460	1.75	61.20	1.87	1.460	1.689	1.75		
H02'b	H03'	1.689	0.924	7.88			1.460	0.924	7.65		
H02'b	H04'a	1.689	1.270	7.08			1.460	1.270	6.79		
H02'b	H04'b	1.689	1.361	6.90			1.460	1.361	6.35		
H02'b	H05'a	1.689	1.817	5.79			1.460	1.562	7.21		
H02'b	H05'b	1.689	1.562	5.73			1.460	1.817	7.33		
H03'	H01a	0.924	2.527	5.57			0.924	2.267	4.25		
H03'	H01b	0.924	2.267	5.08			0.924	2.527	5.48		
H03'	H02	0.924	2.002	6.82			0.924	2.002	7.48		
H03'	H03	0.924	4.166	7.63			0.924	4.166	8.10		
H03'	H04a	0.924	2.561	7.06			0.924	2.561	6.90		
H03'	H04b	0.924	3.273	7.35			0.924	3.273	7.77		
H03'	H06	0.924	4.305	4.50			0.924	4.305	5.44		
H03'	H07	0.924	3.414	3.46			0.924	3.414	3.36		
H03'	H01'	0.924	1.047	7.75			0.924	1.047	9.00		
H03'	H02'a	0.924	1.460	7.39			0.924	1.689	7.60		
H03'	H02'b	0.924	1.689	1.76			0.924	1.460	1.76		
H03'	H04'a	0.924	1.270	2.62			0.924	1.270	2.61		
H03'	H04'b	0.924	1.361	2.62			0.924	1.361	2.62		
H03'	H05'a	0.924	1.817	2.95	2.90	3.10	0.924	1.562	2.92	2.36	3.48
H03'	H05'b	0.924	1.562	2.95	2.36	3.21	0.924	1.817	3.03	2.90	3.37
H04'a	H01a	1.270	2.527	4.42			1.270	2.267	4.12		
H04'a	H01b	1.270	2.267	4.14			1.270	2.527	4.63		
H04'a	H02	1.270	2.002	5.86			1.270	2.002	6.20		
H04'a	H03	1.270	4.166	6.75			1.270	4.166	7.17		
H04'a	H04a	1.270	2.561	5.95			1.270	2.561	5.58		
H04'a	H04b	1.270	3.273	6.09			1.270	3.273	6.73		
H04'a	H06	1.270	4.305	3.17	2.27	3.23	1.270	4.305	4.22	2.27	3.51
H04'a	H07	1.270	3.414	2.77	3.23	3.05	1.270	3.414	3.05	3.21	3.31
H04'a	H01'	1.270	1.047	7.10			1.270	1.047	7.66		
H04'a	H02'a	1.270	1.460	6.68			1.270	1.689	7.36		
H04'a	H02'b	1.270	1.689	7.08			1.270	1.460	6.79		
H04'a	H03'	1.270	0.924	2.62			1.270	0.924	2.61		
H04'a	H04'b	1.270	1.270	1.75			1.270	1.361	1.75		
H04'a	H05'a	1.270	1.817	2.88			1.270	1.562	2.85		
H04'a	H05'b	1.270	1.562	2.52			1.270	1.817	2.49		
H04'b	H01a	1.361	2.527	4.70			1.361	2.267	3.70	2.07	
H04'b	H01b	1.361	2.267	4.41	2.07		1.361	2.527	4.64		
H04'b	H02	1.361	2.002	5.52			1.361	2.002	6.21		
H04'b	H03	1.361	4.166	6.48			1.361	4.166	6.81		
H04'b	H04a	1.361	2.561	5.66			1.361	2.561	5.58		
H04'b	H04b	1.361	3.273	5.80			1.361	3.273	6.41		
H04'b	H06	1.361	4.305	2.68	5.14	2.82	1.361	4.305	3.85	5.14	3.06
H04'b	H07	1.361	3.414	2.68	5.36	2.80	1.361	3.414	2.59	5.36	3.04
H04'b	H01'	1.361	1.047	6.92			1.361	1.047	7.60		
H04'b	H02'a	1.361	1.460	6.69			1.361	1.689	6.93		
H04'b	H02'b	1.361	1.689	6.90			1.361	1.460	6.35		
H04'b	H03'	1.361	0.924	2.62			1.361	0.924	2.62		

H04'b	H04'a	1.361	1.361	1.75			1.361	1.270	1.75		
H04'b	H05'a	1.361	1.817	2.52			1.361	1.562	2.57		
H04'b	H05'b	1.361	1.562	2.88			1.361	1.817	2.86		
H05'a	H01a	1.817	2.527	3.80			1.562	2.267	4.60	16.16	2.53
H05'a	H01b	1.817	2.267	2.61	9.72	2.54	1.562	2.527	4.05		
H05'a	H02	1.817	2.002	5.28			1.562	2.002	6.24		
H05'a	H03	1.817	4.166	5.14			1.562	4.166	6.61		
H05'a	H04a	1.817	2.561	4.30			1.562	2.561	5.06		
H05'a	H04b	1.817	3.273	4.93			1.562	3.273	5.66		
H05'a	H06	1.817	4.305	2.65	12.53	2.43	1.562	4.305	3.12	2.38	3.48
H05'a	H07	1.817	3.414	2.60	8.97	2.57	1.562	3.414	2.48	4.04	3.18
H05'a	H01'	1.817	1.047	6.44			1.562	1.047	8.43		
H05'a	H02'a	1.817	1.460	5.33			1.562	1.689	7.49		
H05'a	H02'b	1.817	1.689	5.79			1.562	1.460	7.21		
H05'a	H03'	1.817	0.924	2.95	7.59	3.17	1.562	0.924	2.92		
H05'a	H04'a	1.817	1.270	2.88			1.562	1.270	2.85		
H05'a	H04'b	1.817	1.361	2.52			1.562	1.361	2.57		
H05'a	H05'b	1.817	1.562	1.75			1.562	1.817	1.75		
H05'b	H01a	1.562	2.527	3.85			1.817	2.267	4.73	9.72	2.75
H05'b	H01b	1.562	2.267	2.51	16.16	2.33	1.817	2.527	3.97		
H05'b	H02	1.562	2.002	5.29			1.817	2.002	5.61		
H05'b	H03	1.562	4.166	5.14			1.817	4.166	6.82		
H05'b	H04a	1.562	2.561	3.76			1.817	2.561	4.81		
H05'b	H04b	1.562	3.273	4.97			1.817	3.273	5.82		
H05'b	H06	1.562	4.305	3.21	2.38	3.21	1.817	4.305	2.86	12.53	2.64
H05'b	H07	1.562	3.414	2.72	4.04	2.94	1.817	3.414	2.98	8.97	2.79
H05'b	H01'	1.562	1.047	6.17			1.817	1.047	8.30		
H05'b	H02'a	1.562	1.460	5.15			1.817	1.689	7.65		
H05'b	H02'b	1.562	1.689	5.73			1.817	1.460	7.33		
H05'b	H03'	1.562	0.924	2.95			1.817	0.924	3.03	7.59	3.44
H05'b	H04'a	1.562	1.270	2.52			1.817	1.270	2.49		
H05'b	H04'b	1.562	1.361	2.88			1.817	1.361	2.86		
H05'b	H05'a	1.562	1.817	1.75			1.817	1.562	1.75		

Table S24: Experimental ^1H - ^1H distances **10B**. η^{ref} was 87.40 (H1a-H1b) and r^{ref} set to 1.894Å for **10-RRRS** and 1.829Å for **10-SRRS**.

F1 Label	F2 Label	10-RRRS					10-SRRS				
		$\delta_{exp} \text{ F1} / \text{ppm}$	$\delta_{exp} \text{ F2} / \text{ppm}$	$r^{effective} / \text{Å}$	η	$r_{exp}^{10B} / \text{Å}$	$\delta_{exp} \text{ F1} / \text{ppm}$	$\delta_{exp} \text{ F2} / \text{ppm}$	$r^{effective} / \text{Å}$	η	$r_{exp}^{10B} / \text{Å}$
H01a	H01b	2.435	2.710	1.75	70.04	1.97	2.710	2.435	1.76	87.43	1.83
H01a	H02	2.435	1.735	2.49	13.63	2.58	2.710	1.735	2.97	5.58	2.89
H01a	H03	2.435	4.235	3.91			2.710	4.235	3.68	1.27	3.70
H01a	H04a	2.435	2.653	4.40			2.710	2.653	3.57		
H01a	H04b	2.435	3.138	4.62			2.710	3.138	4.06	5.07	2.94
H01a	H06	2.435	4.140	5.33			2.710	4.140	4.65		
H01a	H07	2.435	3.259	3.89			2.710	3.259	2.31	20.45	2.33
H01a	H01'	2.435	1.039	2.70	8.79	3.34	2.710	1.039	3.76	4.28	3.63
H01a	H02'a	2.435	1.622/1.592	2.68			2.710	1.622/1.592	3.08		
H01a	H02'b	2.435	1.592/1.622	3.03			2.710	1.592/1.622	2.77		
H01a	H03'	2.435	0.916	5.57			2.710	0.916	4.25		
H01a	H04'a	2.435	1.229/1.283	4.42			2.710	1.229/1.283	4.12		
H01a	H04'b	2.435	1.229/1.283	4.70			2.710	1.229/1.283	3.70		
H01a	H05'a	2.435	2.029	3.80	3.14	3.30	2.710	2.029	4.60		
H01a	H05'b	2.435	1.955	3.85	2.17	3.51	2.710	1.955	4.73		
H01b	H01a	2.710	2.710	1.75	87.43	1.89	2.435	2.710	1.76	70.04	1.90
H01b	H02	2.710	1.735	2.99	5.58	3.00	2.435	1.735	2.58	13.63	2.49
H01b	H03	2.710	4.235	2.91	1.27	3.83	2.435	4.235	4.19		
H01b	H04a	2.710	2.653	3.30			2.435	2.653	3.92		
H01b	H04b	2.710	3.138	3.76	5.07	3.04	2.435	3.138	4.88		

H01b	H06	2.710	4.140	4.00			2.435	4.140	5.22		
H01b	H07	2.710	3.259	4.15	20.45	2.41	2.435	3.259	3.72		
H01b	H01'	2.710	1.039	3.45	4.28	3.76	2.435	1.039	2.72	8.79	3.22
H01b	H02'a	2.710	1.622/1.592	2.65			2.435	1.622/1.592	3.07		
H01b	H02'b	2.710	1.592/1.622	3.07			2.435	1.592/1.622	2.48		
H01b	H03'	2.710	0.916	5.08			2.435	0.916	5.48		
H01b	H04'a	2.710	1.229/1.283	4.14			2.435	1.229/1.283	4.63		
H01b	H04'b	2.710	1.229/1.283	4.41			2.435	1.229/1.283	4.64		
H01b	H05'a	2.710	2.029	2.61			2.435	2.029	4.05	3.14	3.18
H01b	H05'b	2.710	1.955	2.51			2.435	1.955	3.97	2.17	3.39
H02	H01a	1.735	2.435	2.49	10.69	2.69	1.735	2.710	2.97		
H02	H01b	1.735	2.710	2.99			1.735	2.435	2.58	10.69	2.60
H02	H03	1.735	4.235	2.59	14.97	2.54	1.735	4.235	2.46	14.97	2.45
H02	H04a	1.735	2.653	3.65	9.90	2.72	1.735	2.653	2.44	9.90	2.63
H02	H04b	1.735	3.138	3.11			1.735	3.138	3.31		
H02	H06	1.735	4.140	5.25			1.735	4.140	4.91		
H02	H07	1.735	3.259	2.87			1.735	3.259	4.40		
H02	H01'	1.735	1.039	2.93	9.68	3.28	1.735	1.039	2.89	9.68	3.17
H02	H02'a	1.735	1.622/1.592	2.72			1.735	1.622/1.592	2.65		
H02	H02'b	1.735	1.592/1.622	2.57			1.735	1.592/1.622	2.70		
H02	H03'	1.735	0.916	6.82			1.735	0.916	7.48		
H02	H04'a	1.735	1.229/1.283	5.86			1.735	1.229/1.283	6.20		
H02	H04'b	1.735	1.229/1.283	5.52			1.735	1.229/1.283	6.21		
H02	H05'a	1.735	2.029	5.28			1.735	2.029	6.24		
H02	H05'b	1.735	1.955	5.29			1.735	1.955	5.61		
H03	H01a	4.235	2.435	3.91			4.235	2.710	3.68	1.10	3.79
H03	H01b	4.235	2.710	2.91	1.10	3.93	4.235	2.435	4.19		
H03	H02	4.235	1.735	2.59	16.87	2.49	4.235	1.735	2.46	16.87	2.41
H03	H04a	4.235	2.653	2.43	12.54	2.62	4.235	2.653	2.71	12.54	2.53
H03	H04b	4.235	3.138	2.52	15.07	2.54	4.235	3.138	2.25	15.07	2.45
H03	H06	4.235	4.140	4.88			4.235	4.140	4.96		
H03	H07	4.235	3.259	5.42			4.235	3.259	4.48		
H03	H01'	4.235	1.039	3.09	9.87	3.27	4.235	1.039	2.89	9.87	3.16
H03	H02'a	4.235	1.622/1.592	2.92			4.235	1.622/1.592	2.36		
H03	H02'b	4.235	1.592/1.622	2.57			4.235	1.592/1.622	3.13		
H03	H03'	4.235	0.916	7.63			4.235	0.916	8.10		
H03	H04'a	4.235	1.229/1.283	6.75			4.235	1.229/1.283	7.17		
H03	H04'b	4.235	1.229/1.283	6.48			4.235	1.229/1.283	6.81		
H03	H05'a	4.235	2.029	5.14			4.235	2.029	6.61		
H03	H05'b	4.235	1.955	5.14			4.235	1.955	6.82		
H04a	H01a	2.653	2.435	4.40			2.653	2.710	3.57		
H04a	H01b	2.653	2.710	3.30			2.653	2.435	3.92		
H04a	H02	2.653	1.735	3.65	11.31	2.66	2.653	1.735	2.44	11.31	2.57
H04a	H03	2.653	4.235	2.43	13.54	2.58	2.653	4.235	2.71	13.54	2.50
H04a	H04b	2.653	3.138	1.76	94.58	1.87	2.653	3.138	1.75	94.58	1.81
H04a	H06	2.653	4.140	3.30	5.66	2.99	2.653	4.140	2.67	5.66	2.89
H04a	H07	2.653	3.259	4.43	1.09	3.93	2.653	3.259	3.44	1.09	3.80
H04a	H01'	2.653	1.039	4.09			2.653	1.039	5.01		
H04a	H02'a	2.653	1.622/1.592	2.83			2.653	1.622/1.592	4.39		
H04a	H02'b	2.653	1.592/1.622	2.85			2.653	1.592/1.622	4.64		
H04a	H03'	2.653	0.916	7.06			2.653	0.916	6.90		
H04a	H04'a	2.653	1.229/1.283	5.95			2.653	1.229/1.283	5.58		
H04a	H04'b	2.653	1.229/1.283	5.66			2.653	1.229/1.283	5.58		
H04a	H05'a	2.653	2.029	4.30			2.653	2.029	5.06		
H04a	H05'b	2.653	1.955	3.76			2.653	1.955	4.81		
H04b	H01a	3.138	2.435	4.62			3.138	2.710	4.06	4.84	2.96
H04b	H01b	3.138	2.710	3.76	4.84	3.07	3.138	2.435	4.88		
H04b	H02	3.138	1.735	3.11			3.138	1.735	3.31		
H04b	H03	3.138	4.235	2.52	16.99	2.49	3.138	4.235	2.25	16.99	2.40
H04b	H04a	3.138	2.653	1.76	105.94	1.83	3.138	2.653	1.75	105.94	1.77
H04b	H06	3.138	4.140	3.40	1.53	3.72	3.138	4.140	3.36	1.53	3.59

H04b	H07	3.138	3.259	4.41	4.23	3.14	3.138	3.259	3.83	4.23	3.03
H04b	H01'	3.138	1.039	5.17			3.138	1.039	5.22		
H04b	H02'a	3.138	1.622/1.592	4.35			3.138	1.622/1.592	4.45		
H04b	H02'b	3.138	1.592/1.622	4.16			3.138	1.592/1.622	4.78		
H04b	H03'	3.138	0.916	7.35			3.138	0.916	7.77		
H04b	H04'a	3.138	1.229/1.283	6.09			3.138	1.229/1.283	6.73		
H04b	H04'b	3.138	1.229/1.283	5.80			3.138	1.229/1.283	6.41		
H04b	H05'a	3.138	2.029	4.93			3.138	2.029	5.66		
H04b	H05'b	3.138	1.955	4.97			3.138	1.955	5.82		
H06	H01a	4.140	2.435	5.33			4.140	2.710	4.65		
H06	H01b	4.140	2.710	4.00			4.140	2.435	5.22		
H06	H02	4.140	1.735	5.25			4.140	1.735	4.91		
H06	H03	4.140	4.235	4.88			4.140	4.235	4.96		
H06	H04a	4.140	2.653	3.30	5.44	3.01	4.140	2.653	2.67	5.44	2.91
H06	H04b	4.140	3.138	3.40	1.70	3.65	4.140	3.138	3.36	1.70	3.53
H06	H07	4.140	3.259	2.44	8.82	2.78	4.140	3.259	2.93	8.82	2.68
H06	H01'	4.140	1.039	7.32			4.140	1.039	7.50		
H06	H02'a	4.140	1.622/1.592	5.93			4.140	1.622/1.592	6.66		
H06	H02'b	4.140	1.592/1.622	6.13			4.140	1.592/1.622	6.70		
H06	H03'	4.140	0.916	4.50			4.140	0.916	5.44		
H06	H04'a	4.140	1.229/1.283	3.17			4.140	1.229/1.283	4.22		
H06	H04'b	4.140	1.229/1.283	2.68			4.140	1.229/1.283	3.85		
H06	H05'a	4.140	2.029	2.65	5.80	2.98	4.140	2.029	3.12	5.80	2.88
H06	H05'b	4.140	1.955	3.21	4.73	3.08	4.140	1.955	2.86	4.73	2.97
H07	H01a	3.259	2.435	3.89	17.33	2.48	3.259	2.710	2.31	17.33	2.40
H07	H01b	3.259	2.710	4.15			3.259	2.435	3.72		
H07	H02	3.259	1.735	2.87			3.259	1.735	4.40		
H07	H03	3.259	4.235	5.42			3.259	4.235	4.48		
H07	H04a	3.259	2.653	4.43			3.259	2.653	3.44		
H07	H04b	3.259	3.138	4.41	4.11	3.15	3.259	3.138	3.83	4.11	3.04
H07	H06	3.259	4.140	2.44			3.259	4.140	2.93		
H07	H01'	3.259	1.039	6.03			3.259	1.039	6.26		
H07	H02'a	3.259	1.622/1.592	5.89			3.259	1.622/1.592	5.14		
H07	H02'b	3.259	1.592/1.622	5.77			3.259	1.592/1.622	4.90		
H07	H03'	3.259	0.916	3.46	4.56	3.72	3.259	0.916	3.36	4.56	3.59
H07	H04'a	3.259	1.229/1.283	2.77			3.259	1.229/1.283	3.05		
H07	H04'b	3.259	1.229/1.283	2.68			3.259	1.229/1.283	2.59		
H07	H05'a	3.259	2.029	2.60	4.92	3.06	3.259	2.029	2.48	4.92	2.95
H07	H05'b	3.259	1.955	2.72	11.04	2.67	3.259	1.955	2.98	11.04	2.58
H01'	H01a	1.039	2.435	2.70	2.39	3.45	1.039	2.710	3.76	1.22	3.73
H01'	H01b	1.039	2.710	3.45	1.22	3.86	1.039	2.435	2.72	2.39	3.33
H01'	H02	1.039	1.735	2.93	3.58	3.23	1.039	1.735	2.89	3.58	3.12
H01'	H03	1.039	4.235	3.09	3.29	3.27	1.039	4.235	2.89	3.29	3.16
H01'	H04a	1.039	2.653	4.09			1.039	2.653	5.01		
H01'	H04b	1.039	3.138	5.17			1.039	3.138	5.22		
H01'	H06	1.039	4.140	7.32			1.039	4.140	7.50		
H01'	H07	1.039	3.259	6.03			1.039	3.259	6.26		
H01'	H02'a	1.039	1.622/1.592	2.62			1.039	1.622/1.592	2.61		
H01'	H02'b	1.039	1.592/1.622	2.61			1.039	1.592/1.622	2.62		
H01'	H03'	1.039	0.916	7.75			1.039	0.916	9.00		
H01'	H04'a	1.039	1.229/1.283	7.10			1.039	1.229/1.283	7.66		
H01'	H04'b	1.039	1.229/1.283	6.92			1.039	1.229/1.283	7.60		
H01'	H05'a	1.039	2.029	6.44			1.039	2.029	8.43		
H01'	H05'b	1.039	1.955	6.17			1.039	1.955	8.30		
H02'a	H01a	1.622/1.592	2.435	2.68			1.622/1.592	2.710	3.08		
H02'a	H01b	1.622/1.592	2.710	2.65			1.622/1.592	2.435	3.07		
H02'a	H02	1.622/1.592	1.735	2.72			1.622/1.592	1.735	2.65		
H02'a	H03	1.622/1.592	4.235	2.92			1.622/1.592	4.235	2.36		
H02'a	H04a	1.622/1.592	2.653	2.83			1.622/1.592	2.653	4.39		
H02'a	H04b	1.622/1.592	3.138	4.35			1.622/1.592	3.138	4.45		
H02'a	H06	1.622/1.592	4.140	5.93			1.622/1.592	4.140	6.66		

H02'a	H07	1.622/1.592	3.259	5.89			1.622/1.592	3.259	5.14		
H02'a	H01'	1.622/1.592	1.039	2.62			1.622/1.592	1.039	2.61		
H02'a	H02'b	1.622/1.592	1.592/1.622	1.75			1.622/1.592	1.592/1.622	1.75		
H02'a	H03'	1.622/1.592	0.916	7.39			1.622/1.592	0.916	7.60		
H02'a	H04'a	1.622/1.592	1.229/1.283	6.68			1.622/1.592	1.229/1.283	7.36		
H02'a	H04'b	1.622/1.592	1.229/1.283	6.69			1.622/1.592	1.229/1.283	6.93		
H02'a	H05'a	1.622/1.592	2.029	5.33			1.622/1.592	2.029	7.49		
H02'a	H05'b	1.622/1.592	1.955	5.15			1.622/1.592	1.955	7.65		
H02'b	H01a	1.592/1.622	2.435	3.03			1.592/1.622	2.710	2.77		
H02'b	H01b	1.592/1.622	2.710	3.07			1.592/1.622	2.435	2.48		
H02'b	H02	1.592/1.622	1.735	2.57			1.592/1.622	1.735	2.70		
H02'b	H03	1.592/1.622	4.235	2.57			1.592/1.622	4.235	3.13		
H02'b	H04a	1.592/1.622	2.653	2.85			1.592/1.622	2.653	4.64		
H02'b	H04b	1.592/1.622	3.138	4.16			1.592/1.622	3.138	4.78		
H02'b	H06	1.592/1.622	4.140	6.13			1.592/1.622	4.140	6.70		
H02'b	H07	1.592/1.622	3.259	5.77			1.592/1.622	3.259	4.90		
H02'b	H01'	1.592/1.622	1.039	2.61			1.592/1.622	1.039	2.62		
H02'b	H02'a	1.592/1.622	1.622/1.592	1.75			1.592/1.622	1.622/1.592	1.75		
H02'b	H03'	1.592/1.622	0.916	7.88			1.592/1.622	0.916	7.65		
H02'b	H04'a	1.592/1.622	1.229/1.283	7.08			1.592/1.622	1.229/1.283	6.79		
H02'b	H04'b	1.592/1.622	1.229/1.283	6.90			1.592/1.622	1.229/1.283	6.35		
H02'b	H05'a	1.592/1.622	2.029	5.79			1.592/1.622	2.029	7.21		
H02'b	H05'b	1.592/1.622	1.955	5.73			1.592/1.622	1.955	7.33		
H03'	H01a	0.916	2.435	5.57			0.916	2.710	4.25		
H03'	H01b	0.916	2.710	5.08			0.916	2.435	5.48		
H03'	H02	0.916	1.735	6.82			0.916	1.735	7.48		
H03'	H03	0.916	4.235	7.63			0.916	4.235	8.10		
H03'	H04a	0.916	2.653	7.06			0.916	2.653	6.90		
H03'	H04b	0.916	3.138	7.35			0.916	3.138	7.77		
H03'	H06	0.916	4.140	4.50			0.916	4.140	5.44		
H03'	H07	0.916	3.259	3.46	1.15	3.90	0.916	3.259	3.36	1.15	3.76
H03'	H01'	0.916	1.039	7.75			0.916	1.039	9.00		
H03'	H02'a	0.916	1.622/1.592	7.39			0.916	1.622/1.592	7.60		
H03'	H02'b	0.916	1.592/1.622	1.76			0.916	1.592/1.622	1.76		
H03'	H04'a	0.916	1.229/1.283	2.62			0.916	1.229/1.283	2.61		
H03'	H04'b	0.916	1.229/1.283	2.62			0.916	1.229/1.283	2.62		
H03'	H05'a	0.916	2.029	2.95	2.06	3.54	0.916	2.029	2.92	2.06	3.42
H03'	H05'b	0.916	1.955	2.95	2.58	3.41	0.916	1.955	3.03	2.58	3.29
H04'a	H01a	1.229/1.283	2.435	4.42			1.229/1.283	2.710	4.12		
H04'a	H01b	1.229/1.283	2.710	4.14			1.229/1.283	2.435	4.63		
H04'a	H02	1.229/1.283	1.735	5.86			1.229/1.283	1.735	6.20		
H04'a	H03	1.229/1.283	4.235	6.75			1.229/1.283	4.235	7.17		
H04'a	H04a	1.229/1.283	2.653	5.95			1.229/1.283	2.653	5.58		
H04'a	H04b	1.229/1.283	3.138	6.09			1.229/1.283	3.138	6.73		
H04'a	H06	1.229/1.283	4.140	3.17			1.229/1.283	4.140	4.22		
H04'a	H07	1.229/1.283	3.259	2.77			1.229/1.283	3.259	3.05		
H04'a	H01'	1.229/1.283	1.039	7.10			1.229/1.283	1.039	7.66		
H04'a	H02'a	1.229/1.283	1.622/1.592	6.68			1.229/1.283	1.622/1.592	7.36		
H04'a	H02'b	1.229/1.283	1.592/1.622	7.08			1.229/1.283	1.592/1.622	6.79		
H04'a	H03'	1.229/1.283	0.916	2.62			1.229/1.283	0.916	2.61		
H04'a	H04'b	1.229/1.283	1.229/1.283	1.75			1.229/1.283	1.229/1.283	1.75		
H04'a	H05'a	1.229/1.283	2.029	2.88			1.229/1.283	2.029	2.85		
H04'a	H05'b	1.229/1.283	1.955	2.52			1.229/1.283	1.955	2.49		
H04'b	H01a	1.229/1.283	2.435	4.70			1.229/1.283	2.710	3.70		
H04'b	H01b	1.229/1.283	2.710	4.41			1.229/1.283	2.435	4.64		
H04'b	H02	1.229/1.283	1.735	5.52			1.229/1.283	1.735	6.21		
H04'b	H03	1.229/1.283	4.235	6.48			1.229/1.283	4.235	6.81		
H04'b	H04a	1.229/1.283	2.653	5.66			1.229/1.283	2.653	5.58		
H04'b	H04b	1.229/1.283	3.138	5.80			1.229/1.283	3.138	6.41		
H04'b	H06	1.229/1.283	4.140	2.68			1.229/1.283	4.140	3.85		
H04'b	H07	1.229/1.283	3.259	2.68			1.229/1.283	3.259	2.59		

H04'b	H01'	1.229/1.283	1.039	6.92	1.229/1.283	1.039	7.60
H04'b	H02'a	1.229/1.283	1.622/1.592	6.69	1.229/1.283	1.622/1.592	6.93
H04'b	H02'b	1.229/1.283	1.592/1.622	6.90	1.229/1.283	1.592/1.622	6.35
H04'b	H03'	1.229/1.283	0.916	2.62	1.229/1.283	0.916	2.62
H04'b	H04'a	1.229/1.283	1.229/1.283	1.75	1.229/1.283	1.229/1.283	1.75
H04'b	H05'a	1.229/1.283	2.029	2.52	1.229/1.283	2.029	2.57
H04'b	H05'b	1.229/1.283	1.955	2.88	1.229/1.283	1.955	2.86
H05'a	H01a	2.029	2.435	3.80	2.029	2.710	4.60
H05'a	H01b	2.029	2.710	2.61	2.029	2.435	4.05
H05'a	H02	2.029	1.735	5.28	2.029	1.735	6.24
H05'a	H03	2.029	4.235	5.14	2.029	4.235	6.61
H05'a	H04a	2.029	2.653	4.30	2.029	2.653	5.06
H05'a	H04b	2.029	3.138	4.93	2.029	3.138	5.66
H05'a	H06	2.029	4.140	2.65	2.029	4.140	3.12
H05'a	H07	2.029	3.259	2.60	2.029	3.259	2.48
H05'a	H01'	2.029	1.039	6.44	2.029	1.039	8.43
H05'a	H02'a	2.029	1.622/1.592	5.33	2.029	1.622/1.592	7.49
H05'a	H02'b	2.029	1.592/1.622	5.79	2.029	1.592/1.622	7.21
H05'a	H03'	2.029	0.916	2.95	2.029	0.916	2.92
H05'a	H04'a	2.029	1.229/1.283	2.88	2.029	1.229/1.283	2.85
H05'a	H04'b	2.029	1.229/1.283	2.52	2.029	1.229/1.283	2.57
H05'a	H05'b	2.029	1.955	1.75	2.029	1.955	1.75
H05'b	H01a	1.955	2.435	3.85	1.955	2.710	4.73
H05'b	H01b	1.955	2.710	2.51	1.955	2.435	3.97
H05'b	H02	1.955	1.735	5.29	1.955	1.735	5.61
H05'b	H03	1.955	4.235	5.14	1.955	4.235	6.82
H05'b	H04a	1.955	2.653	3.76	1.955	2.653	4.81
H05'b	H04b	1.955	3.138	4.97	1.955	3.138	5.82
H05'b	H06	1.955	4.140	3.21	1.955	4.140	2.86
H05'b	H07	1.955	3.259	2.72	1.955	3.259	2.98
H05'b	H01'	1.955	1.039	6.17	1.955	1.039	8.30
H05'b	H02'a	1.955	1.622/1.592	5.15	1.955	1.622/1.592	7.65
H05'b	H02'b	1.955	1.592/1.622	5.73	1.955	1.592/1.622	7.33
H05'b	H03'	1.955	0.916	2.95	1.955	0.916	3.03
H05'b	H04'a	1.955	1.229/1.283	2.52	1.955	1.229/1.283	2.49
H05'b	H04'b	1.955	1.229/1.283	2.88	1.955	1.229/1.283	2.86
H05'b	H05'a	1.955	2.029	1.75	1.955	2.029	1.75

Comparison of ${}^nJ_{\text{HH}}$ measured from the ${}^1\text{H}$ spectra and the computational ${}^nJ_{\text{HH}}$ (Figure S53) show that the lowest deviations (MAD 0.8-0.9 Hz) between datasets are found when comparing **10A** with **10-RRRS** and **10B** with **10-SRRS** (Table S25).

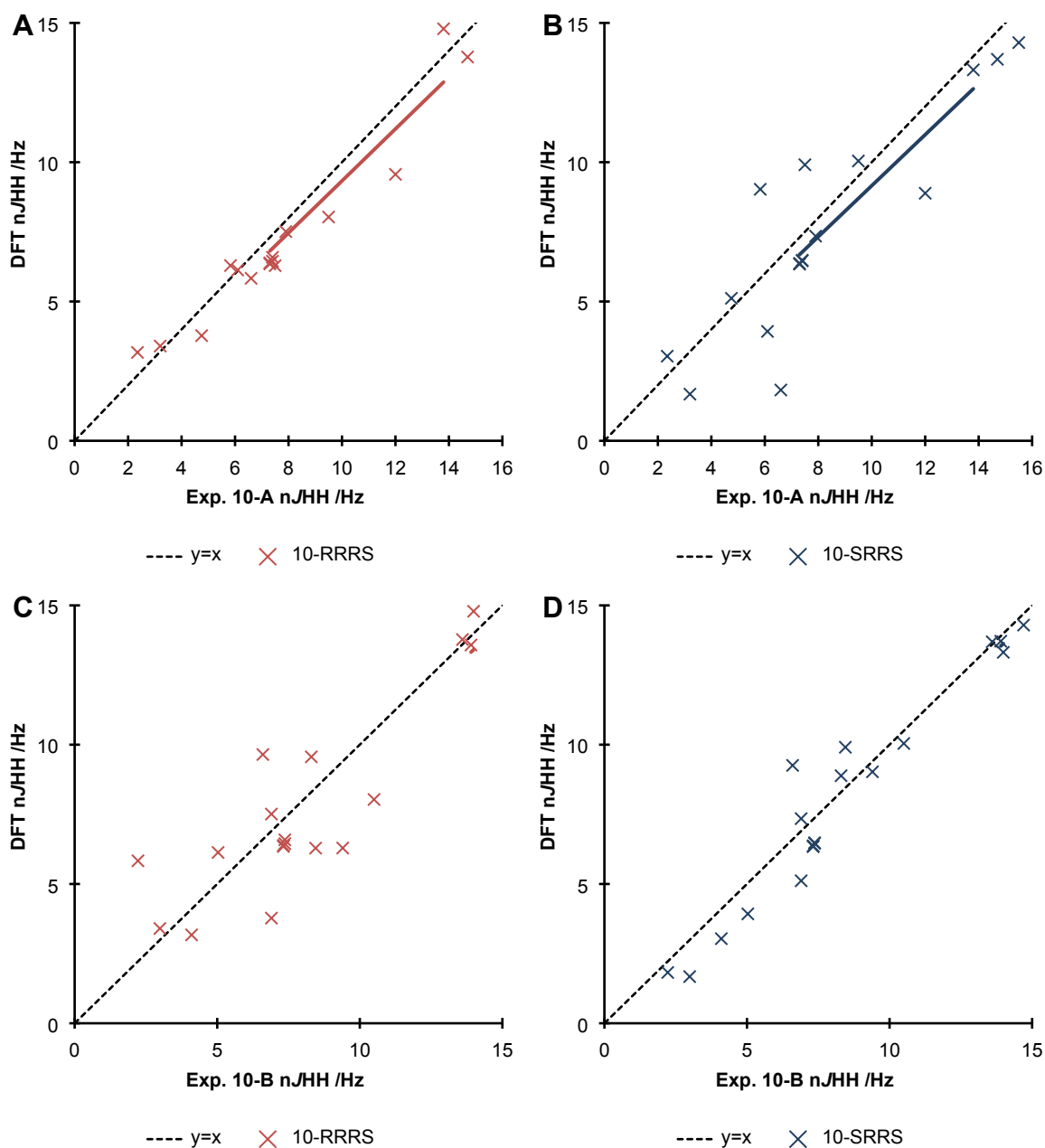


Figure S53: ${}^nJ_{HH}$ measured experimentally for A,B) **10A** and C,D) **10B** compared to DFT-derived values for **10-RRRS** and **10-SRRS**. The coloured solid lines indicate the line of best fit between the data.

Table S25: Summary of all statistics comparing ${}^nJ_{HH}$ from experimental data (**10A** and **10B**) to the computational data (**10-RRRS** and **10-SRRS**).

	10A		10B	
	10-RRRS	10-SRRS	10-RRRS	10-SRRS
MAD /Å	0.84	1.44	1.42	0.88
SD /Å	0.84	1.81	1.82	1.04
RMSD /Å	0.99	1.87	1.79	1.07

Comparison of experimentally determined ^1H - ^1H distances and the computational values (Figure S54) confirm the findings from $^1J_{\text{HH}}$ showing that the lowest deviations (MA%D 4.8-9.5%) between datasets are found when comparing **10A** with **10-RRRS** and **10B** with **10-SRRS** (Table S26).

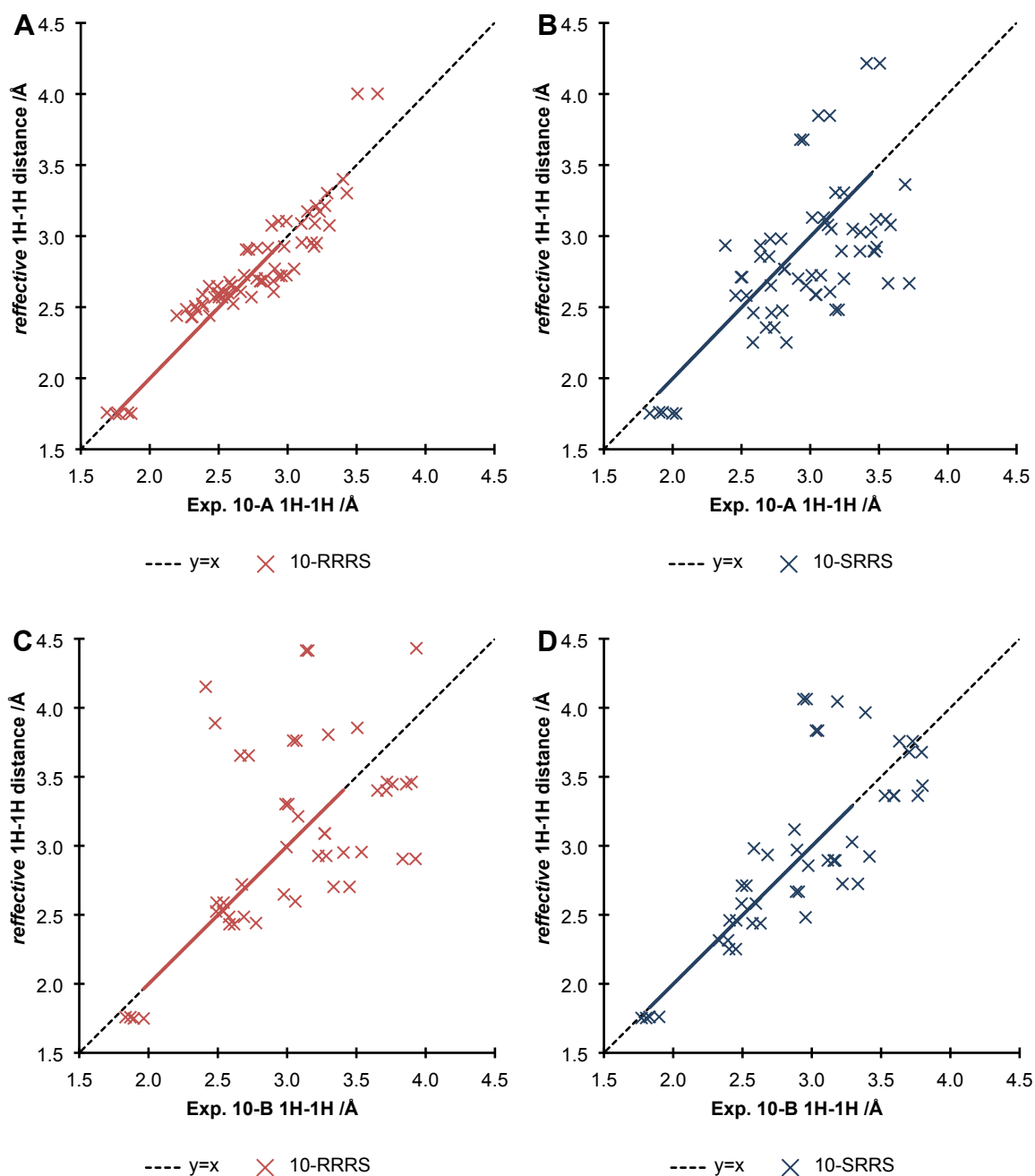


Figure S54: Experimental ^1H - ^1H distances determined by NOE (Equations 2-3) for A,B) **10A** and C,D) **10B** compared to DFT-derived effective distances (Equation 10-11) for **10-RRRS** and **10-SRRS**. The coloured solid lines indicate the line of best fit between the data.

Table S26: Summary of all statistics comparing ^1H - ^1H distances from experimental data (**10A** and **10B**) to the DFT-derived data (**10-RRRS** and **10-SRRS**).

	10A		10B	
	10-RRRS	10-SRRS	10-RRRS	10-SRRS
MA%	4.8%	15.9%	14.8%	9.5%
%SD	5.8%	22.9%	20.8%	13.1%
MAD /Å	0.13	0.47	0.45	0.29
SD /Å	0.16	0.66	0.61	0.40
RMSD /Å	0.16	0.65	0.60	0.40

Note that calculations for the diastereomers **10A** and **10B** were performed before the absolute configuration of **1** was known and used the *enantiomeric* structures of **10A** and **10B**. This does not alter the conclusion that the *2S, 3S, 6S, 7R* stereoisomer is the best match for **10A**.

25 Crystallisation of Cornexistin and X-ray Analysis

Cornexistin (2 mg) was dissolved in dichloromethane (75 μl) in an open tube. Isohexane (50 μl) was added, the solution went cloudy, then dichloromethane (15 μl) was added to homogenise. This tube was placed upright in a larger outer vessel that had a small amount isohexane in the bottom, and the outer vessel was sealed and allowed to stand at room temperature. Needles formed in the inner tube and were submitted for X-ray crystallography (Figure S55).

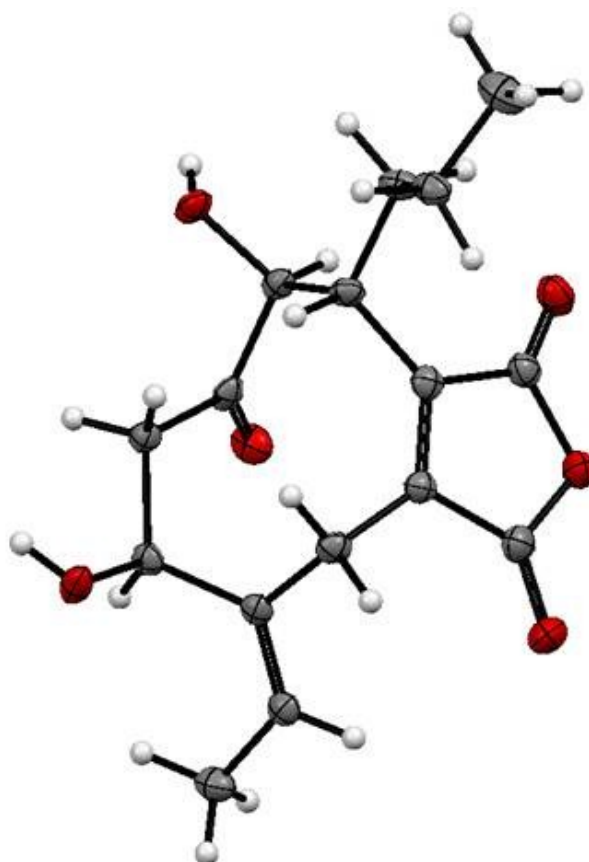


Figure S55: X-ray crystal structure of cornexistin 1 with 50% probability of the thermal ellipsoids.

There is very clear H-bonding between molecules in the crystal lattice (H-bonds depicted as dotted orange lines, Figure S56), with geometrical details available in the CIF.

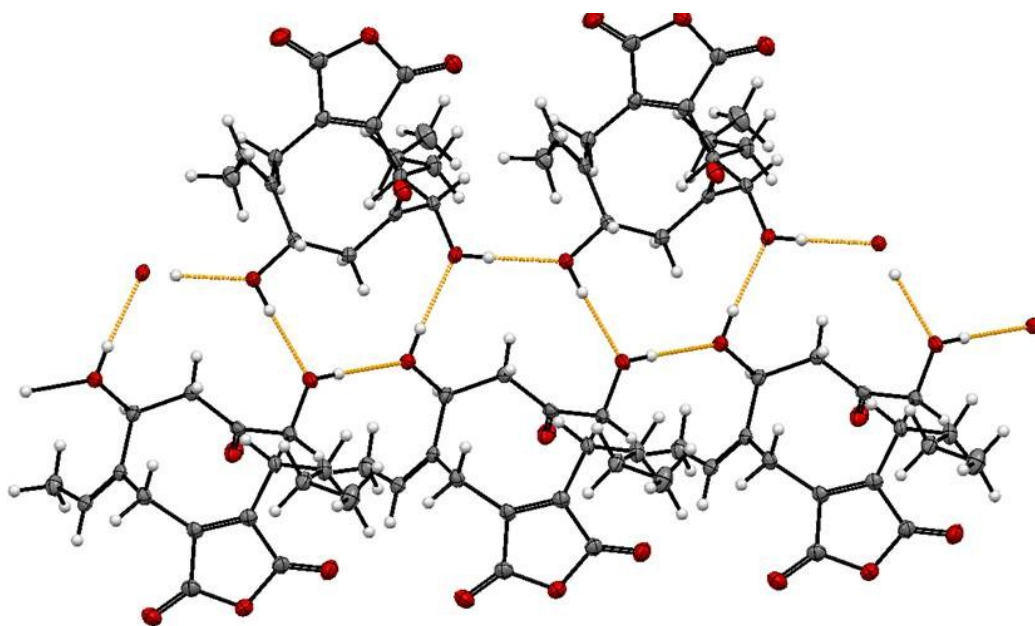


Figure S56: Intermolecular hydrogen bonding in the crystal of cornexistin 1 with 50% probability of the thermal ellipsoids.

Four molecules pack together in the crystal unit cell (Figure S57)

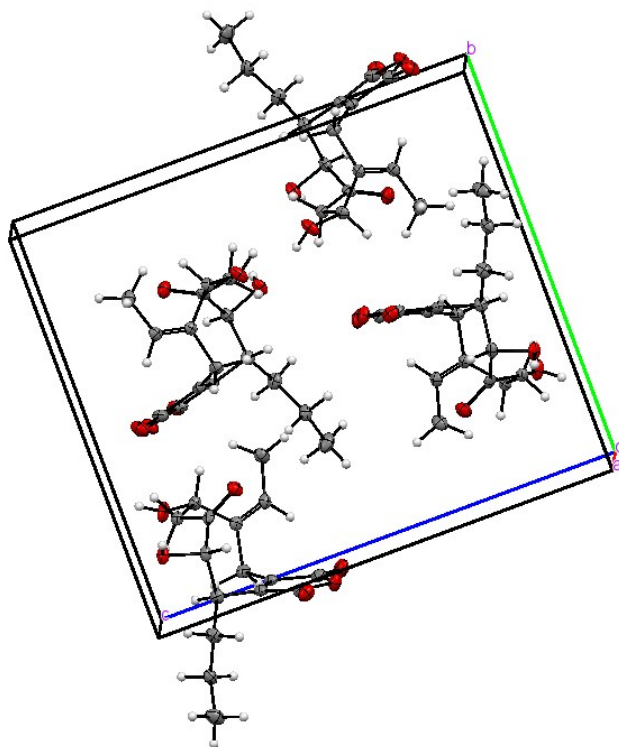


Figure S57: Unit cell of cornexistin 1 crystal structure with 50% probability of the thermal ellipsoids.

The value of the Flack parameter [-0.05(14)] establishes the absolute configuration of cornexistin 1. It can be stated with 99% confidence that this absolute stereochemistry is the correct one:

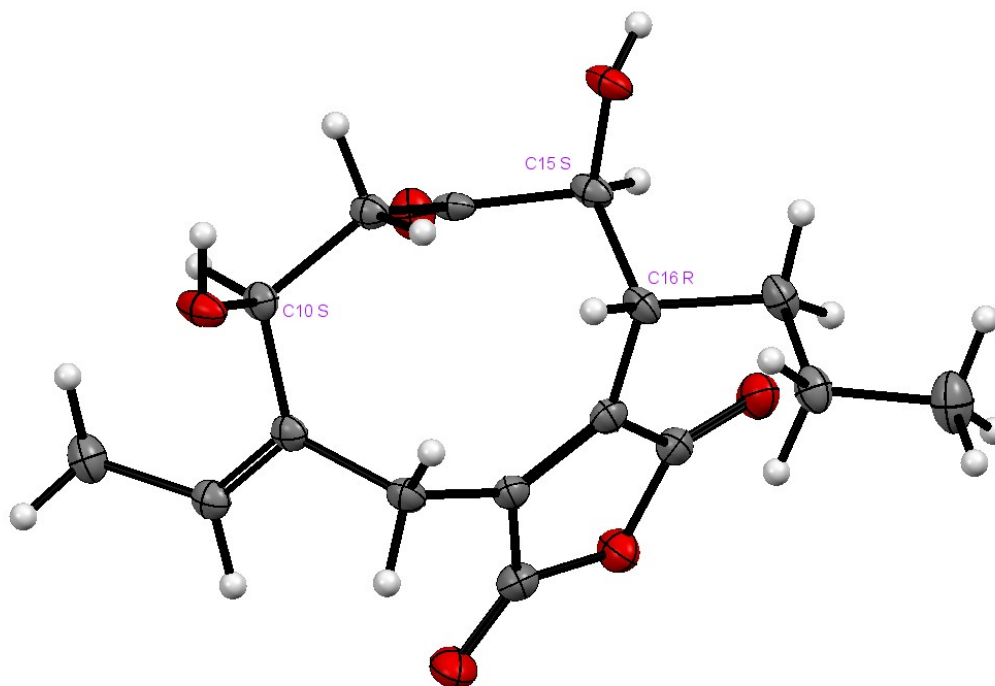


Figure S58: Absolute configuration of cornexistin 1 with 50% probability of the thermal ellipsoids.

26 References

1. J. Sambrook and D. W. Russell, *Molecular Cloning: A Laboratory Manual*, Cold Spring Harbor Laboratory Press, New York, 3rd ed., 2001.
2. J. T. Simpson, K. Wong, S. D. Jackman, J. E. Schein, S. J. M. Jones and I. Birol, *Genome Res.*, 2009, **19**, 1117-1123.
3. M. Boetzer, C. V. Henkel, H. J. Jansen, D. Butler and W. Pirovano, *Bioinformatics*, 2011, **27**, 578-579.
4. C. Trapnell, L. Pachter and S. L. Salzberg, *Bioinformatics*, 2009, **25**, 1105-1111.
5. V. Solovyev, P. Kosarev, I. Seledsov and D. Vorobyev, *Genome Biol.*, 2006, **7**, S10.
6. S. Altschul, T. Madden, A. Schaffer, J. Zhang, Z. Zhang, W. Miller and D. Lipman, *Nucleic Acids Res.*, 1997, **25**, 3389 - 3402.
7. S. Hunter, P. Jones, A. Mitchell, R. Apweiler, T. K. Attwood, A. Bateman, T. Bernard, D. Binns, P. Bork, S. Burge, E. de Castro, P. Coggill, M. Corbett, U. Das, L. Daugherty, L. Duquenne, R. D. Finn, M. Fraser, J. Gough, D. Haft, N. Hulo, D. Kahn, E. Kelly, I. Letunic, D. Lonsdale, R. Lopez, M. Madera, J. Maslen, C. McAnulla, J. McDowall, C. McMenamin, H. Mi, P. Mutowo-Muellenet, N. Mulder, D. Natale, C. Orengo, S.

-
- Pesseat, M. Punta, A. F. Quinn, C. Rivoire, A. Sangrador-Vegas, J. D. Selengut, C. J. A. Sigrist, M. Scheremetjew, J. Tate, M. Thimmajananathan, P. D. Thomas, C. H. Wu, C. Yeats and S.-Y. Yong, *Nucleic Acids Res.*, 2012, **40**, 4725-4725.
8. D. W. Brown, S. H. Lee, L. H. Kim, J. G. Ryu, S. Lee, Y. Seo, Y. H. Kim, M. Busman, S. H. Yun, R. H. Proctor and T. Lee, *Mol. Plant-Microbe Interact.*, 2015, **28**, 319-332.
 9. L. Blank, J. Green and J. R. Guest, *Microbiology*, 2002, **148**, 133-146.
 10. P. A. Nunes, S. Tenreiro and I. Sa-Correia, *Antimicrob. Agents Chemother.*, 2001, **45**, 1528-1534.
 11. N. E. J. Appleford, D. J. Evans, J. R. Lenton, P. Gaskin, S. J. Croker, K. M. Devos, A. L. Phillips and P. Hedden, *Planta*, 2006, **223**, 568-582.
 12. Y. C. Huang, Y. H. Chen, S. R. Lo, C. I. Liu, C. W. Wang and W. T. Chang, *Mol. Microbiol.*, 2004, **53**, 81-91.
 13. J. W. Bok, D. Chung, S. A. Balajee, K. A. Marr, D. Andes, K. F. Nielsen, J. C. Frisvad, K. A. Kirby and N. P. Keller, *Infect. Immun.*, 2006, **74**, 6761-6768.
 14. C. Zaugg, O. Jousson, B. Lechenne, P. Staib and M. Monod, *Int. J. Med. Microbiol.*, 2008, **298**, 669-682.
 15. R. C. Vargas, S. Tenreiro, M. C. Teixeira, A. R. Fernandes and I. Sa-Correia, *Antimicrob. Agents Chemother.*, 2004, **48**, 2531-2537.
 16. T. Ishizuka, I. Fujimori, M. Kato, C. Noji-Sakikawa, M. Saito, Y. Yoshigae, K. Kubota, A. Kurihara, T. Izumi, T. Ikeda and O. Okazaki, *J. Biol. Chem.*, 2010, **285**, 11892-11902.
 17. F. K. Crutcher, J. G. Liu, L. S. Puckhaber, R. D. Stipanovic, A. A. Bell, R and L. Nichols, *Microbiology-SGM*, 2015, **161**, 875-883.
 18. R. Fujii, A. Minami, T. Tsukagoshi, N. Sato, T. Sahara, S. Ohgiya, K. Gomi and H. Oikawa, *Biosci., Biotechnol., Biochem.*, 2011, **75**, 1813-1817.
 19. J. Abdoul-Zabar, I. Sorel, V. Helaine, F. Charmantray, T. Devamani, D. Yi, V. de Berardinis, D. Louis, P. Marliere, W. D. Fessner and L. Hecquet, *Adv. Synth. Catal.*, 2013, **355**, 116-128.
 20. A. Hidalgo, M. A. Akond, K. Kita, M. Kataoka and S. Shimizu, *Biosci., Biotechnol., Biochem.*, 2001, **65**, 2785-2788.
 21. M. J. Banfield, R. L. Brady, *J. Mol. Biol.*, 2000, **297**, 1159-1170.
 22. T. J. Carver, K. M. Rutherford, M. Berriman, M. A. Rajandream, B. G. Barrell, J. Parkhill, *Bioinformatics*, 2005, **21**, 3422-3423.
 23. M. L. Nielsen, L. Albertsen, G. Lettier, J. B. Nielsen and U. H. Mortensen, *Fungal Genet. Biol.*, 2006, **43**, 54-64.
 24. M. Nakajima, K. Itoi, Y. Takamatsu, S. Sato, Y. Furukawa, K. Furuya, T. Honma, J. Kadotani, M. Kozasa and T. Haneishi, *J. Antibiot.*, 1991, **44**, 1065-1072.
 25. A. J. Szwalbe, K. Williams, D. E. O'Flynn, A. M. Bailey, N. P. Mulholland, J. L. Vincent,

-
- C. L. Willis, R. J. Cox and T. J. Simpson, *Chem. Commun.*, 2015, **51**, 17088-17091.
26. MestReNova, Version 9.0.1, Mestrelab Research S.L., Santiago de Compostela, Spain, 2014.
27. S. Macura, B. T. Farmer and L.R. Brown, *J. Magn. Reson.*, 1986, **70**, 493-499.
28. G. Esposito and A. Pastore, *J. Magn. Reson.*, 1988, **76**, 331-336.
29. H.T. Hu and K. Krishnamurthy, *J. Magn. Reson.*, 2006, **182**, 173-177.
30. D. Neuhaus and M. P. Williamson, Wiley. *The Nuclear Overhauser Effect in Structural and Conformational Analysis*, Wiley-VCH, New York, 2nd ed., 2000, 99-128.
31. C. P. Butts, C. R. Jones, E. C. Towers, J. L. Flynn, L. Appleby and N. J. Barron, *Org. Biomol. Chem.*, 2011, **9**, 177-184.
32. C. R. Jones, M. D. Greenhalgh, J. R. Bame, T. J. Simpson, R. J. Cox, J. W. Marshall and C. P. Butts, *Chem. Commun.*, 2016, **52**, 2920-2923
33. Schrödinger Release 2011-1: MacroModel, version 9.9, Schrödinger, LLC, New York, NY, 2011.
34. Gaussian 09, Revision D.01, M. J. Frisch, G. W. Trucks, H. B. Schlegel, G. E. Scuseria, M. A. Robb, J. R. Cheeseman, G. Scalmani, V. Barone, B. Mennucci, G. A. Petersson, H. Nakatsuji, M. Caricato, X. Li, H. P. Hratchian, A. F. Izmaylov, J. Bloino, G. Zheng, J. L. Sonnenberg, M. Hada, M. Ehara, K. Toyota, R. Fukuda, J. Hasegawa, M. Ishida, T. Nakajima, Y. Honda, O. Kitao, H. Nakai, T. Vreven, J. A. Montgomery, Jr., J. E. Peralta, F. Ogliaro, M. Bearpark, J. J. Heyd, E. Brothers, K. N. Kudin, V. N. Staroverov, T. Keith, R. Kobayashi, J. Normand, K. Raghavachari, A. Rendell, J. C. Burant, S. S. Iyengar, J. Tomasi, M. Cossi, N. Rega, J. M. Millam, M. Klene, J. E. Knox, J. B. Cross, V. Bakken, C. Adamo, J. Jaramillo, R. Gomperts, R. E. Stratmann, O. Yazyev, A. J. Austin, R. Cammi, C. Pomelli, J. W. Ochterski, R. L. Martin, K. Morokuma, V. G. Zakrzewski, G. A. Voth, P. Salvador, J. J. Dannenberg, S. Dapprich, A. D. Daniels, O. Farkas, J. B. Foresman, J. V. Ortiz, J. Cioslowski, and D. J. Fox, Gaussian, Inc., Wallingford CT, 2013.
35. S. G. Smith and J. M. Goodman, *J. Am. Chem. Soc.*, 2010, **132**, 12946-12959.